From the holdings of the Department of Special Collections , Princeton University Library, Princeton, NJ

These documents are either in the public domain, or can only be used for educational and research purposes (Fair use) as per U.S. Copyright law (text below). By accessing this file, all users agree that their use falls in the public domain or within fair use as defined by the copyrightlaw. We do not charge any permission or usage fees for the publication of images of material inour collections, including those provided by Princeton University Library, via our website, catalog, or directly from staff.For more information regarding copyright, credit, and citation please review the information onthe Copyright, Credit and Citation Guidelines page of our website.
https://library.princeton.edu/special-collections/policies/copyright-credit-and-citation-guidelines. If you have any questions, including how to order higher-quality images from the collection, contact Special Collections Public Services via our Ask Us! Form. https://library.princeton.edu/special-collections/ask-us

---

Doctoral Dissertations, 2011-2026 Neuroscience

2015

Sensory-driven modulation of song structure and amplitude in Drosophila melanogas

Coen, Philip

Princeton, NJ : Princeton University

---

http://arks.princeton.edu/ark:/88435/dsp01vt150m51t

U.S. Copyright law: The copyright law of the United States (Title 17, §108, United States Code) governs the making of photocopies or other reproductions of copyrighted material. Under certain conditions specified in the law, libraries and archives are authorized to furnish a photocopy or other reproduction. One of these specified conditions is that the photocopy or reproduction is not to be used for any purpose other than private study, scholarship, or research. If a user makes a request for, or later uses, a photocopy or reproduction for purposes in excess of fair use that user may be liable for copyright infringement. This institution reserves the right to refuse to accept a copying order if, in its judgment, fulfillment of the order would involve a violation of copyright law. https://www.copyright.gov/title17/title17.pdf

Sensory-driven modulation of song structure and amplitude in *Drosophila melanogaster*

Philip Alexander Poliakoff Coen

A Dissertation
Presented to the Faculty
of Princeton University
in Candidacy for the Degree
of Doctor of Philosophy

Recommended for Acceptance
by the Princeton Neuroscience Institute
Adviser: Mala Murthy

March 2015

© Copyright by Philip Alexander Poliakoff Coen, 2015.

All rights reserved.

Abstract

A fundamental goal of neuroscience is to understand how sensory inputs are transformed into behavioral outputs. Mounting evidence suggests that brains are optimized to process naturalistic stimuli, but natural behaviors involving neural computations of interest are often challenging to accurately quantify. Acoustic communication is a natural behavior which exists throughout the animal kingdom, and can involve a dynamic signal which is both highly quantifiable and necessitates complex neural networks for generation and perception. Here, we use quantitative behavioral assays, computational modeling, and genetic manipulations to dissect the neural computations and circuits underlying this behavior in *Drosophila melanogaster*.

Dorsophila acoustic communication consists of a patterned courtship song produced by males to increase their chance of success with a female. Songs comprise of two modes—pulse and sine—and males alternate between these modes to produce patterns with high variability. Neural noise within pattern generating circuits is widely assumed to be the primary source of such variability. In contrast, we demonstrate that much of the pattern variability in *Drosophila* courtship song can be explained by taking into account the dynamic sensory experience of the male.

Several organisms modulate the amplitude of their acoustic signal in accordance with target distance to optimize for receiver intensity and conserve energy. Previously, this sensorimotor transformation has not been identified in invertebrates. We not only demonstrate that male flies increase pulse amplitude with female distance, but that this sensorimotor transformation takes place within ∼35ms. Further, through genetic and physical manipulations, we establish that amplitude modulation at large distances is exclusively mediated by vision, dependent on naturalistic stimuli, and implemented via the indirect flight muscles.

These results demonstrate that detailed quantification and modeling can reveal unexpected neural complexity underlying seemingly "stereotyped" behaviors.

Acknowledgements

I would like to thank Mala Murthy, not only for her constant support throughout this project, but also for first inspiring my interest in Neuroscience when we worked together in 2006. It has been a privilege to be part of her burgeoning research group, and I can't overstate how grateful I am for the level of intellectual freedom Mala afforded me during this time. With my bizarre schedule, scatterbrained explanations, and unfathomable tangents, I can only imagine the patience required to guide me through graduate school, but I never lacked for encouragement. I couldn't have asked for a better adviser.

The members of my thesis committee, David Tank and William Bialek, have given invaluable advice during this project. In general, the collaborative atmosphere and stimulating courses provided by the Princeton Neuroscience Institute have been fantastic, and I would like to thank David Tank, Jonathan Cohen, Carlos Brody, and Alan Gelprin for their ongoing efforts toward improving the graduate student experience.

Alan and David had the misfortune of dealing with me as both a student and TA of the experimental neuroscience laboratory. I learned so much from both of them during this time, and continued to pepper them with questions throughout my entire PhD. I will always be grateful for their help and guidance. My enjoyment, survival, and correct usage of statistics during those courses all depended on the energy and patience of my laboratory partner and colleague, Te Rutherford. He continues educating me to this day.

I would like to thank the entire Murthy Lab, past and present, for their support, friendship, and scientific insights. Jan Clemens guided me through the murky waters of data analysis and tolerated me as an office-mate, Georgia Guan kept my flies alive and brought a modicum of organization to my life, Diego Pacheco let me win at pool whenever I needed cheering up, and Alexandria Hammons kept my office, and stomach, supplied with delicious baked goods. Kelly LaRue went through the struggles of thesis-writing with me, Amanda Crocker graciously dealt with my stream of questions for more than four years, and Cyrille Girardin gave me an inferiority complex with his spectacular electrophysiology. I have had

the good fortune to work with some exceptionally talented undergraduates, and both Andrew Weinstein and Marjorie Xie made significant contributions to the work described here.

My house-mates of four years, Loren Alegria, Ben Safdi, Brin Rosenthal, and Cynthia Gerlein, made Princeton a great place to live, and I can't thank them enough for that. I will always remember the fussball games, night golf, cooking rotation, and Doctor Who marathons. I know we will remain close for many years to come. When Loren and Ben graduated and abandoned me, Ann Duan and Diego Pacheco moved into the house to save me from the brink of despair, and I thank them for making my final year so much fun.

Finally, I would like to thank my family—my parents, brother Tim, and sister Susie. Whether I need help with a grant application, emotional support, or fashion advice, they are always ready to listen. I cannot express how much they mean to me.

To my family.

Contents

Abstract iii

Acknowledgements iv

List of Tables x

List of Figures xi

1 Introduction **1**

1.1 A naturalistic approach to the study of neural computations 1

1.2 The ant odometer 3

1.3 Internal models of the dragonfly 5

1.4 Fruit fly courtship 6

2 Dynamic Sensory Cues Shape Song Structure in *Drosophila* **8**

2.1 Introduction 8

2.2 Results 9

2.2.1 A novel assay to study *Drosophila* song behavior 9

2.2.2 Using Generalized Linear Models to predict song patterning 9

2.2.3 Identifying the sensory cues responsible for song patterning 21

2.2.4 Both song modes influence female behavior 25

2.3 Discussion 28

2.4 Methods 28

2.4.1 Fly strains and rearing 28

2.4.2 Recording apparatus . . . 29
2.4.3 Courtship assay . . . 30
2.4.4 Dark/Light transition assay . . . 30
2.4.5 Thermogenetic activation experiments . . . 31
2.4.6 Data processing and analysis . . . 31

3 Neural Mechanisms Underlying Rapid Song Intensity Modulation in *Drosophila* 39

3.1 Introduction . . . 39
3.2 Results . . . 40
3.2.1 Distance predicts pulse amplitude . . . 40
3.2.2 Males modulate individual pulses within each train . . . 45
3.2.3 A crucial role for vision in amplitude modulation . . . 49
3.2.4 Changes in light intensity impact pulse amplitude in isolated males . 51
3.2.5 Motion-sensitive neurons affect courtship but not amplitude modulation 55
3.2.6 Amplitude modulation relies on indirect flight muscles . . . 57
3.2.7 Visual information intersects the song pathway upstream of dPR1 . . 58
3.2.8 Using an air-supported ball setup to investigate optimal visual stimuli 62
3.3 Discussion . . . 64
3.4 Methods . . . 66
3.4.1 Fly strains and rearing . . . 66
3.4.2 Behavioral chamber . . . 68
3.4.3 Air-supported ball . . . 68
3.4.4 Courtship assay . . . 69
3.4.5 Wing Measurement . . . 69
3.4.6 Thermogenetic activation in the behavioral chamber . . . 69
3.4.7 Dark/Light transition assay . . . 70
3.4.8 Multi-level light intensity assay . . . 70

3.4.9 Inactivation of motion-sensitive neurons 71
3.4.10 Data processing and analysis 71

4 Future directions and Conclusions **77**

4.1 Future work 77
4.1.1 Fly triplets with automated song segmentation 77
4.1.2 Calcium imaging and electrophysiology during song production 79
4.2 Conclusions 80

Bibliography **82**

List of Tables

2.1 Descriptions and acronyms for all fly strains/genotypes 11

3.1 Descriptions and acronyms for all fly strains/genotypes 43

List of Figures

2.1 A novel assay to study *Drosophila* song behavior 10

2.2 Courtship Behavior with PIBL females 12

2.3 Song bout statistics for WT strains courting PIBL females 13

2.4 Bout Triggered Averages (BTAs) for all nine movement parameters for song starts 14

2.5 Schematic of the generalized linear model. 15

2.6 Song bout patterning is predictable and based on few features. 16

2.7 Model selection criteria examples and comparison of model performance statistics. 17

2.8 fFV changes predict mFV changes in WT and PI males, but not BL or PIBL males. 18

2.9 Relationships between male-female distance, male velocity, and song bout starts. 19

2.10 Failed copulations do not result from differences in song patterning decisions. 20

2.11 Male velocity consistently predicts the current mode of song. 22

2.12 Flies perform distance-based modulations of song structure using vision. . . . 23

2.13 A neural link between locomotor and song-patterning circuits. 24

2.14 Models to predict current song mode during times when the female is stationary. 26

2.15 Song patterning decisions and female responses. 27

3.1 Measuring pulse amplitude 42

3.2 Dis predicts pulse amplitude at a delay of 470ms 45

3.3 Pulse parameters are independent 46
3.4 Flies modulate individual pulses with distance 48
3.5 Vision is responsible for amplitude modulation at larger distances 50
3.6 Modulation at short distances is independent of foreleg tarsi and pheromones 51
3.7 Visual information modulates amplitude within 30ms, but is influenced by history 53
3.8 FRU^{Act} and DSX^{Act} both show a light flash response independent of velocity 54
3.9 Motion-sensitive lamina neurons are not required for amplitude modulation . 56
3.10 T4 and T5 tangential neurons are not required for amplitude modulation . . 57
3.11 Normal IFM function is critical for amplitude modulation 59
3.12 Visual information intersects with the song pathway upstream of dPR1 . . . 61
3.13 Dissecting amplitude modulation using an air-supported ball setup 63

Chapter 1

Introduction

1.1 A naturalistic approach to the study of neural computations

A principal goal of neuroscience is to understand how neural circuits transform sensory information into appropriate behaviors. When attempting to dissect these mechanisms, it is invaluable to know the precise inputs and outputs—sensory cues and behaviors respectively—as these provide critical insights into the underlying neural computations. However, during naturally occurring complex behaviors, such as navigation, social interactions, or decision-making, the sensory environment is usually high-dimensional and difficult to measure. This creates a a dichotomy between the desire to study complex neural computations and the experimental benefit of limited sensory inputs and behavioral outputs.

A common solution to this problem is taken from the field of psychophysics. Animals can be trained to perform a specific action in response to sensory stimuli provided by the experimenter [1]. One such paradigm in extensive use is the go/no-go task, in which the animal simply reports whether it detected a stimulus [2, 3]. With further training, more complex behaviors can be developed, such as two-alternative forced choice tasks wherein the animal must distinguish which of two stimuli has a particular attribute. This task structure

has been used extensively in non-human primates [4, 5], and has recently been utilized in rodent studies [6, 7].

In these studies, the sensory input and behavioral output are well defined. If a mouse is trained to lick for a reward in response to a whisker deflection [8], the experimenter can accurately quantify both the sensory input (whisker deflection) and behavioral output (licking). While such psychophysical experiments have made huge contributions to our understanding of neural computations, they often require extensive training periods and involve behaviors which are relatively unnatural. Efforts are being made to create more naturalistic paradigms, such as those where mice navigate a virtual environment by running on an air-supported ball [9, 10], but the sensory information received by such animals is still disparate from their natural experience. This is problematic given the mounting evidence that sensory systems are more responsive to naturalistic stimuli [11], suggesting that computations performed by the brain are optimized for natural environments.

At the other end of the spectrum, recent studies have taken advantage of advances in computational power and machine vision to automatically categorize the behaviors naturally performed by an organism [12, 13]. The development of video acquisition with exquisite resolution and rapid frame rates has led to an explosion of automated tracking systems used in organisms from bacteria [14] to rodents [15]. When combined with machine vision techniques, this video data can be used to automatically segment the behavioral repertoire of an organism. Such methods have been applied to videos of a freely walking fruit fly and identified a staggering 122 separable behavioral states [16], and unsupervised learning approaches have been used to identify behaviors in individual *Drosophila* larvae and *Caenorhabditis elegans* [17, 18]. This behavioral phenotyping has also been utilized to describe animal interactions, including a study which used geometrical primitives to categorize social behaviors in mice pairs [15].

While the ethograms produced by these methods are valuable tools, they give limited insight into the underlying neural mechanisms. Furthermore, the identified behaviors are

relatively simplistic and the neural computations involved are unlikely to approach the complexity of those studied in trained animals. However, an option exists at the interface between two methodologies: to quantify a specific and complex natural behavior while recording the sensory experience of the organism. In this scenario, the naturalistic quality of sensory inputs is maintained, and the behavioral repertoire of the animal is limited enough to give meaningful insights into the underlying neural computations. If a suitable behavior is chosen, these computations will necessitate complex neural circuitry.

This strategy has been applied to both isolated animals and group behaviors. Recent work tracking the foraging behavior in the nematode worm *Caenorhabditis elegans* identified a transition between different behavioral states which could be quantitatively explained by a maximally informative search strategy [19]. In another study, experimenters allowed real predatory fish to hunt mobile virtual prey and demonstrated that a tendency toward collective motion (i.e. schooling) imparted prey with a survival advantage [20]. In both these examples, accurate quantification of behavior and manipulations of the sensory environment gave insights into underlying neural computations.

Applying these strategies to insects has met with particular success as their behavioral repertoires are large enough to exhibit complexity whilst remaining relatively robust and reproducible. Moreover, their small size and resilience to physical manipulations (such as limb removal) allows for accurate quantification of behaviors and easy manipulation of the sensory environment. Experimenters have taken advantage of these features to identify several complex neural computations in the insect brain.

1.2 The ant odometer

Desert ants navigate their vast habitat when foraging for food, often traveling hundreds of meters (>20,000 body lengths) from their nest. When returning to their home, these tiny insects display the remarkable ability to chose a direct path without retracing their circuitous

foraging route [21]. This behavior requires two types of information: direction steered and distance traveled.

Early experiments demonstrated that polarized light was of critical importance for directional information [22]. Ants were collected at feeding locations, held in darkness for several hours, and then released in an unfamiliar location. Nevertheless, ants repeatedly walked in the direction of their nest. A small vehicle was created to accompany the ants and manipulate the sensory environment, either by blocking the sun altogether, or changing the polarization of sunlight. Experimenters were able to elicit reproducible deviations in homing direction, or completely eliminate the behavior, demonstrating that ants not only rely on polarized light, but compensate for the movement of the sun during the hours they were confined to darkness.

The mechanism by which ants measure distance remained mysterious for a further twenty-five years until Wittlinger and colleagues tested the hypothesis that ants could be counting the number of leg movements [23]. Ants were trained to walk from their nest entrance to a feeder placed 10m away along a linear channel. After reaching the feeder, ants were collected and their leg length was manipulated: either shortened through cutting to create "stumps" or lengthened by gluing short "stilts" to each leg. When released in a new location, ants attempted to navigate back to their nest, but animals with stumps or stilts under- or overestimated the distance respectively. Furthermore, ants treated with stumps or stilts prior to foraging accurately measured distance to the nest on their homeward journey, when the number of outbound and inbound steps were the same. Quantifying the gait of manipulated ants with high speed video confirmed that changes in stride length predicted the error in distance estimation [24].

Thus, through methodical manipulations of the ants sensory environment, combined with a thorough analysis of specific and quantifiable natural behavior (path trajectories), investigators identified a neural computation of striking complexity. Yet the analysis of this behavior is ongoing. New work has demonstrated that ants not only measure distance

and direction, but also elevation, and are able to return directly to their nest even when traversing hills of unpredictable height [25, 26]. This extends the path integration into three dimensions, and the sensory mechanism for this behavior is still unknown. Investigators are currently pursuing the problem using the same methodologies: manipulating the sensory environment (using artificial sloped terrain) and quantifying natural behaviors.

1.3 Internal models of the dragonfly

Humans and non-human primates use internal models to interact with the world [27, 28]. For example, when catching a ball, it is necessary to predict where the ball is going to land and move one's hand accordingly. Whether invertebrates used such mechanisms to interact with the environment has remained unclear. Indeed, it has traditionally been assumed that invertebrates rely purely on reactive control to perform sensorimotor behaviors such as intercepting prey during flight [29].

Mischiati and colleagues used exquisite quantification of dragonfly prey capture to test whether this complex, natural behavior depended upon the use of internal models [30]. By placing retro-reflective markers on the dragonfly, high speed video (200Hz) from 18 cameras was used to track the body and head orientation of dragonflies throughout hundreds of prey capture sequences, including both live and artificial prey. In contrast to prior assumptions, the researchers demonstrated that reactive control in response to prey movements could not explain dragonfly movements.

Many changes in the the dragonfly's acceleration were not in response to prey movement, establishing that their interception path was not simply a concatenation of reactive flight corrections. Further, dragonflies adjusted their head orientation during flight to account not only for the foveal drift imposed by their own motion, but also to nullify the predicted movement of their prey. These changes in head position occurred within 4ms of the change in visual environment, an impossibly short time period for sensory-driven re-

sponses. This demonstrated that dragonflies utilize both forward models (to predict the sensory consequences of self-motion) and inverse models (to predict, and account for, future prey location).

Thus, by selecting a complex natural behavior, and accurately quantifying both dragonfly motion and the sensory space, experimenters uncovered the necessity for novel and highly complex neural computations.

1.4 Fruit fly courtship

While the path integration of desert ants and prey capture of the dragonfly are complex behaviors which rely on intriguing computations, limited experimental tools exist to help dissect the underlying neural circuits. Conversely, the range of genetic, optical, and electrophysiological tools available to study neural circuit structure and function in the fruit fly, *Drosophila melanogaster*, is extensive and continually increasing [31, 32]. Multiple binary expression systems and intersection strategies can be combined to express a protein of choice in sparse neural subsets. Thus, once a novel behavior is identified, neurons of interest can be activated or inactivated to assess their contribution without even dissecting the fly [33], a manipulation currently impossible in any other insect. Genetic techniques can be combined with calcium imaging or electrophysiology to record activity from identifiable neural subsets [34]; such experiments have been performed in tethered flies, both during walking and flight [35, 36]. These tools are invaluable aids during the search for, and functional analysis of, neural circuits underlying behavior and represent a tremendous advantage over systems such as the ant and dragonfly. However, as with these organisms, it is desirable to first establish which computations are performed by fruit flies during complex natural behaviors. When these are known, the nervous system can then be probed with advanced knowledge of the optimal sensory information to deliver and the behavioral output to expect.

One such behavior in *Drosophila* is the production and perception of courtship song. During courtship, males carry out a range of behaviors: they orient toward and chase the female, tap her abdomen, lick her genitalia, attempt copulation, and produce a courtship song by extending and vibrating their wing [37]. Females arbitrate the mating decision, and males will continue to court for many minutes until they are allowed to copulate. Of the courtship behavioral elements, song is the most complex cue to generate and perceive as it involves a dynamic and time-varying signal (unlike pheromones or gustatory cues). The production of courtship song dramatically improves a male's chance of successful copulation [38] and is an important cue for females to distinguish between different fly species [39]. Moreover, as with ant path trajectories and dragonfly interception maneuvers, courtship song highly quantifiable.

Despite this, a quantitative analysis of the relationship between the male's song production and his sensory environment had never been performed. This presented an opportunity to examine the computational underpinnings of a complex social behavior which is naturally and robustly produced. Here, we undertake to dissect this behavior with a combination of quantitative behavioral assays and modeling, and to use the genetic and neural circuit tools available in *Drosophila* to investigate the underlying neural mechanisms.

Chapter 2

Dynamic Sensory Cues Shape Song Structure in *Drosophila*

2.1 Introduction

The generation of acoustic communication signals is widespread across the animal kingdom [40, 41], and males of many species, including *Drosophilids*, produce patterned courtship songs to increase their chance of success with a female. For some animals, song structure can vary considerably from one rendition to the next [42]; neural noise within pattern generating circuits is widely assumed to be the primary source of such variability, and statistical models that incorporate neural noise are successful at reproducing the full variation present in natural songs [43]. In direct contrast, we demonstrate that much of the pattern variability in *Drosophila* courtship song can be explained by taking into account the dynamic sensory experience of the male. In particular, using a quantitative behavioral assay combined with computational modeling, we find that males use fast modulations in visual and self motion signals to pattern their songs, a relationship we show is evolutionarily conserved. Using neural circuit manipulations, we also identify the pathways involved in song patterning choices, and show that females are sensitive to song features. Our data not only demonstrate that

Drosophila song production is not a fixed action pattern [44, 45], but establish *Drosophila* as a valuable new model for studies of rapid decision-making under both social and naturalistic conditions.

2.2 Results

2.2.1 A novel assay to study *Drosophila* song behavior

Drosophila melanogaster males chase females during courtship and produce song via wing vibration; females, meanwhile, arbitrate mating decisions. We developed a behavioral chamber to record acoustic signals and fly movements simultaneously (Figure 2.1a); fly movements provide information on the sensory cues that may influence song production. We collected a large data set ($>$ 100,000 song bouts) to model the relationship between sensory cues and song patterning. Most experiments involve females that are pheromones-insensitive [46] and blind (termed PIBL) to facilitate auditory response measurements. All fly types used are described in Table 2.1.

For one wild type strain (WT1), we show that using AC (arista-cut/deaf) females, or WC (wing-cut/mute) males increased the time to copulation and decreased the percentage of mated pairs (Figure 2.1c). This corroborates prior work [38, 39] in demonstrating the importance of song for courtship success. Pairing WT1 males with WT, rather than PIBL, females did not alter these results (Figure 2.1c), nor any of the results described below (not shown). All WT strains showed similar success with PIBL females (Figure 2.2b). Courtship songs comprise two modes (sine and pulse; Figure 2.1b) and are part of a genetically-hardwired mating ritual, thought to be stereotyped [45, 47]. However, we find frequent mode transitions and variable mode durations individualize song bouts (Figure 2.1d and Figure 2.3).

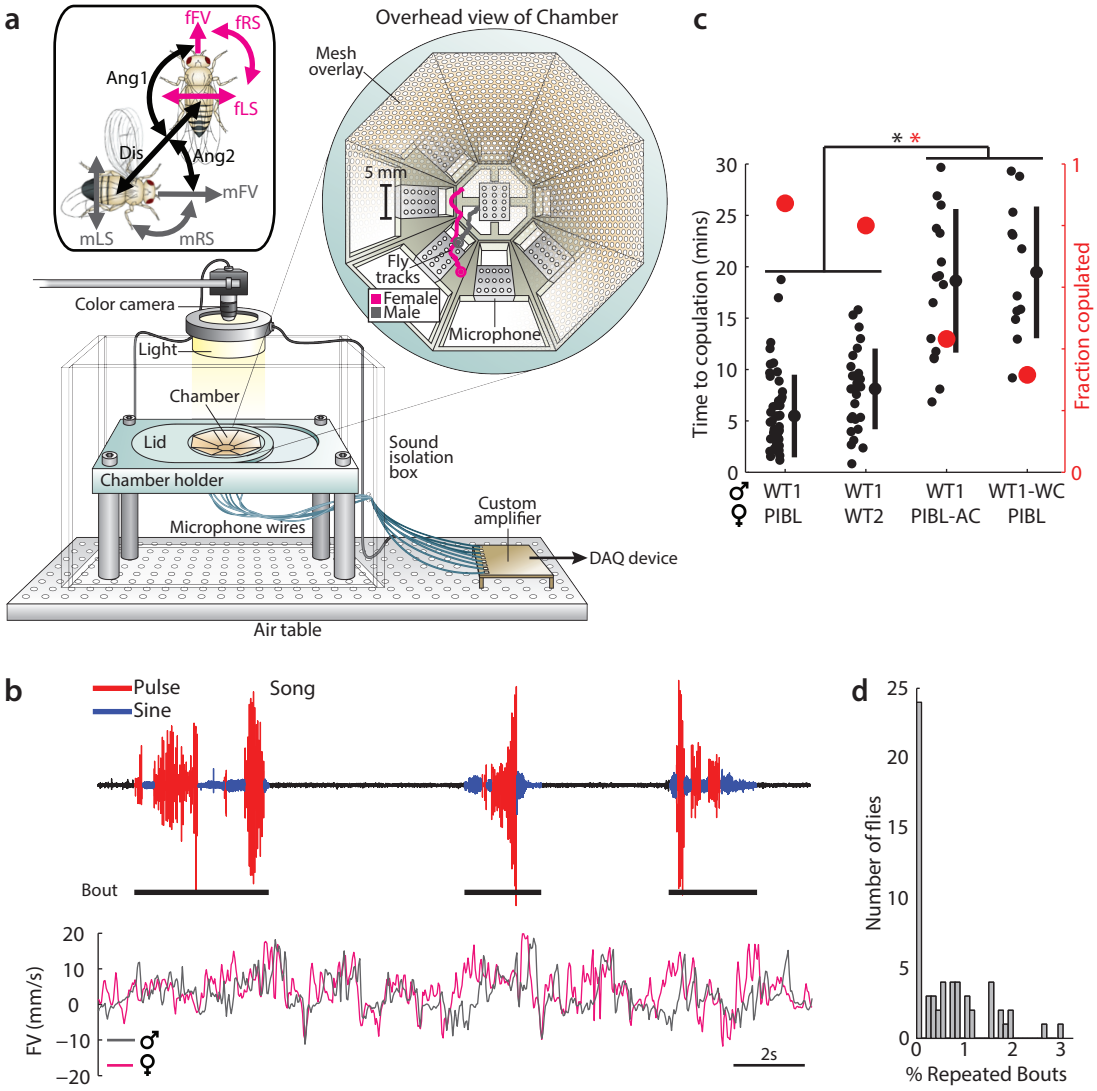

Figure 2.1: A novel assay to study *Drosophila* song behavior. **a**, Behavioral chamber with tracked fly movements (see Methods). Fly movements are divided into: male/female forward velocity (mFV/fFV), male/female lateral and rotational speeds (mLS/fLS and mRS/fRS), the distance between fly centers (Dis), the absolute angle from female/male heading to male/female center (Ang1/Ang2). **b**, (top) Segmentation of song bouts into pulse (red) and sine (blue) elements. (bottom) Corresponding traces for mFV and fFV. **c**, Song is important for mating. Time to copulation increases (black, * = $p < 0.001$) and fraction of copulated pairs decreases (red, * = $p < 0.01$) when females are deaf or males are mute. Individual points, mean, and s.d. are given for each genotype (n = 35-48 pairs). **d**, Song is variable. The number of identical mixed (containing pulse and sine) bouts per fly (see Methods). n = 60 WT males.

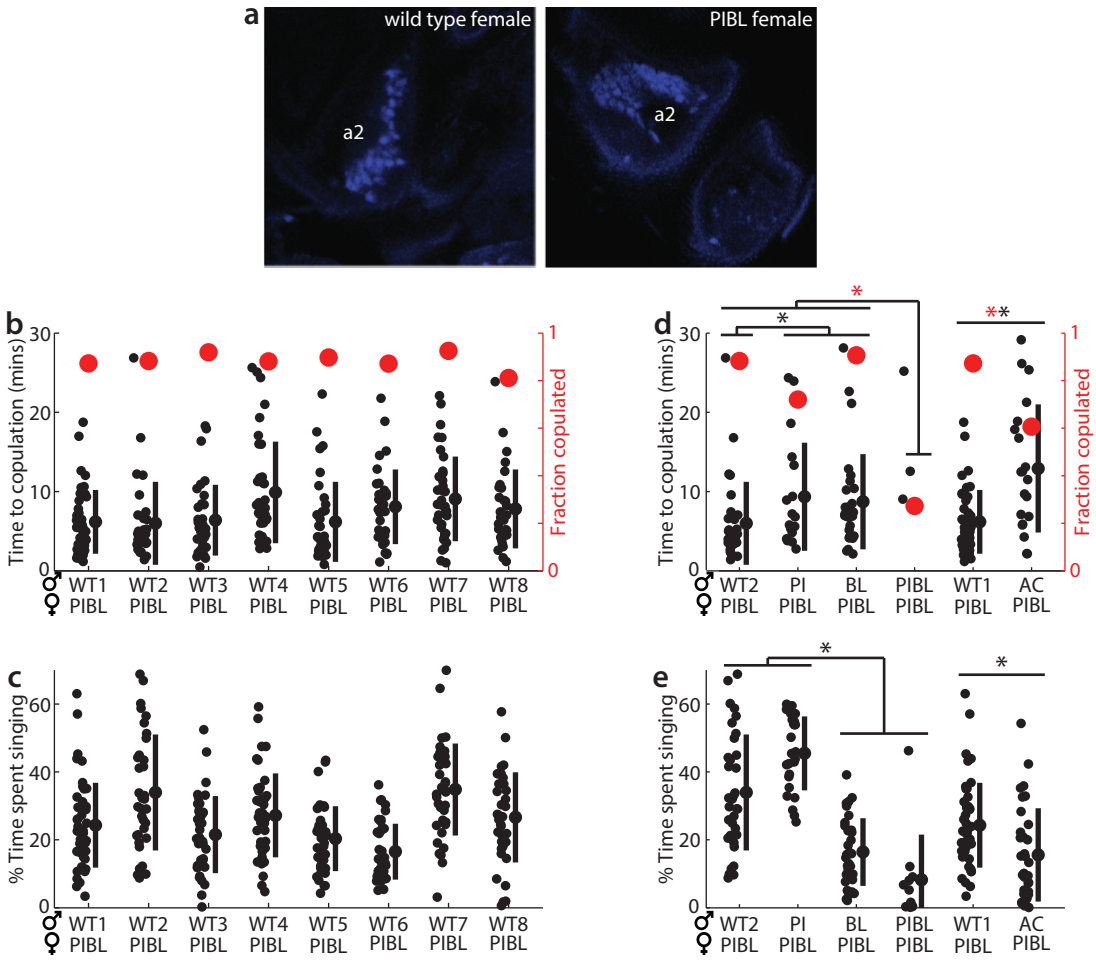

Figure 2.2: Courtship Behavior with PIBL females. **a**, Recently, genes involved in photoreceptor development have been implicated in JO function [48], so we confirmed that the GMR-hid mutation (which induces photoreceptor apoptosis) did not affect JO neuron development. Here, we show a single z plane image of the antenna of a wild type (left) or PIBL (right) female fly, labeled with anti-elav (blue) to mark the nuclei of JO neurons. **b**, Time to copulation (black) and fraction of copulating pairs (red) are similar for all 8 wild type strains. n = 34-48 males for each strain. **c**, The percentage of time males spent singing for all 8 wild type strains. n = 34-48 males for each strain. **d**, As in **b**, but for AC, PI, BL and PIBL males compared with WT strains of matched genetic background (WT2 for PI, BL, and PIBL and WT1 for AC). * = $p < 0.05$, n = 11-48 males for each genotype. **e**, As in **c**, but for AC, PI, BL and PIBL males compared with WT strains of matched genetic background. * = $p < 0.01$, n = 11-48 males for each genotype. **b-d** Individual points, mean, and s.d. are given for each strain/genotype.

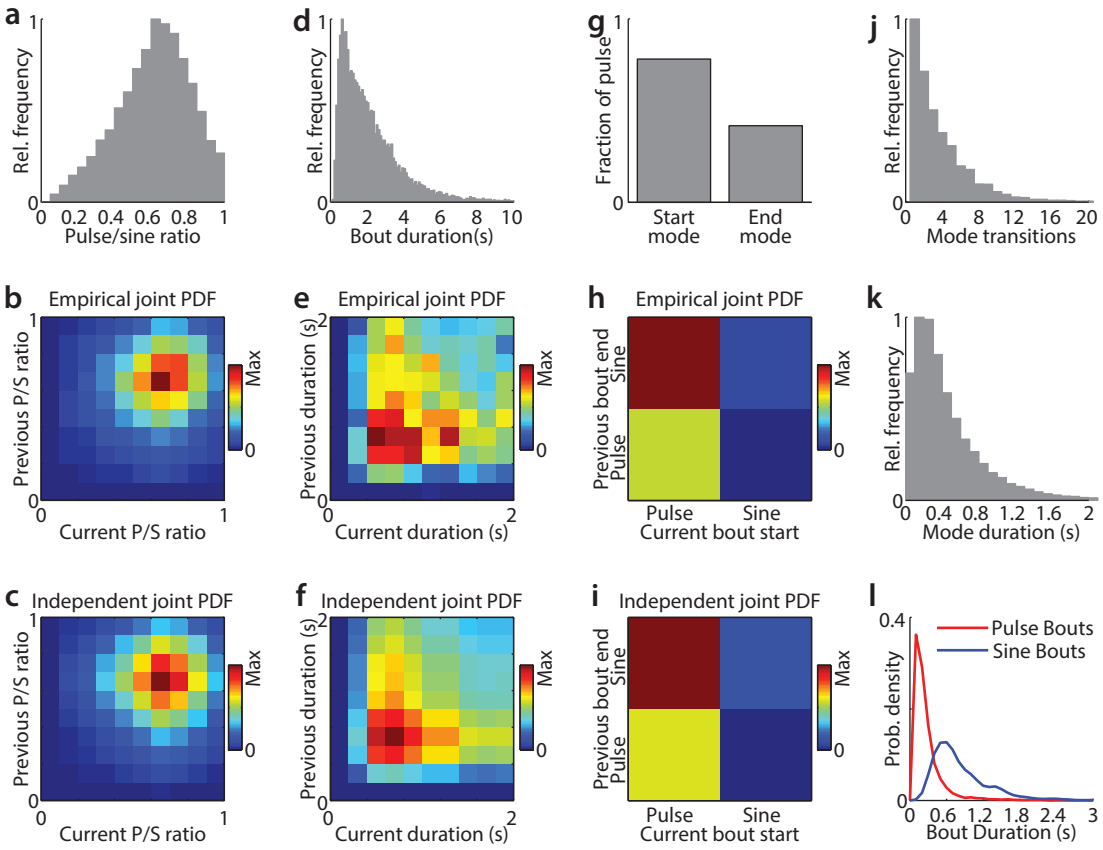

Figure 2.3: Song bout statistics for WT strains courting PIBL females. For all panels, data came from the 116 males singing more than 100 song bouts. **a**, Relative frequency of the pulse/sine ratio for mixed bouts (containing both sine and pulse). n = 15,489 bouts. **b**, The empirical joint probability density function (PDF) of pulse/sine ratios for consecutive pairs of mixed bouts (see Methods). n = 10,805 bouts. **c**, As in **b**, but the independent, rather than empirical, joint PDF. The distributions in **b** and **c** are not significantly different (p = 0.99, two-sample Kolmogorov-Smirnov test). **d**, Relative frequency of bout durations for mixed bouts. n = 15,489 bouts. **e**, The empirical joint PDF of bout durations for consecutive pairs of mixed bouts lasting less than 2s. n = 3,535 bouts. **f**, As in **e**, but the independent, rather than empirical, joint PDF. The distributions in **e** and **f** are not significantly different (p = 0.19, two-sample Kolmogorov-Smirnov test). **g**, The fraction of mixed bouts starting and ending in pulse mode. n = 10,805 bouts. **h**, The empirical joint PDF of the ending and starting modes for consecutive pairs of mixed bouts. n = 10,805 bouts. **i**, As in **h**, but the independent, rather than empirical, joint PDF. The distributions in **h** and **i** are not significantly different (p = 0.99, two-sample Kolmogorov-Smirnov test). **j**, Relative frequency of the number of mode (sine or pulse) transitions within mixed bouts. n = 15,489 transitions. **k**, Relative frequency of the durations of each song mode (sine or pulse) within mixed bouts. n = 76,979 song modes. **l**, Relative frequency of durations of non-mixed song bouts, comprising a single song mode. n = 8,624/772 for pulse only/sine only.

Acronym	Description
WT1	Wild type from Nairobi, Kenya; collected by Andolfatto & Bachtrog (2006)
WT2	Canton-S laboratory strain
WT3	Wild type from San Diego, California; collected by Andolfatto (2006)
WT4	Wild type from Cartagena, Colombia; collected by Andolfatto (2009)
WT5	Wild type from the Netherlands; collected by Davis (2000)
WT6	Wild type from Zanzibar, Tanzania; collected by Andolfatto & Bachtrog (2006)
WT7	Wild type from Harare, Zimbabwe; collected by Begun (1993)
WT8	Wild type from Victoria Falls, Zimbabwe; collected by Ballard (2002)
PI	Genetic manipulation to remove all volatile pheromone receptors and many general olfactory receptors
BL	Genetic manipulation to remove photoreceptors
PIBL	Genetic manipulation to remove photoreceptors and volatile pheromone receptors
AC	PIBL (female) or WT1 (male) flies had aristae removed > 20 hours before recording
WC	Male flies had wings removed > 20 hours before recording
SP	PIBL females injected with *Drosophila melanogaster* sex peptide > 20 hours before recording
In-C	PIBL females injected with *Drosophila melanogaster* SIFamide peptide > 20 hours before recording
oe^{-}	Genetic manipulation to remove pheromone producing cells (in PIBL females)
sim	*Drosophila simulans* strain from UCSD species stock center
Fru-A	Males expressing thermosensitive TrpA1 channels in all *fruitless* positive neurons.
Fru-B	Males expressing thermosensitive TrpA1 channels in all *fruitless* positive neurons, but with suppressed expression in the ventral nerve cord via the GAL80 system.
P1	Males expressing thermosensitive TrpA1 channels sparsely in putative song command (P1) neurons

Table 2.1: Descriptions and acronyms for all fly strains/genotypes

2.2.2 Using Generalized Linear Models to predict song patterning

Males spend $\sim$ 20% of courtship time singing (Figure 2.2c), and bouts can begin with either song mode. Using reverse correlation, we found that all tracking parameters correlate with bout initiations (Figure 2.4). We therefore turned to the GLM (generalized linear model; Figure 2.5), widely used to analyze binary response data with several explanatory variables [49, 50, 51]. Unlike reverse correlation [52], the GLM we employ includes a sparsity prior, which disentangles the contributions of correlated parameters to song patterning (see Methods) this represents a major difference between our approach and previous studies [53].

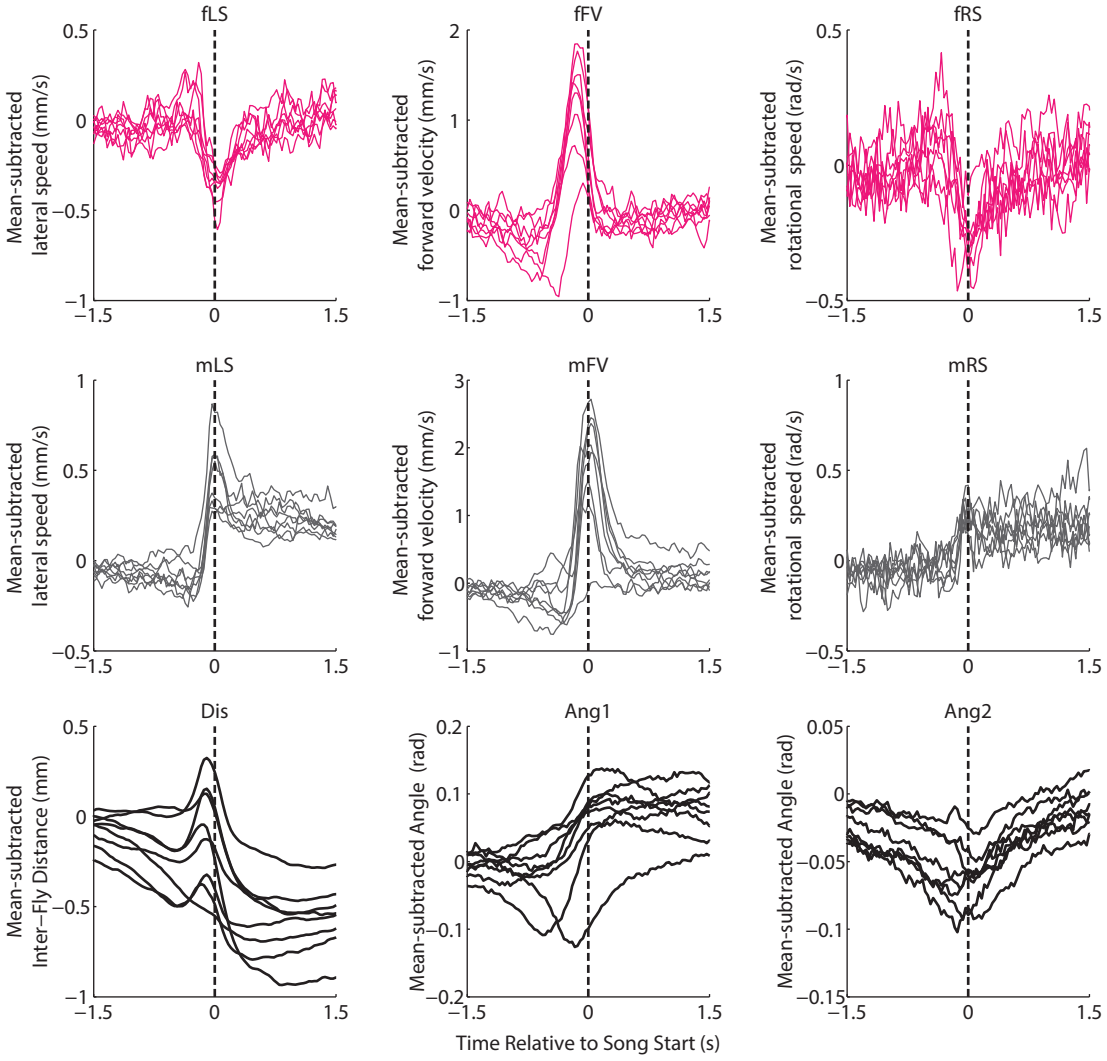

Figure 2.4: Bout Triggered Averages (BTAs) for all nine movement parameters for song starts. BTAs are formed similar to spike-triggered averages (STAs) for neural data. Movement parameters for each of the 8 wild type strains were aligned to the start of song (n = 2,427-7,586 bouts from 34-48 males). All males were paired with PIBL females. Female and male parameters are colored magenta and gray, respectively. For each trial, movement parameters were mean-subtracted before averaging (see Methods).

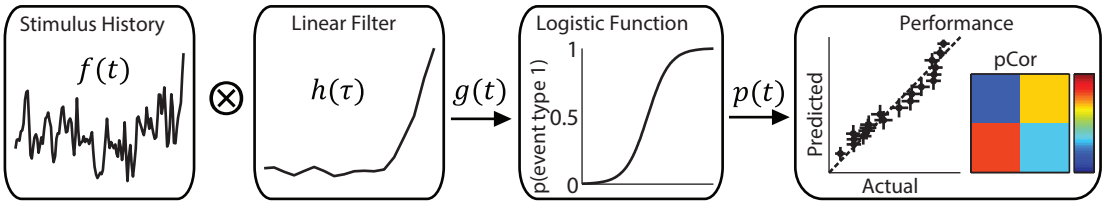

Figure 2.5: Schematic of the generalized linear model. Inputs—stimulus histories (features; *f(t)*) for each movement parameter—are used to predict binary event probabilities. Significant features are convolved with a linear filter, $h(\tau)$, and the result, *g(t)*, is transformed into a probability, *p(t)*, via a logistic function. Performance plots show the predicted and actual event probability relationships. Confusion matrices, from which we derive pCor values, quantify model performance.

Given similarities across fly strains (Figure 2.4), we combined data from all WT flies (315 pairs, 84904 song bouts) for GLM analyses. We selected the most predictive features ($\leq 600ms$ of tracking parameter history) for each model based on deviance reduction (Figure 2.7). For pulse song starts, combining two features (mFV and mLS) strongly improved model fit (Figure 2.6a). When tested on separate data, the fraction of correctly classified song starts (pCor) was 0.67 (Figure 2.6b) a 34% improvement over the null model (pCor = 0.5). This compares favorably with fMRI-based predictions of human behavior [54] and with two-alternative forced choice behavioral performance in *Drosophila* [55]. pCor values are equivalent ($r^2 = 0.98$) to area under the curve values, an alternative performance measure (Figure 2.7c-d). We used a similar GLM framework to identify fFV as the best predictor of changes in male motion (mFV (Figure 2.8a-c) and mLS (data not shown)): that is, when the female speeds up, the male accelerates to follow her. Therefore, any correlation between male motion and song mode choice ultimately establishes a link between a sensory cue (e.g., female motion) and song patterning. We address this point further below.

For songs that start in sine mode, the optimal model included only Dis (Figure 2.6b-c and Figure 2.9a). Song start filters derived from PI (pheromone-insensitive) or AC males paired with PIBL females, or from WT males paired with AC or SP (unreceptive/sex peptide-injected [56]) females, were indistinguishable from WT filters (Figure 2.6c), even though males take longer to copulate with AC females (Figure 2.1c), and never copulate with SP

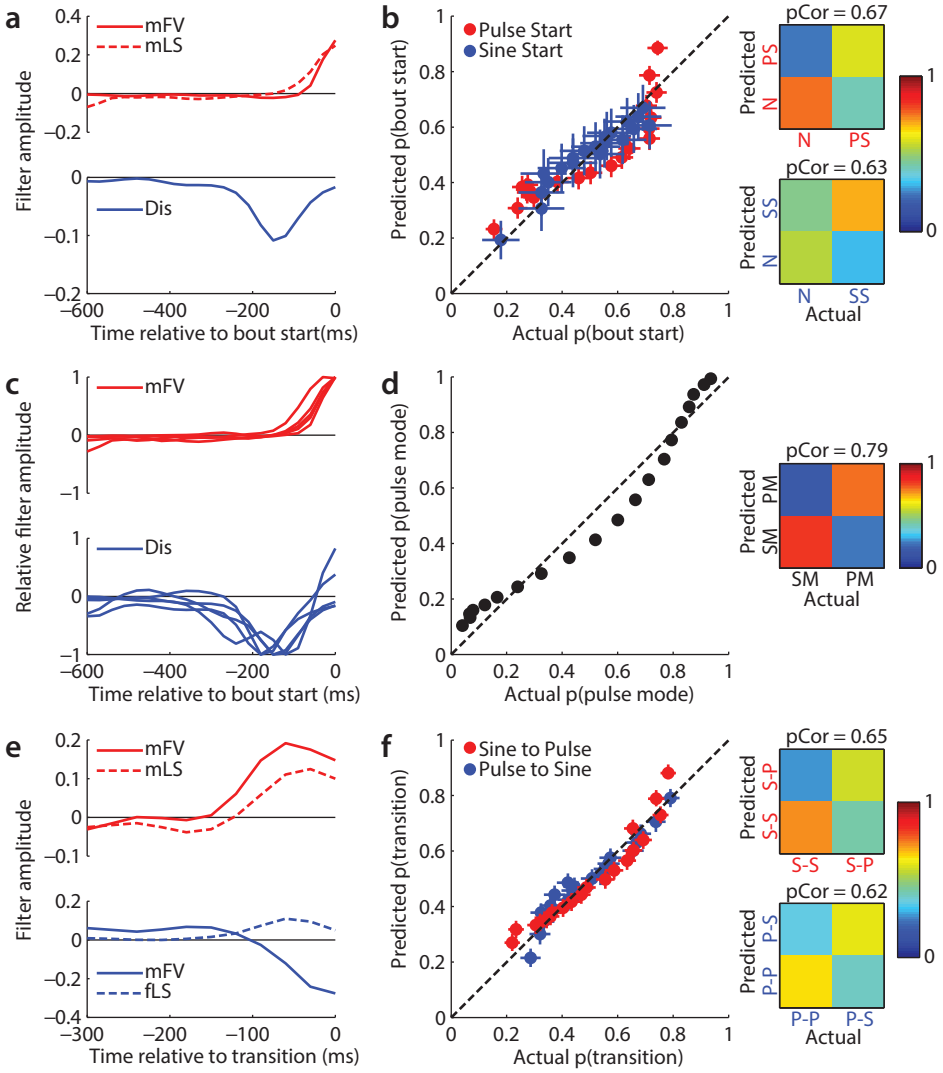

Figure 2.6: Song bout patterning is predictable and based on few features. a, Filters for pulse and sine song initiation GLMs. Unlike mLS or mLV, the Dis filter indicates a time lag between distance estimation and sine song initiation. **b**, GLM performance for identifying pulse song starts (PS) using mFV and mLS filters (n = 11020 test events from 315 males) and sine song starts (SS) using the Dis filter (n = 2476 test events from 315 males). N = no song start. **c**, mFV pulse song start filters and Dis sine song start filters are similar for data from PI or AC males or males paired with AC or SP females; filters from WT males are also plotted. **d**, GLM performance for classifying current song mode (PM = pulse mode, SM = sine mode) using mean mFV and mLS (n = 55464 test events from 315 males). **e**, Filters for sine to pulse (S-P) transitions (top) and the pulse to sine (P-S) transitions (bottom). **f**, GLM performance for identifying S-P transitions (versus continued sine song (S-S)) using mFV and mLS filters (n = 17118 test events from 315 males) and P-S transitions (versus continued pulse song (P-P)) using mFV and fLS filters (n = 11748 test events from 315 males). **b**, **d**, and **f**, error bars (most too small to visualize) indicate 95% confidence intervals (CIs).

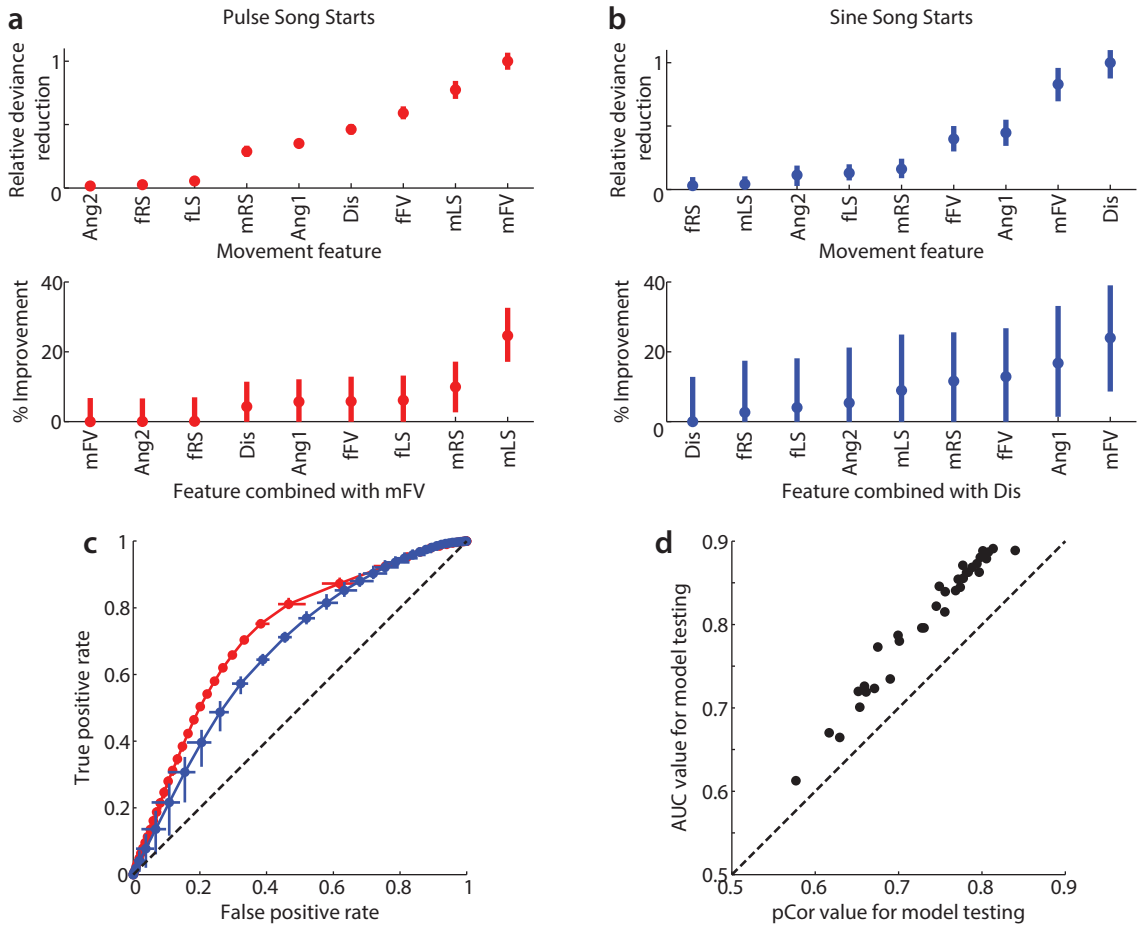

Figure 2.7: Model selection criteria examples and comparison of model performance statistics. **a**, Top: first, we train nine separate GLMs, each based on a single feature, followed by cross-validation on two thirds of the data, with 1000 repetitions. The single feature which gives the greatest reduction in deviance is chosen—here mFV for the detection of song bouts that start in pulse mode. Bottom: a second feature is included in the model if the additional reduction in deviance improves the model by a minimum of 10%—here mLS. **b**, Top: as in **a** but for song bouts that start in sine mode. Dis is selected as the most predictive feature. Bottom: as in **a**, but no second feature results in a significant model improvement, so only the one feature model is used. **c**, Receiver operating characteristic curves for GLM models designed to identify pulse (red) and sine (blue) song starts. Integrating the area under the curve (AUC) shows that both models perform significantly better than chance, for which AUC would be 0.5. AUC = 0.72 (for the pulse starts model) and 0.62 (for the sine starts model). **d**, Comparison between the pCor and AUC values for every model presented in this study, showing a high correlation between the two measures—$r^2 = 0.98$. For every model tested, the pCor value is a more conservative measure of performance. **a-c**, Error bars indicate 95% confidence intervals, although some are too small to visualize.

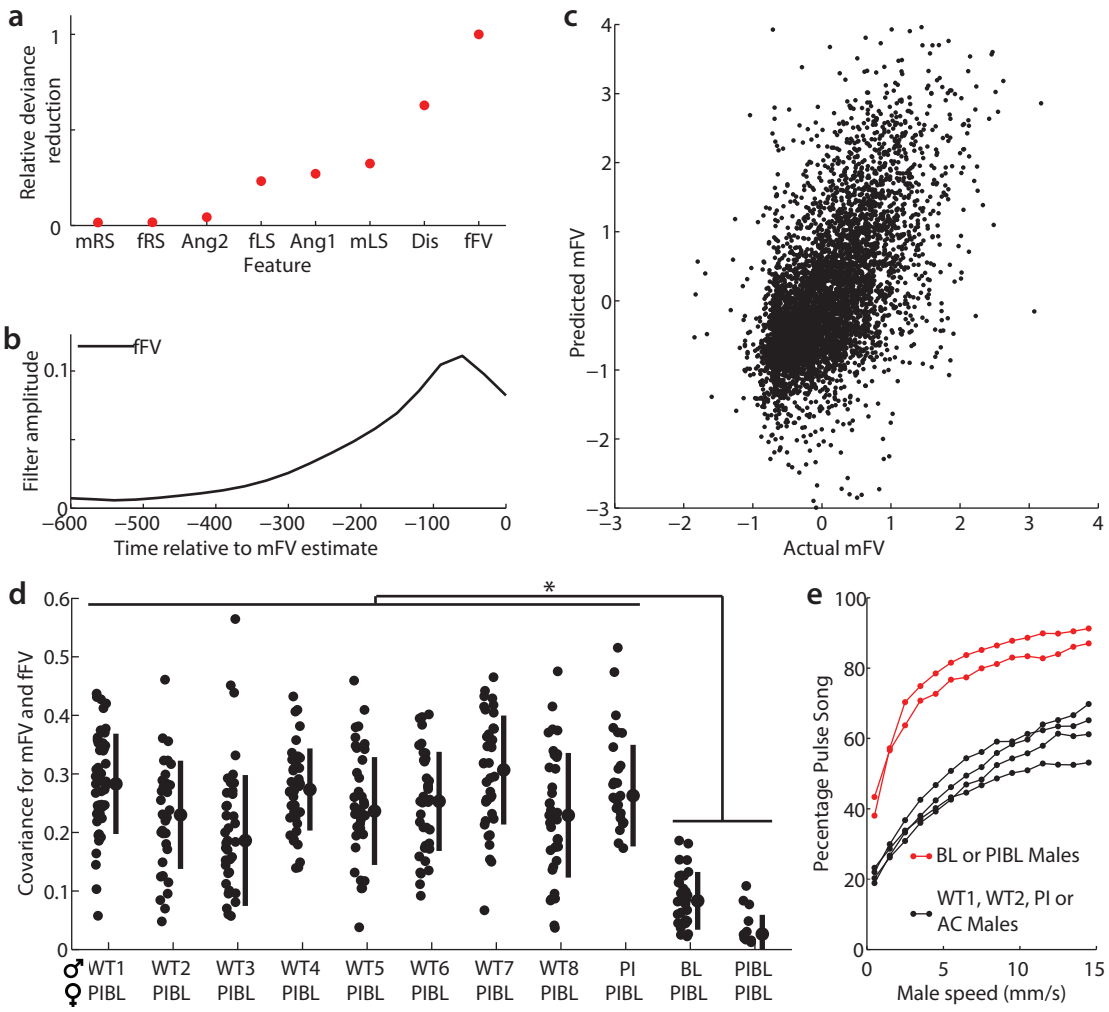

Figure 2.8: fFV changes predict mFV changes in WT and PI males, but not BL or PIBL males. a, Relative deviance reduction for GLMs, one for each movement feature, to predict mFV at timepoints during song. fFV (female forward velocity) is the optimal predictor. Error bars indicate 95% confidence intervals, although some are too small to visualize. **b**, The fFV linear filter is most predictive of mFV values at a lag of $\sim 60ms$. **c**, GLM performance for predicting mFV based only on mean fFV (n = 58,1814 test events from 315 pairs, $r^2 = 0.39$). Values of mFV and fFV were normalized such that mean is 0 and standard deviation is 1 (see Methods). 1% of the data is plotted here for illustrative purposes. **d**, As an estimate of the time males spent following females, we measured the maximum cross-covariance (normalized by the auto-covariance) between male and female forward velocities, n = 11-48 males for each strain. Perfect following behavior, over the entire trial, would produce a value of 1. We tested all following delays between 0 and 300ms. BL and PIBL, but not PI, males show significantly reduced following compared with all other WT strains, * = $p < 0.05$. Individual points, mean, and s.d. are given for each strain/genotype. **e**, The two blind male genotypes (BL and PIBL, red) sing a higher percentage of pulse song at all male speeds (binned to nearest mm/s) compared with WT males or males with other sensory manipulations (WT1, WT2, PI, and AC, black). In all cases, females were PIBL. Speeds $> 15mm/s$ were excluded due to sparsity of data. For each point, n = 1,208-1,5736 samples.

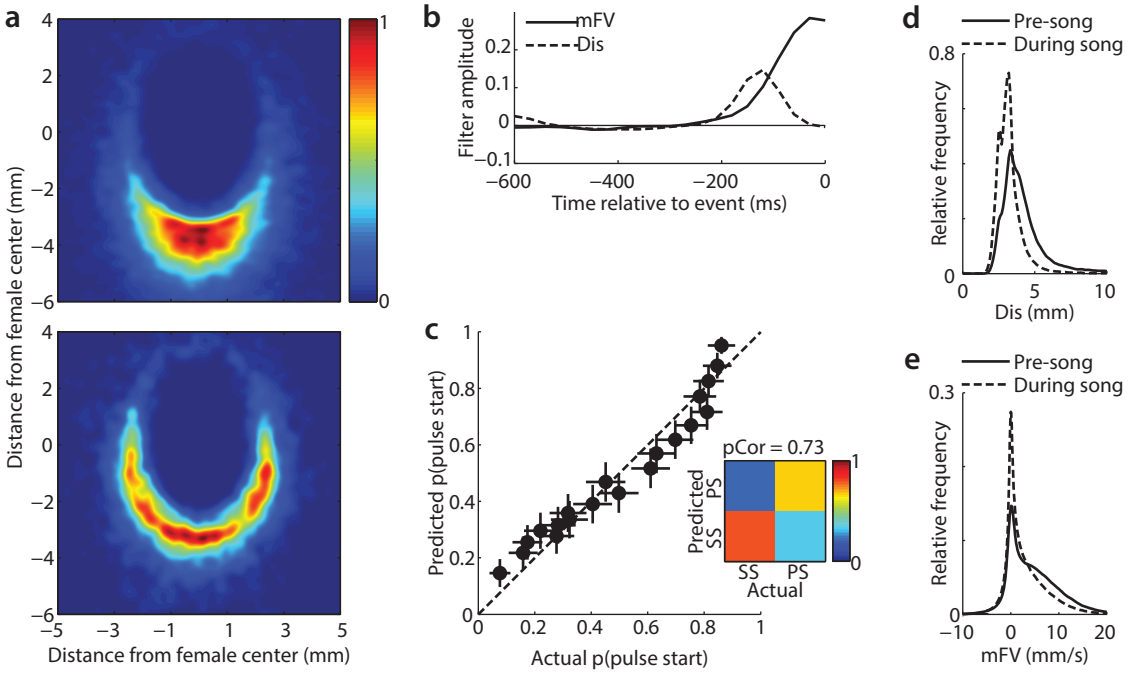

Figure 2.9: Relationships between male-female distance, male velocity, and song bout starts. **a,** A 2-dimensional normalized kernel density estimate of the male center relative to the female center (0,0) at the time of song bout initiation using combined data from all wild type males. Males are positioned further from the female when they start a song bout in pulse mode (top, n = 27,820 bouts from 315 males) versus sine mode (bottom, n = 5,749 bouts from 315 males). **b**, Linear filters for mFV and Dis, the most predictive features for the song start mode classification GLM (predicting sine song starts (SS) versus pulse song starts (PS)). **c**, GLM performance for classifying song start mode with mFV and Dis filters (pCor = 0.73, n = 3,904 test events from 315 males). Error bars indicate 95% confidence intervals. **d**, Relative frequency distribution of Dis for periods 150ms prior to the start of song bouts (solid) and during song (dashed), $n \geq 201,414$ time points from 315 males. The variance in Dis is larger, by 229%, for time points before song. **e**, As in **d**, but for mFV. The variance increase in mFV for time points prior to song is 58% - much smaller than the increase observed with Dis.

females (Figure 2.10a). A model designed to distinguish song bouts beginning in sine versus pulse mode retains mFV and Dis as the most predictive features, but with significantly increased performance (Figure 2.9b-c). Therefore, we focus hereafter on song patterning decisions, rather than the males decision to sing versus perform another courtship behavior. Here, a decision refers to a behavioral choice biased by sensory information [57].

During song bouts, males typically alternate between sine and pulse modes, with each mode lasting 10s to 100s of milliseconds. Can the GLM also predict the current mode of song within bouts? Model performance was optimal using only two features: mFV and mLS

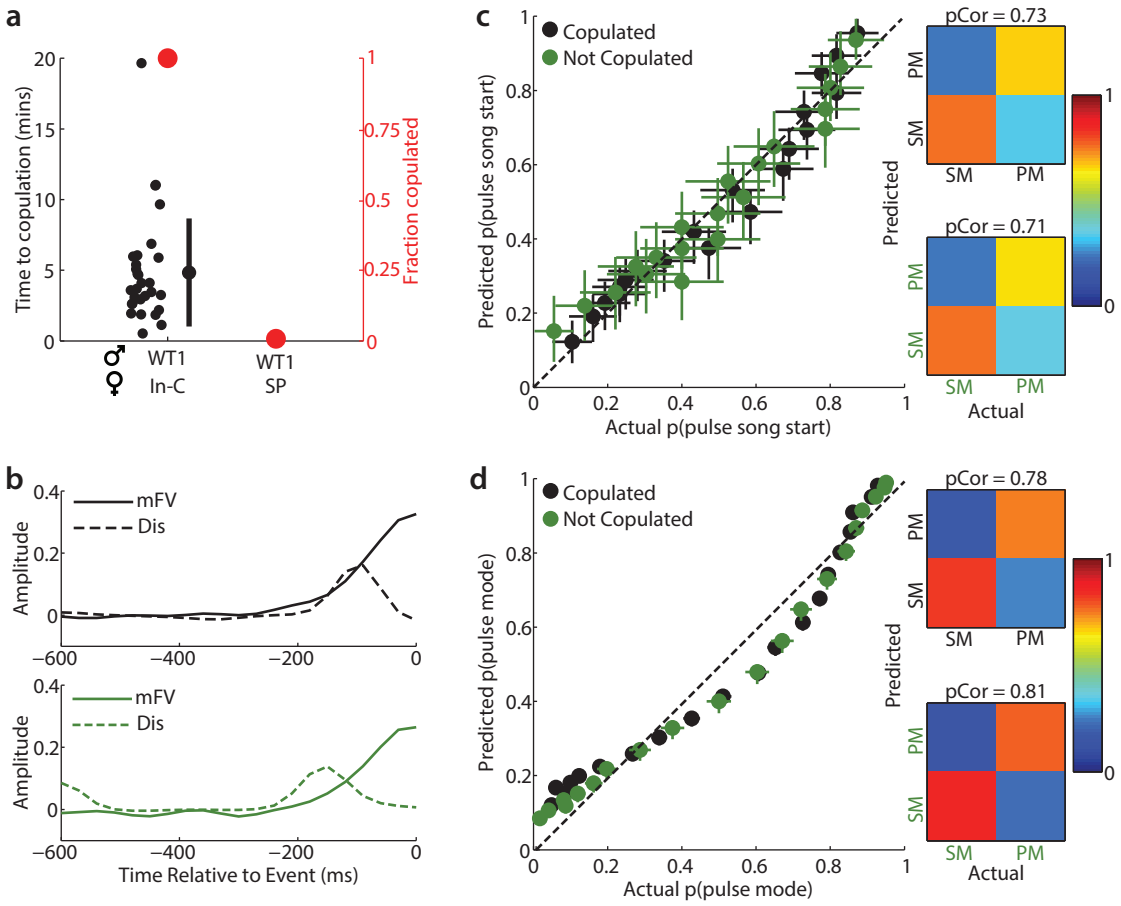

Figure 2.10: Failed copulations do not result from differences in song patterning decisions. **a**, Time to copulation (black) and fraction of copulating pairs (red) for sex peptide injected (SP) and control peptide injected (In-C) females paired with WT1 males (n = 28-30 males for each). Individual points, mean, and s.d. are given for In-C females (no SP females copulated). **b**, mFV (solid) and Dis (dashed) linear filters for song start classification (predicting songs that start in pulse mode versus sine mode). The GLM is based on data from either wild type flies that copulated (top, black) or did not copulate (bottom, green). **c**, GLM performance for classifying song starts with mFV and Dis filters for wild type flies that copulated (black, pCor = 0.72, n = 2,490 test events from 278 males) or did not copulate (green, pCor = 0.71, n = 1458 test events from 37 males). **d**, GLM performance for classifying current song mode (based on mean mFV and mLS) for wild type flies that copulated (black, pCor = 0.78, n = 36,094 test events from 278 males) or did not copulate (green, pCor = 0.81, n = 17,666 test events from 37 males). **c-d** Error bars indicate 95% confidence intervals, although some are too small to visualize.

(a 58% improvement over the null model; Figure 2.6d). The absence of Dis in this model is likely due to its reduced variance during song (Figure 2.9d-e). Using different, male-centric features only decreased model performance (Figure 2.11). We then went on to predict all mode transitions within a bout: increases in mFV and mLS predict transitions to pulse mode, while decreases in mFV and increases in fLS predict transitions to sine mode (Figure 2.6e). Mode transitions represent a subtle change in behavior (e.g., whether 300ms of pulse song is followed by 30ms of sine song or 30ms of continued pulse song); nonetheless, our model predictions produced a combined pCor of 0.64 (Figure 2.6f). Thus, taking into account male motion and inter-fly distance can largely explain variability in song patterning. While studies in birds have shown that auditory cues, either produced by the singer itself [58] or by a duetting partner [59], impact acoustic sequence generation, to the best of our knowledge, ours is the first demonstration of a role for non-auditory sensory inputs in dynamically patterning the structure of individual song sequences.

2.2.3 Identifying the sensory cues responsible for song patterning

Which sensory pathways mediate the males decision-making during song production? While male motion is the primary contributor to song patterning in our models, we observed a strong correlation ($r^2 = 0.95$) during song bouts between Dis (beyond the tactile range of $\sim 5mm$; the tail of the distribution in Figure 2.9d) and the pulse/sine ratio (Figure 2.12a; correlation is independent of male movement). We conclude that flies use vision to measure distance over this range, because blind males or WT males placed in the dark, sing significantly more pulse song (Figure 2.12b-c); this is not true for any other sensory deficit and cannot be explained by changes in male speed (Figure 2.8e).

Previous studies have demonstrated that separate neurons control pulse and sine song production [60, 61] indicating that male locomotion and song patterning are not mechanically coupled. In support of this, males sing both song modes at all velocities (Figure 2.13a). We further conclude that visual measurements of optic flow are not used to convey male motion

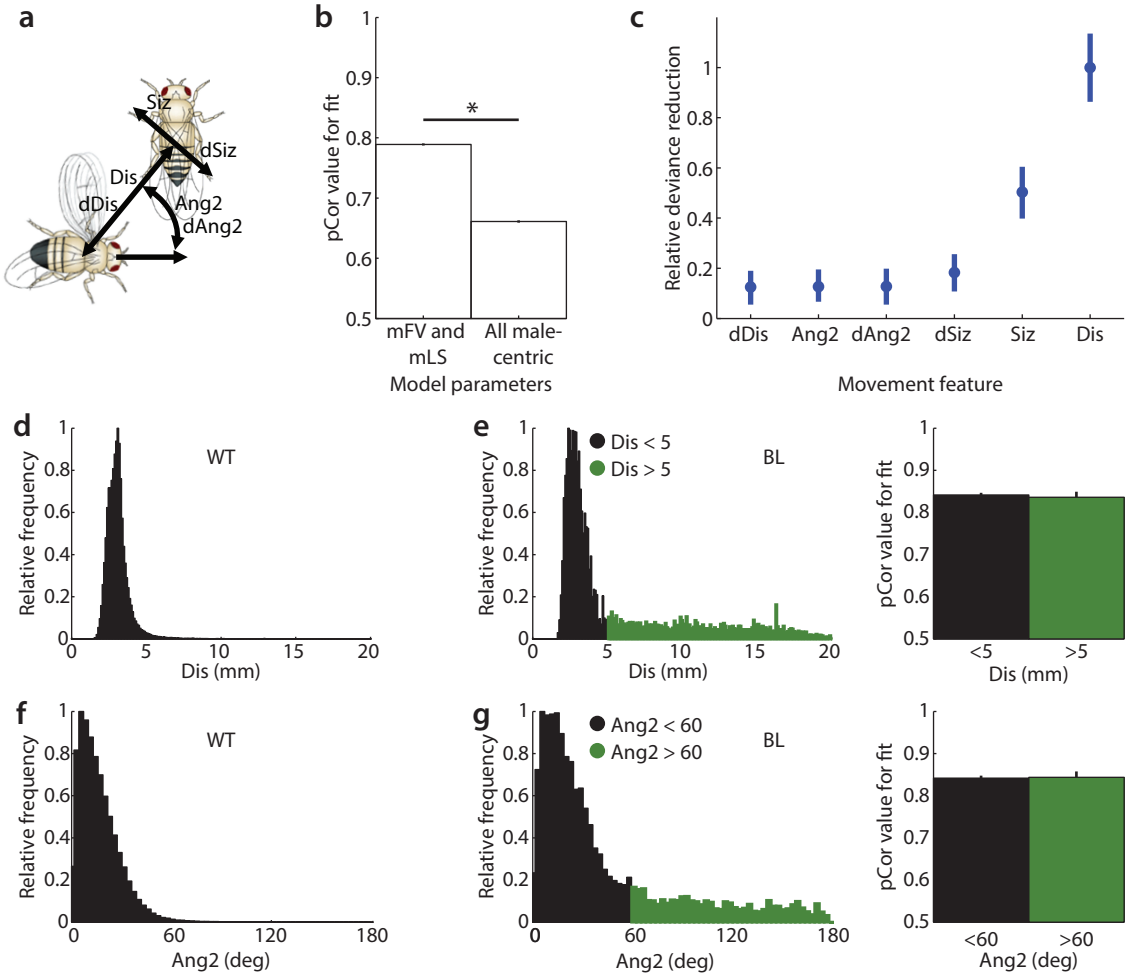

Figure 2.11: Male velocity consistently predicts the current mode of song. **a**, Male-centric features used to examine model performance. Dis and Ang2 are the same as described in Figure 2.1a. Siz represents a projection of the females body axis onto a plane perpendicular to a line joining the two fly centers. Thus, when Siz = 0 or 1, the female occupies a minimal or maximal region of the males visual space respectively. dDis, dAng2, and dSiz represent the rate of change of Dis, Ang2 and, Siz. **b**, Comparison of models to classify current song mode based on only mFV and mLS versus all 6 male-centric features combined (* = $p < 0.001$). Models were tested using the same dataset (n = 55,464 test events from 315 males). **c**, Deviance reduction statistics for models predicting song bouts starting in sine mode, using only male-centric features as inputs. Dis remains the most important feature (compare with Figure 2.6). **d**, The distribution of Dis during song for WT males (n = 338,238 time points from 315 males). **e**, (left) The distribution of Dis during song for BL males (n = 10,802 time points from 33 males) is broader than for WT. However, model performance (right) for GLMs using mFV and mLS to classify current song mode remains high for song samples produced at $< 5mm$ (black, n = 2074 test events) or $> 5mm$ (green, n = 650 test events) from 33 males. **f**, As in **d**, but for Ang2 rather than Dis. **g**, As in **e**, but for Ang2 rather than Dis and splitting the data for Ang2 < 60deg (black, n = 2,258 test events) or $> 60deg$ (green, n = 534 test events). **b-c**, **e**, and **g**, Error bars indicate 95% confidence intervals, although some are too small to visualize.

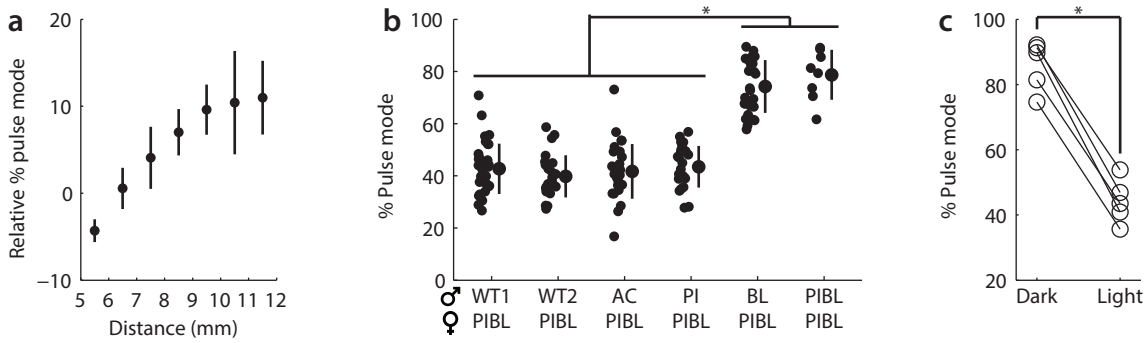

Figure 2.12: Flies perform distance-based modulations of song structure using vision. **a**, Percentage of song in pulse mode (mean and s.d.) increases with inter-fly distance ($r^2 = 0.95$; see Methods). **b**, Pulse song percentage increase in blind males (n = 11-48 flies, * = $p < 0.001$). Individual points, mean, and s.d. are shown for each group. **c**, Individual WT2 males (paired with PIBL females) produce more pulse song in dark versus light (n = 5 flies, * = $p < 0.0001$).

signals to song patterning networks, because a model based on only mFV and mLS predicts current song mode for blind males (Figure 2.13b). This left two likely possibilities (Figure 2.13c): either 1) a cue from the female induces males to change speed and concomitantly affects song patterning or 2) neural circuits that carry information about male motion (via either a copy of the motor commands or proprioceptive feedback from the legs) modulate song patterning circuits. Because fFV predicts male motion (Figure 2.8a-c), song patterning would ultimately be dependent on sensory cues for both mechanisms.

To distinguish between these mechanisms, we abrogated the link between female cues and male motion. mLS and mFV still predicted current song mode when males are pheromone-insensitive and/or blind (Figure 2.13b). Given that blind males do not follow females (Figure 2.8d), and produce song over a wide range of inter-fly distances/orientations (Figure 2.11d-g), it seems unlikely that a non-visual, long-range cue from the female patterns song in these males. Further, model performance remains high when females provide no motion cues (Figure 2.13d) and (Figure 2.14). Finally, we examined the link between male motion and song patterning without a female present. We artificially activated song and targeted three neural subsets (see Methods). For all genotypes, levels of inter-bout variability were similar to WT levels despite constitutive thermal activation (Figure 2.13e). Again, mLS and mFV predicted current song mode (Figure 2.13f), within the performance range for WT strains

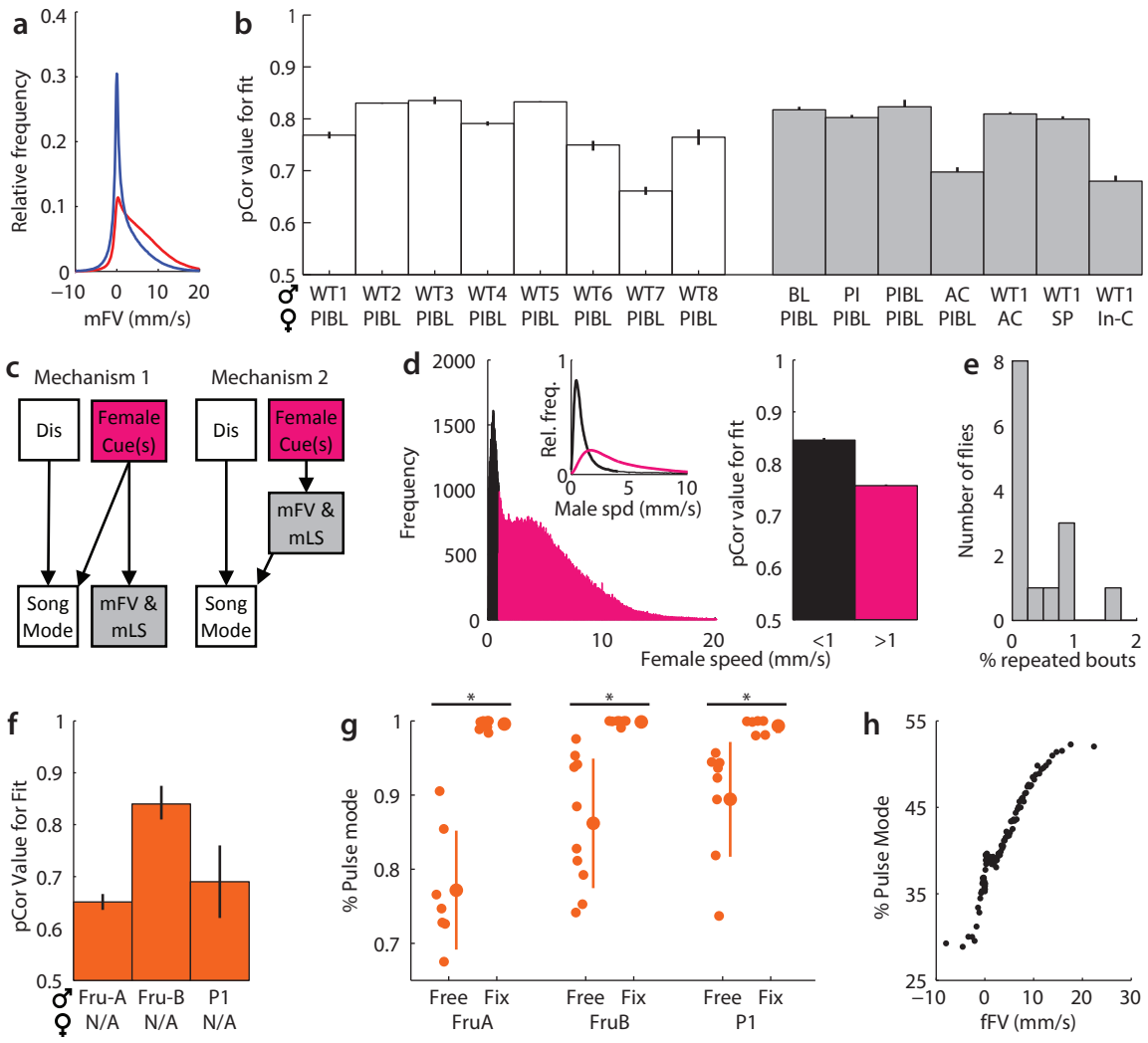

Figure 2.13: A neural link between locomotor and song-patterning circuits. **a**, Normalized event frequency for pulse/sine song (red/blue, n = 570,225/952,541 from 315 males) at each mFV, across all WT strains. **b**, pCor values from classifying current song mode (using mean mFV and mLS) for WT strains (white bars) and various sensory manipulations (n = 924-16,256 test events from 11-48 flies for each model). **c**, Two potential neural circuit mechanisms underlying the correlation between male motion and song. (left) Female cue(s) directly modulate both song patterning and locomotor circuits or (right) circuits carrying information about male motion modulate song patterning circuits. **d**, (left) WT data was split into songs produced when females were not moving/moving (black/magenta, n = 9,454/46,204 test events from 315 males; see Methods). (inset) Corresponding male speeds. (right) Corresponding pCor values from classifying current song mode using mean mFV and mLS. **e**, Song variability with TrpA1-activated flies (n = 14 males from 3 genotypes) is similar to WT (Figure 2.1d). **f**, pCor values from classifying current song mode using mean mFV and mLS for Fru-A, Fru-B, and P1 activated males (n = 100-1,987 test events from 7-10 males). **g**, For each genotype, the percentage of pulse song increases (* = $p < 0.01$) when flies are fixed. Individuals, mean, and s.d. are shown. **h**, Correlation between fFV and the percentage of pulse song (n = 16,092 from 315 WT male/PIBL female pairs, binned by percentile) at a 60ms lag ($r^2 = 0.91$). **b**, **d**, and **g**, error bars indicate 95% CI.

(Figure 2.13b). By preventing these males from moving, we observed a dramatic reduction in sine song (Figure 2.13g); because this song mode is typically produced at lower male speeds, our results suggest that a copy of the locomotor commands (presumably still active in fixed males) is more likely (than proprioceptive feedback) to pattern song. Thus, our data support the conclusion that activity in locomotor circuits influences song patterning, favoring Mechanism 2 (Figure 2.13c). Consistent with this, we observed the strongest correlation (r^2 = 0.91) between fFV and the pulse/sine ratio in WT flies at the delay at which males follow females (Figure 2.13h and Figure 2.13b).

As a final test of the importance of sensory cues in song patterning, we considered song bout terminations. The exponential distribution of syllable durations in songbirds has been proposed to support a stochastic mechanism for syllable termination [62]. Bout durations in *Drosophila* are also well fit by an exponential function (r^2 = 0.98; Figure 2.3b). However, we identified fLS as a significant predictor of bout ends (Figure 2.15e-f). We posit that when males sense changes in fLS they either transition to sine song (Figure 2.6e-f), or they end song altogether.

2.2.4 Both song modes influence female behavior

Based on the data presented, we propose that, for *Drosophila*, detection of a female [63] gates the song production. Once gated, sensory cues act directly (Dis and fLS) or indirectly (via mFV and mLS) to pattern song on short timescales (Figure 2.15c). While trial-to-trial variability in acoustic signals may be useful for song learning in birds [64], *Drosophila* males do not learn their songs. What then is the role of patterning decisions in fly mating behaviors? Because female speed decreases prior to copulation (Figure 2.15d), we reasoned that female slowing was a sign of receptivity. Indeed, using the GLM framework, we found a negative correlation between the amount of either song mode, in a given time window, and female speed (Figure 2.15e). This relationship was reduced for deaf females, while unreceptive (SP) females showed a positive correlation between speed and song amount, a reversal

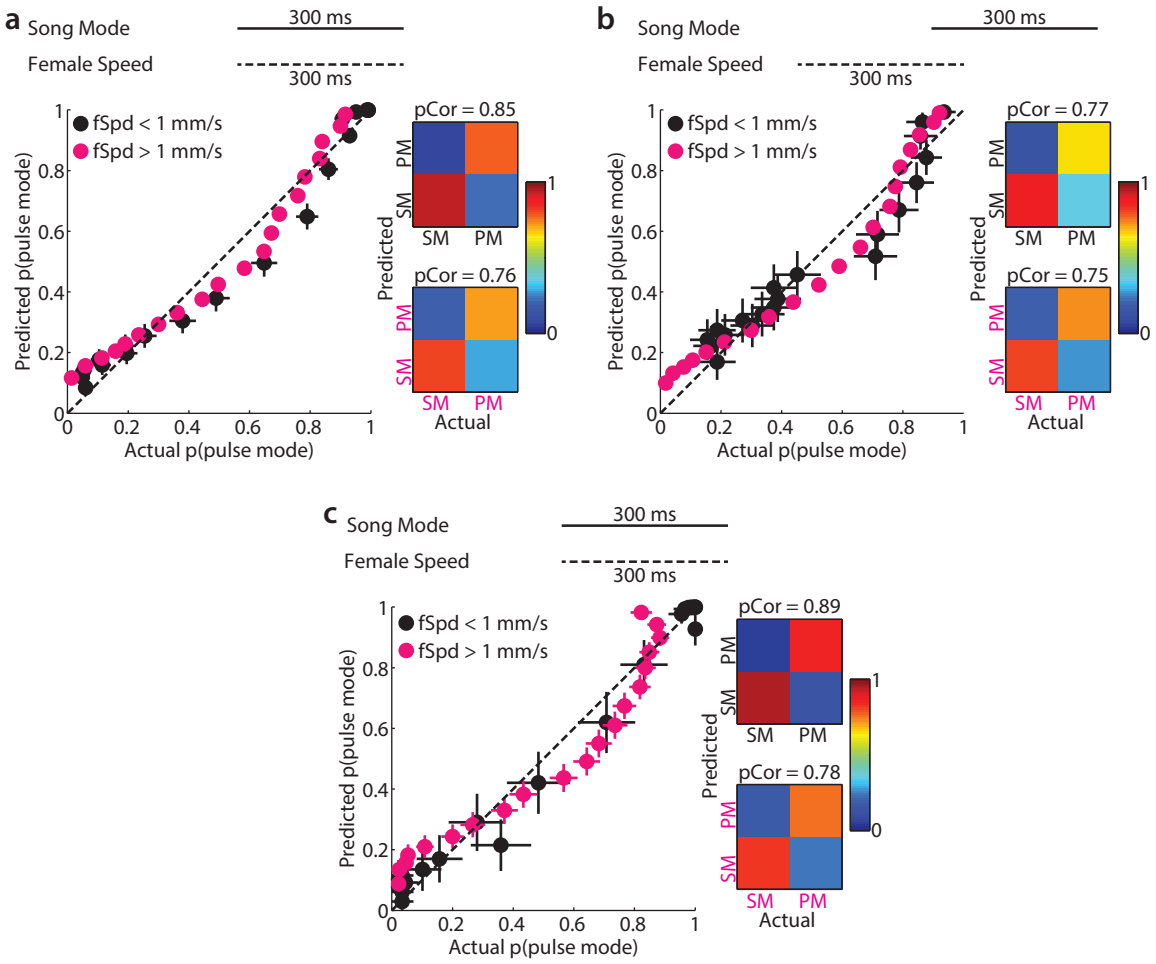

Figure 2.14: Error bars in all plots indicate 95% confidence intervals, although some are too small to visualize. **a**, GLM performance for classifying current song mode (based on mean mFV and mLS) for wild type flies. The dataset was divided into samples for which the female was effectively stationary during the song sample (black, pCor = 0.85, n = 9,454 test events from 315 males), and those where she was moving (magenta, pCor = 0.76, n = 46,204 test events from 315 males). Model performance remains high even without any motion cues from the female. **b**, As in **a**, but the dataset is divided according to a shifted estimate of female speed 240ms prior to the song sample. This matches the most predictive region of the female BTA (Figure 2.4). Model performance remains high whether the female is stationary (black, pCor = 0.77, n = 3,110 test events from 315 males), or moving (magenta, pCor = 0.75, n = 44,314 test events from 315 males) 240ms prior to the song sample. **c**, As in **a**, but using data from PI males. Male velocity remains a successful predictor even when males cannot detect pheromones and when the female is stationary (black, pCor = 0.89, n = 1,788 test events from 25 males) or moving (magenta, pCor = 0.78, n = 9,018 test events from 25 males) during the song sample. .

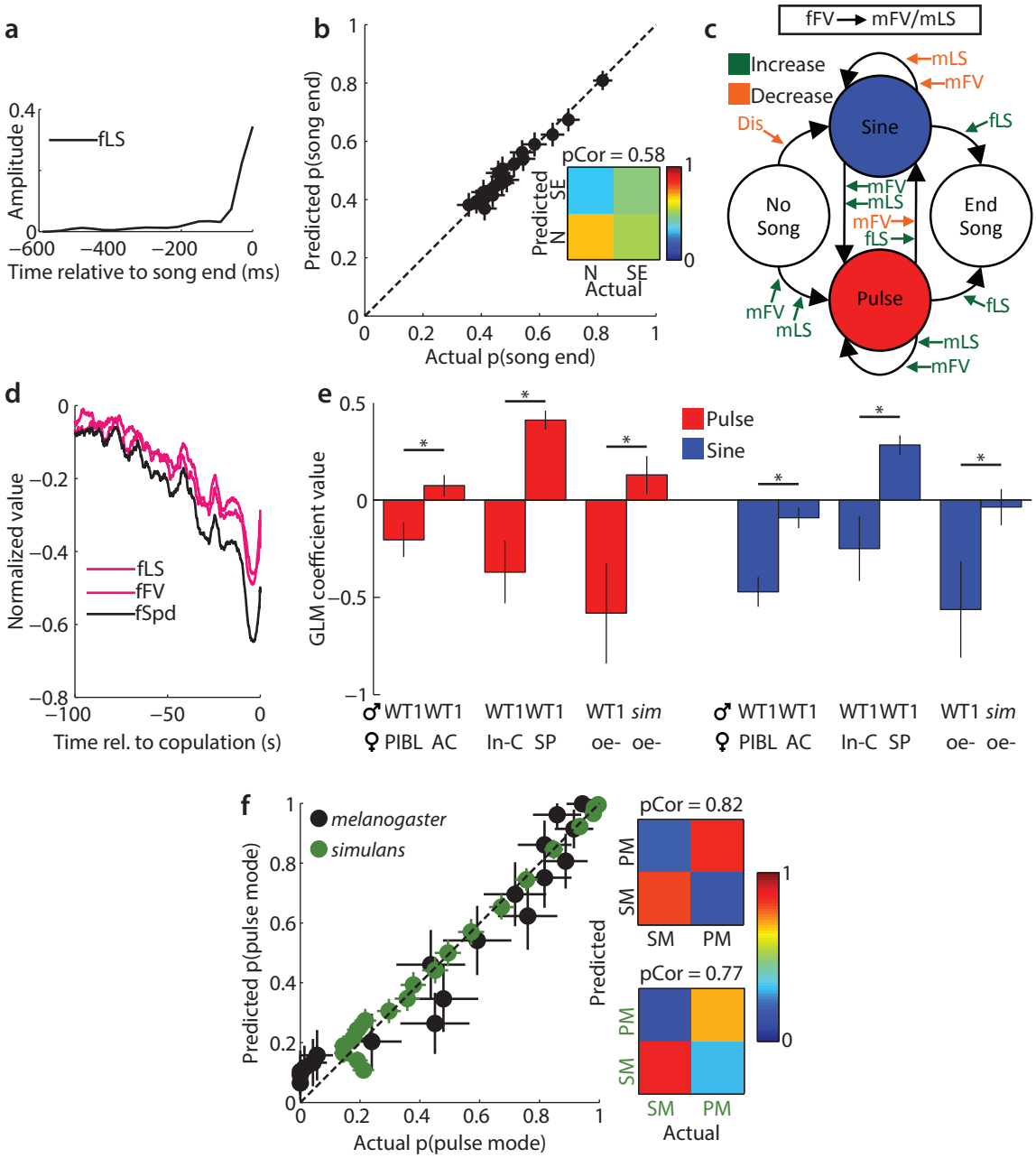

Figure 2.15: Song patterning decisions and female responses. **a**, Filter from GLM for song ends (SE). **b**, GLM performance for identifying SE using fLS (n = 10708 events from 315 males). N = no song end. **c**, Summary of the influence of sensory inputs on song patterning, as revealed by GLM analysis. **d**, Normalized changes in female motion prior to copulation (n = 233 flies). **e**, GLM coefficient values between pulse or sine song density and female speed (* = $p < 0.01$, n = 40-1429 samples from 7-38 pairs; see Methods). **f**, GLM performance for classifying current song mode using mean mFV and mLS for WT2/sim (black/green, n = 1,424/9,854 test events from 31/40 flies) males paired with oe- females. **b**, **e**, and **f** error bars are 95% CI.

of WT behavior. In addition, females increased or decreased speed in response to song from *Drosophila simulans* (heterospecific) or WT1 (conspecific) males, respectively. This is particularly striking when considering that, for the same experiment, male motion predicts song mode choice for both simulans and melanogaster males (Figure 2.15f). Therefore, male song patterning choices are unlikely to be used by females for mate selection. Indeed, successful males (those that copulated within 30min) and unsuccessful males pattern song similarly (Figure 2.10b-d). We hypothesize that males bias toward their louder form of song (pulse) when far from the female (captured by the Dis feature) or when trying to catch up to, or locate, the female (captured by the mFV and mLS features); this would maximize the probability of the female hearing his song and decreasing her locomotion. It remains to be determined, however, over what specific distances and angles, females can detect each song mode (and amplitude modulations therein).

2.3 Discussion

Instinctive behaviors, like acoustic signal production, have been generally considered to comprise a series of fixed action patterns, elicited and oriented by sensory information [65]. Courtship song production in *Drosophila* has long been regarded as an example of such a fixed action sequence [44, 45], with the female serving as the trigger stimulus. In contrast to this view, we show that even the simple fly utilizes sensory information to pattern his song sequences over short timescales. These data therefore offer a new window into the study of instinctive behaviors, and suggest that song production in flies may be more analogous to complex motor behaviors, such as prey capture, known to rely heavily on sensory feedback for patterning. More broadly, and consistent with recent studies of fly flight and human mobility [66, 67], we suspect that seemingly stochastic behaviors may be more predictable than expected.

2.4 Methods

2.4.1 Fly strains and rearing

For all experiments we used 3-7 day old virgin flies. All flies were raised in density-controlled bottles seeded with 8 males and 8 females for 4 days. Bottles were kept at 25C and 60% relative humidity. Virgined flies were then housed individually and kept in behavioral incubators (TriKinetics) under 12hr/12hr light/dark cycling. Male flies were painted with a small spot of opaque ultraviolet-cured glue (Norland Electronic Adhesives) on the dorsal mesothorax to facilitate identification during tracking. All wild-type strains, except for the laboratory colony Canton-S (WT2), were supplied by the Andolfatto group at Princeton University. These strains descended from single females caught in geographically diverse locations (Table 2.1). For several experiments, we used genetically modified flies. All genetic mutations were recombined into the Canton-S genetic background; their genotypes are:

PIBL (pheromone-insensitive and blind): *w+/w+; GMR-hid/+; orco-/ orco-*

oe- (oenocyte-less and PIBL): *GMR-hid/+; PromE800-Gal4, Tub-Gal80ts/UAS-hid,UAS-stringerll; orco-/orco-*

PI (pheromone-insensitive): *w+/w+; ; orco-/ orco-*

BL (blind): *w+/w+; GMR-hid/GMR-hid*

Fru-A (TrpA1 expressed in all fruitless-positive neurons): *UAS-TrpA1/sco; fruP1-GAL4/TM6B*

Fru-B (TrpA1 expressed in mostly brain-specific fruitless-positive neurons): *tsh-Gal80/UAS-TrpA1; fruP1-GAL4/TM6B*

P1 (TrpA1 expressed in P1 song command neurons): *NP2631/UAS-frtstopfrt-TrpA1; fru P1-FLP/TM6B*

We acquired *GMR-hid* flies from the Bloomington Stock Center, *PromE800-Gal4, Tub-Gal80ts; UAS-hid, UAS-stingerII* flies from Joel Levine, *orco-* flies from Leslie Vosshall, *fru P1-GAL4* and *fru P1-FLP* from Barry Dickson, and NP2631 from the Kyoto stock center.

For arista- and wing- cutting paradigms (AC and WC), to render flies deaf (AC) or mute (WC), WT1 flies were anesthetized with CO^2, and aristae or wings were removed, with fine forceps, >20 hours prior to recording. *Drosophila melanogaster* sex peptide [56] or a control peptide (SIFamide [68]) were injected into PIBL virgin females 12-24 hours prior to recording. These flies were anesthetized on ice during injections.

2.4.2 Recording apparatus

The recording chamber (Figure 2.1a) is octagonal and covered in a layer of copper mesh; the chamber itself was milled from white delrin by Schmit Prototypes (Menomonie, WI). The floor is sloped at an angle such that the effective chamber diameter is 25mm ($\sim$ 10 fly body lengths); this is large enough to permit a range of fly motions and interactions. Using sloped chamber sides facilitates fly tracking [69]. The lid was made from clear plexiglass. The floor of the chamber is tiled with 9 NR23158 microphones (Knowles Electronics) to capture male song throughout the chamber. Each microphone connects to a custom-built amplifier [70]. The open areas around the microphones increase signal-to-noise ratio. The entire chamber is enclosed inside an acrylic box with a door for loading flies and placed on an air table to minimize microphone noise. The camera for recording fly movement, a Unibrain 540c with a Fujinon HF16HA-1B lens, was suspended above the acrylic box, and a DigiSlave L-Ring 3200 LED light was used to illuminate the behavioral chamber. Room lighting was off during all recordings.

2.4.3 Courtship assay

Before the first recording of each day, the chamber was prepared in two steps. First, the underside of the cover glass was rinsed and coated with Sigmacote (Sigma-Aldrich) to prevent flies from walking on the chamber ceiling. Second, to odorize the environment, >4 flies (strain WT2) were placed inside the chamber for 10 minutes. Flies were loaded individually into the chamber using a custom-built aspirator. To optimize for peak fly activity, we began

recordings within 150 minutes of the behavioral incubator lights switching on. Recordings were terminated when copulation occurred or after 30 minutes (classified as no copulation). Recordings with no song in the first 5 minutes (excepting the WC paradigm) were terminated early and disregarded. Data from flies that moved $<$ 1.5mm per minute, or sang at low amplitudes relative to other flies of the same strain, were excluded on the basis of possible poor health (this criteria applied to 25 males).

2.4.4 Dark/Light transition assay

For acute transitions between dark/light conditions (see Figure 2.12c), the chamber was covered completely with BK5 Blackout Fabric (Thor Labs), and flies were loaded in darkness using a Spot 90-Lumen LED headlamp (Black Diamond) on the red light setting. After 10 minutes of courtship in the dark, the LED L-Ring light was switched on. If flies copulated in the dark then the trial was disregarded.

2.4.5 Thermogenetic activation experiments

For thermogenetic activation of Fru-A, Fru-B, and P1 neurons in males (no female in the chamber), the chamber was heated with a coil (HSTAT, BriskHeat) to 25C (for FruA activation), 27C (for FruB activation), and 32C (for P1 activation). In the Fix condition, each flys legs were fixed in place with UV-curable glue. Songs from these males were segmented as described above, except that the criteria for bout, pulse, and sine identification were relaxed to account for small differences between heat-activated and naturally produced song (e.g., increased variability in inter-pulse interval). Song from both freely moving and fixed flies were analyzed with the same modified criteria.

2.4.6 Data processing and analysis

All data processing and analysis was conducted in MATLAB (MathWorks, Inc.).

Significance Testing

Unless otherwise specified in the text, significance tests were as follows: To determine significant differences between means, we used one-way ANOVA or KruskalWallis analyses, depending on whether the distributions in question were non-normal (as identified by the Jarque-Bera test for normality). For confidence intervals, both for model selection and in Figure 2.15e, non-overlap was used as a conservative estimate of significant differences. For normally distributed data, variance was estimated to be similar between groups, as required for applying ANOVA. Given variability in behavior, we sampled a large number of flies for each wild type strain ($\sim$ 40) before performing any statistical tests. After observing the effect size in wild type data, we then collected between 5 and 40 flies (depending on the analysis) for other genotypes and manipulations. Blinding was not necessary for these experiments because all data analyses were automated. As all statistical tests were performed between different fly strains (with the exception of Fig. Figure 2.12c, for which there is an internal control), randomization of animal groups was not necessary.

Fly tracking and song segmentation

Fly positional tracking was achieved by optimizing (for flies) an algorithm originally developed for tracking bacteria [14]. Tracking errors occurred at a low rate ($\sim$ 1 switch in fly identity or orientation every 25 or 12 minutes respectively) and were corrected manually using custom software. We performed song segmentation using automated software [70]. We combined segmentation results from the 9 microphones into a single song with false positive and negative rates similar to those reported in 5. Audio (10KHz) and video (30Hz) sampling frequencies were synchronized using a Master 8 (A.M.P.I.), to simultaneously drive an LED and buzzer.

Quantification of movement parameters

Males can approach the female from either side during courtship. As a result, distinctions between left/right lateral movement and anticlockwise/clockwise rotations or angles are not meaningful for the analyses we performed. For this reason, only forward velocities were allowed to take negative vales and we use absolute values for lateral movements and rotations. It should be noted that the relative contributions of forward and lateral movements to song patterning could be better established with a faster video frame rate.

Quantifying the percentage of repeated bouts

Bouts were down-sampled to 50Hz (from 10KHz). This temporal resolution was chosen to match the pulse rate in fly song; events on this timescale are likely to have ethological significance. Mixed bouts (containing both sine and pulse trains) were converted into strings of ones (sine) and zeros (pulses) at the 50Hz sampling rate. For males singing more than 100 mixed bouts of song, we calculated the number of repeated bouts to be: 1 - (number of unique binary strings/total number of binary strings). Therefore, a Percentage of Repeated Bouts of zero for a fly indicates that no two mixed bouts produced by this fly had the same pulse/sine patterning, when sampled at 50Hz.

Analyzing song statistics

For Figure 2.3a-k, only mixed bouts (those containing both sine and pulse elements) were included in analyses. Empirical joint probability density functions (PDFs) were calculated by binning data in 2 dimensions. Independent PDFs were calculated as the outer product of the empirical marginal PDFs. For bout durations (Figure 2.3e-f), only bouts shorter than 2s were included in PDF estimation due to the sparsity of the matrix beyond this cutoff. The kernel density estimates seen in Figure 2.3l were calculated using the ksdensity function in MATLAB.

Bout Triggered Averages (BTAs)

Given the difference between audio/video sampling rates, we resampled relevant sections of our tracking data, keeping the sampling rate the same (30Hz) but aligning motion samples with song bout onset. For each movement parameter, we subtracted the mean between 3s and 2.5s prior to song initiation; subtracting the mean of the entire courtship session (many minutes) instead artificially increased variability, as some flies had long periods of quiescence when not singing. Mean-subtracted trials were aligned and averaged to calculate BTAs and corresponding SEM shown in Figure 2.4l.

GLM implementation

For all models, data were first split into groups hereafter termed fitting data (66%) and testing data (34%). We fit all models using the method described in [49], which uses a sparseness prior to penalize redundant features. When fitting or testing models over 1000 iterations, data were randomly subsampled each time to equalize the frequency of each event type (a common method for dealing with uneven event frequencies). For models where we sought to determine the predictive power of a model based on mLV and mFV, rather than identify the most predictive feature, model selection was not performed. If a model combined data from multiple fly strains, we first z-scored movement features for each strain before running the model to account for any genetic differences in behavior.

Model selection

The fitting procedure for the binomial GLM takes as inputs features (stimulus histories for movement parameters) and binary events associated with each feature (e.g., no song start versus song start, encoded as 0 and 1). All stimulus histories are convolved with a linear filter yielding a linear prediction. The filter represents the weight for time points prior to each event; positive/negative deviations in the filter indicate that an increase/decrease in the stimulus is predictive of event type 1/0. The linear prediction is then transformed to

the predicted event probability using a logistic function. We first fit separate models for each movement feature, repeating each fit 1000 times (the data were split evenly for fitting and cross-validation) to calculate 95% confidence intervals for the deviance reduction (for example, see Figure 2.7). If the deviance reduction for a single feature was greater than zero, we then re-ran models with paired inputs (e.g. mFV and mLV), to determine if adding a second feature improved model performance. We continued to add features until the relative improvement from an additional feature was not significantly greater than 10%.

Model performance

We convolved each of the 1000 filters generated during fitting iterations with the testing data; the convolved data were then passed through a non-linear logistic function to calculate a probability score for each stimulus history predicting event 1 versus event 0 (see Figure 2.5). For each test, pCor values were calculated by comparing the actual outcome (whether events were type 0 or type 1) with the predicted outcome. A predicted probability >0.5 was counted as an outcome of type 1. Receiver operating characteristic (ROC) curves where generated by varying this 0.5 threshold between 0 and 1 and running the test 1000 times for each threshold to get estimates of the false positive and true positive rates; AUC statistics were then calculated from these generated ROC curves. Performance plots were generated by sorting predictions in ascending order and grouping data using 5% intervals and plotting the mean prediction value against the percentage of type 1 events for each of the 20 groups. These plots serve as a visualization tool.

Song start prediction

GLMs were trained to distinguish song starts (either pulse or sine start) from potential song starts. We considered a stimulus history of 600ms prior to events for all features. For potential song starts (times when the male is not singing), we constrained selected time points to those times when Dis $< 8mm$ and Ang2 $< 60deg$, for the entire 600ms period. We

also only included actual song starts that met these criteria ($\sim 65\%$ of song starts). These winnowing criteria were only used for models presented in Figure 2.6b-d and Figure 2.11c. As well as song start predictions, we also ran a model to classify between sine and pulse starts, given that a song start had occurred; the goal of this analysis was to eliminate noise arising from unidentified behaviors (such as attempted copulation) that prevent song starts. For this, we used the same stimulus histories described above, but only for times when song starts actually occurred and without applying any winnowing criteria (Figure 2.9).

Current song mode prediction

GLMs were trained to distinguish pulse mode from sine mode. We extracted movement features during 600ms of pulse or sine song and considered only the central 300ms (with a 150ms buffer either side) of this time window. This prevented contamination of the data with behaviors related to transitions, song ends, or song starts. Temporal information for this model was not relevant, as the GLM was trained and tested using the mean values of each movement feature within the central 300ms window. Results were not significantly different for models generated using 10 separate time points rather than taking the mean (data not shown). For current song mode models applied to subsets of data the dataset was split prior to the separation of fitting and testing data. To examine model performance when females were effectively stationary, we split the data into samples when female speed was $< 1mm/s$ or $> 1mm/s$ (Figure 2.13f and Figure 2.14). Similarly, to examine model performance or when blind males were at large distances, or facing away from the female, we split the data into samples when Dis was $< 5mm$ or $> 5mm$, or Ang2 was $< 60deg$ or $> 60deg$, respectively (Figure 2.11).

Transition prediction

GLMs were trained to distinguish transitions (pulse-to-sine or sine-to-pulse) from continual song (pulse-to-pulse or sine-to-sine). Due to the fast nature of transitions, we considered

300ms of stimulus history—this represents half the length considered for song starts or song ends. Song was classified as a transition if there was a switch in mode immediately following this 300ms window.

Song end prediction

GLMs were trained to distinguish song bout ends from potential song bout ends. We included all bout ends with at least 600ms of song preceding the bout end. Potential song bout ends were considered to be any 600ms period of song that did not precede the end of a bout.

Male velocity prediction

GLMs were trained to predict male forward velocity values (at time points during male song) using the preceding 600ms of each of the other 8 movement parameters. Due to the analog nature of the output data (male velocities can take a wide range of values), a non-linear logistic function was not applied to the values after convolving with linear filters. As a result, model performance is demonstrated with the comparison of all predicted and actual mFVs (and corresponding r^2 value for the fit), and not with a pCor (Figure 2.8). The r^2 value is, as expected, similar to the covariance value for the most predictive feature with mFV.

Female response to song

Female speed, along with male song data, were extracted using a sliding window of width 1 minute, with 50% overlap. A range of window sizes were tested, but the results were not significantly affected unless windows became smaller than 15s (data not shown), at which point estimates became too noisy. To eliminate female behaviors relating to initial introduction or copulation, time windows within 1 minute of fly introduction and less than 1 minute prior to copulation were not used. A GLM was used to determine if the amount of pulse or sine song within a window predicted the mean female speed within the same window.

Female speed was calculated using only time points within the window $> 300ms$ from any song (sine or pulse), to prevent confounding effects related to male singing decisions. Only windows containing $> 5\%$ (some courtship) or $< 95\%$ (to allow for speed estimates) song were included.

Effect of distance on pulse/sine ratio

To eliminate the effect of velocity on song patterning (discovered in this study), we binned velocities into 1 mm/s windows and analyzed the relationship between inter-fly distance and the pulse/sine ratio of song within each velocity bin (see Figure 2.12a). Due to the rarity of song at significant inter-fly distances, all wild type fly strains were combined in this analysis. For each velocity window, we subtracted the mean pulse/sine ratio for all song at that velocity. Thus, negative values indicate that the pulse/sine ratio at that distance was lower than the overall ratio for that velocity. Ratios were only included if 100 song samples existed for a particular velocity/distance combination; means and standard deviations were calculated using all relative ratios that met these criteria at a particular distance. Distances below 5mm were excluded to eliminate confounding effects of tactile interactions.

Fraction of song in pulse mode

Flies were included in this analysis (see Figure 2.12b-c and Figure 2.13j) only if they sang more than 25 bouts during the courtship period. For acute dark/light transitions (Figure 2.12c), flies were required to sing at least 25 bouts during both dark and light conditions.

Female behavior prior to copulation

Data from all wild type strains courting PIBL females were combined for this analysis (see Figure 2.15d). Only flies that took longer than 3 minutes to copulate were included. The first minute of each recording was eliminated to avoid analyzing behaviors associated with chamber introduction, and we examined only the 100s preceding copulation. Each movement

parameter was normalized by subtracting the mean value during 120-100s period prior to copulation and dividing by the standard deviation within the final 100s. Data were analyzed similarly to the BTAs (see above).

Chapter 3

Neural Mechanisms Underlying Rapid Song Intensity Modulation in *Drosophila*

3.1 Introduction

Acoustic signals play a critical role in social communication throughout the animal kingdom and senders will often alter their positioning or orientation to improve signal transmission [71, 72, 73]. Some organisms (e.g. humans and song birds [74, 75]) are also capable of modulating the amplitude of their signal in accordance with the distance of their target to optimize for receiver intensity and conserve energy. This behavior has never been observed in invertebrates. The closest corollary exists in the field cricket, wherein males produce a secondary courtship song—which is quieter than their calling song—after contact with a female [76]. However, this binary switch in song type is clearly distinct from ongoing amplitude modulation of a single acoustic pattern in response to changes in the receiver distance. That this sensorimotor transformation remains undiscovered in lower organisms may indicate a lack of capacity, but it's also possible that technical challenges inherent to

studying naturalistic acoustic communication have obscured such behaviors. Here, we use our novel assay to test for this complex behavior in *Drosophila*.

As described in Chapter 2, courtship song comprises two modes: pulse and sine. Pulse mode consists of pulse trains with an inter-pulse interval of approximately 35ms. We found significant variability in the amplitude of individual pulses, satisfying one precondition for directed amplitude modulation. By examining $> 460,000$ pulses from 8 wild type strains, we not only demonstrate that male flies actively increase pulse amplitude with distance from the female, but that this sensorimotor transformation is performed in milliseconds to modulate the production of ongoing acoustic signals on a pulse-by-pulse basis.

Through genetic and physical manipulations, we establish that amplitude modulation at large distances is exclusively mediated by vision, but is independent of the commonly studied visual motion detection pathways. Further, we identify the indirect flight muscles as a critical component of the motor output. To examine song without confounding sensory cues, we thermogenetically activated males in the absence of any female. Even males whose song circuits have been artificially activated increase amplitude with target distance, and global changes in light intensity produced transient amplitude responses. Building on this success, we developed the first system for recording activated song while tethered flies walk on an air-supported ball, to map the stimulus-response transformation. Our results identify an unprecedented level of complexity in insect acoustic communication and establish a novel link between visual information and acoustic signal production.

3.2 Results

3.2.1 Distance predicts pulse amplitude

Drosophila melanogaster males extend and vibrate their wings to produce pulse trains as part of their courtship ritual. These trains can be interspersed with sinusoids or produced independently, and individual pulses are easily separated to calculate amplitude, inter-pulse

interval (IPI), and fundamental frequency (Figure 3.1a). Sine song is generally softer than pulse song, and tends to be produced when males are in close proximity to the female [77]. This suggests that males may actively adjust their song amplitude in accordance with their distance from the female. In addition, pulse amplitudes produced by individual flies can be highly variable (Figure 3.2a), and recent work has demonstrated that variability in courtship song can be explained by sensory cues [77]. Building from this, we hypothesized that males could actively modulate pulses in response to their environment, perhaps increasing amplitude when females are at larger distances. This form of acoustic amplitude modulation has never been identified in insects, and if males were capable of regulating individual pulses, it would represent the fastest example of this sensorimotor transformation in any organism. To test for amplitude modulation requires a large sample of pulses produced at a range of inter-fly distances (Dis—defined here as the distance between the fly centers, Figure 3.1d). To achieve this, we paired individual males from 8 wild type strains (WT1 through WT8, see Table 3.1) with virgin females (genetically engineered to be pheromone insensitive and blind, termed PIBL) in our large behavioral chamber (Figure 2.1a, [77]).

We simultaneously tracked fly movements throughout naturalistic courtship rituals and recorded $> 460,000$ pulses produced at a range of distances up to 15mm ($\sim$6 female body lengths). Signals recorded on each microphone will vary both with the amplitude produced by the male and his position relative to the microphone. This technical difficulty has prevented prior studies from investigating song amplitude [78]. In our chamber, variations in the recording sensitivity of microphones added a further level of complexity. Unlike previous studies, we also tracked the male's location at each point in time. We used this tracking information to normalize the amplitude of each pulse (Figure 3.1b and Methods), but could not account for variability introduced through male orientation or wing choice; this likely reduced the significance of our results. When possible, we measured the wing length of each fly post-recording (see Methods, [79]) and discovered a positive correlation between wing length and pulse amplitude (Figure 3.1c, $r^2 = 0.5$). Prior work has established that wing

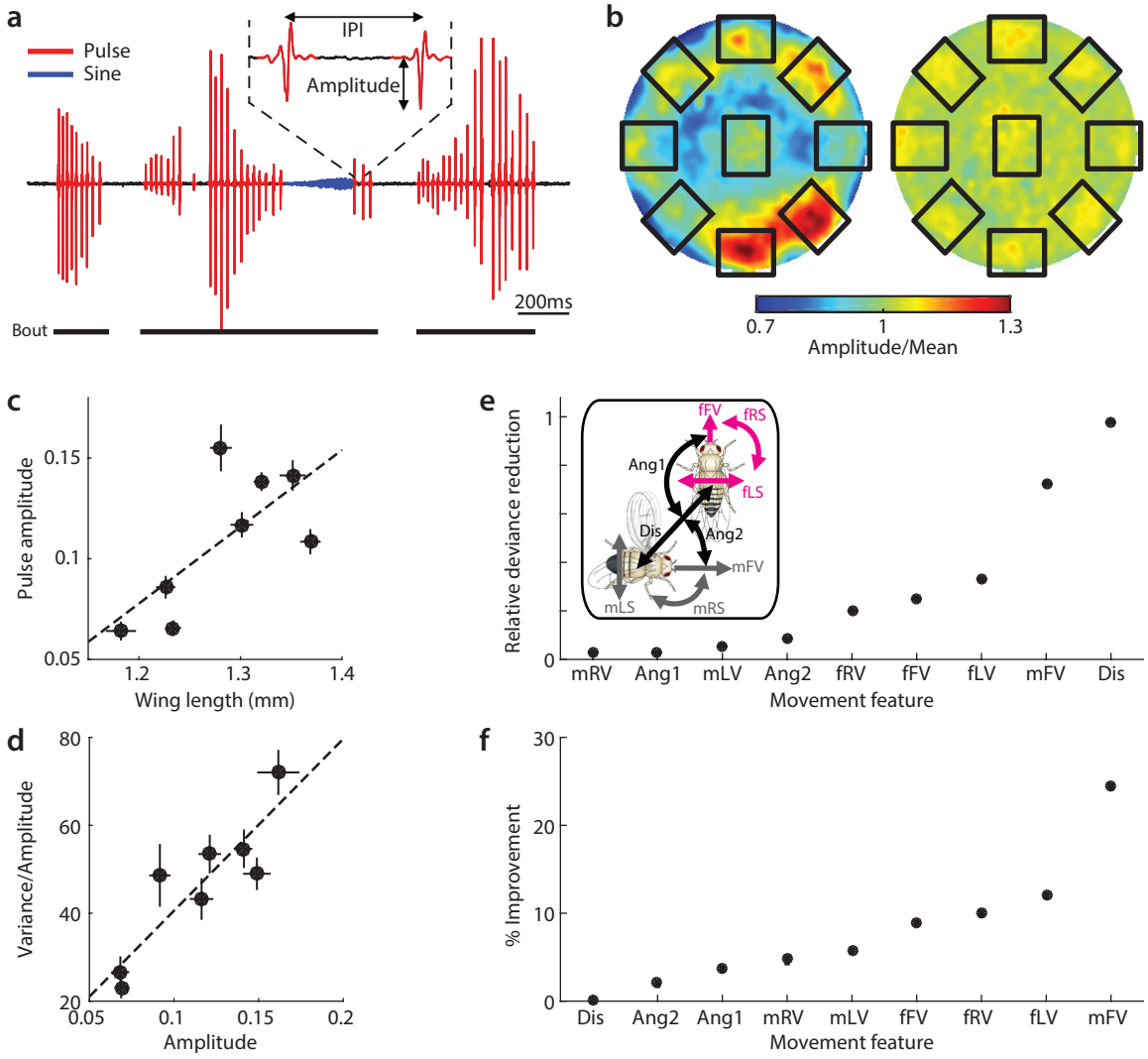

Figure 3.1: Measuring pulse amplitude. **a**, Segmentation of song bouts into pulse (red) and sine (blue) elements. Three song bouts, two pulse-only bouts and one containing sine song, are shown. Magnified section illustrates amplitude and inter-pulse interval (IPI). **b**, Distribution of pulse amplitudes with male position as a fraction of the mean across all positions before (left) and after (right) normalization (see Methods). Microphone positions are indicated (black rectangles). Pulses produced $> 11mm$ from the center were excluded from all analyses due to data limitations ($\sim$ 10% of pulses). **c**, Mean pulse amplitude (arbitrary units) increases with wing length across 8 wild type strains. Standard errors and linear fit (dashed line, $r^2 = 0.5$) are shown. n = 18-36 flies. **d**, As in **c**, but comparing the variance/amplitude ratio to the mean amplitude for each strain. $r^2 = 0.79$. **e**, The relative deviance reduction for GLMs designed to predict amplitude from a single movement feature. **Inset**, Illustration of 9 movement features used: Male/female forward velocity (mFV/fFV), male/female lateral and rotational speeds (mLS/fLS and mRS/fRS), the distance between fly centers (Dis), the absolute angle from female/male heading to male/female center (Ang1/Ang2). **f**, The percentage improvement in deviance reduction from including a second movement feature in the GLM. n = 271,287 pulses from 226 flies. Error bars indicate 95% confidence intervals. **b-e**, Included flies sang > 500 pulses.

Acronym	Description
WT1	Wild type from Nairobi, Kenya; collected by Andolfatto & Bachtrog (2006)
WT2	Canton-S laboratory strain
WT3	Wild type from San Diego, California; collected by Andolfatto (2006)
WT4	Wild type from Cartagena, Colombia; collected by Andolfatto (2009)
WT5	Wild type from the Netherlands; collected by Davis (2000)
WT6	Wild type from Zanzibar, Tanzania; collected by Andolfatto & Bachtrog (2006)
WT7	Wild type from Harare, Zimbabwe; collected by Begun (1993)
WT8	Wild type from Victoria Falls, Zimbabwe; collected by Ballard (2002)
PI	Genetic manipulation to remove all volatile pheromone receptors and many general olfactory receptors
BL	Genetic manipulation to remove photoreceptors
PIBL	Genetic manipulation to remove photoreceptors and volatile pheromone receptors
TCBL	BL male flies had their foreleg tarsi removed > 20 hours before recording
AC	WT1 male flies had aristae removed > 20 hours before recording
SP	PIBL females injected with Drosophila melanogaster sex peptide > 20 hours before recording
oe-	Genetic manipulation to remove pheromone producing cells (in PIBL females)
FRU^{Act}	Activated (~26ºC) males expressing thermosensitive TrpA1 channels in all *fruitless* positive neurons
DSX^{Act}	Activated (~27ºC) males expressing thermosensitive TrpA1 channels in all *doublesex* positive neurons
$P1^{Act}$	Activated (~33ºC) males expressing thermosensitive TrpA1 channels in putative song command neurons (P1)
$pIP10^{Act}$	Activated (~33ºC) males expressing thermosensitive TrpA1 channels in descending song neurons (pIP10)
$dPR1^{Act}$	Activated (~33ºC) males expressing thermosensitive TrpA1 channels in prothoracic song neurons (dPR1)
$Cont^{Kir}$	Male controls for Kir-silencing of motion-sensitive neurons, expressing half of a split-GAL4 in the Kir background
$C1C2^{Kir}$	Males expressing an inward-rectifying potassium channel (Kir2.1) in motion-sensitive lamina neurons (C1 and C2)
$L1L2^{Kir}$	Males expressing an inward-rectifying potassium channel (Kir2.1) in motion-sensitive lamina neurons (L1 and L2)
$L4^{Kir}$	Males expressing an inward-rectifying potassium channel (Kir2.1) in motion-sensitive lamina neurons (L4)
$Cont^{TNT}$	Male controls for TNT-silencing of motion-sensitive neurons, expressing half of a split-GAL4 in the TNT background
$C1C2^{TNT}$	Males expressing tetanus toxin light chain (TNT) in motion-sensitive lamina neurons (C1 and C2)
$L1L2^{TNT}$	Males expressing tetanus toxin light chain (TNT) in motion-sensitive lamina neurons (L1 and L2)
$L4^{TNT}$	Males expressing tetanus toxin light chain (TNT) in motion-sensitive lamina neurons (L4)
$T4T5^{Kir}$	Males expressing an Kir2.1 in motion-sensitive lobula plate neurons (T4 and T5)
$Cont^{Shi}$	Control males expressing a temperature sensitive synaptic inhibitor at a permissive temperature (~22ºC)
$T4T5^{Shi}$	Control males expressing a temperature sensitive synaptic inhibitor at a non-permissive temperature (~26ºC)
$Cont^{Dm}$	A rescused null strain for the myosin light regulatory strain Dmlc2
Phos	Males expressing a Dmlc2 protein with alanine substitutions at two kinase phosphorylation sites
Dual	Males expressing a two mutations of the Dmlc2 protein: Phos combined with a truncated N-terminal

Table 3.1: Descriptions and acronyms for all fly strains/genotypes

area is an important component of courtship success [80], but this is the first direct evidence that flies with larger wings produce louder song. In addition to the mean amplitude, wing length also impacts the distribution of amplitudes produced (Figure 3.1d). Given these results, we focused on relative changes in amplitude and normalized pulse amplitude for individual flies before combining data in later analyses. This "Normalized amplitude" is measured in standard deviations (STDs) from the mean pulse amplitude (see Methods) and necessitates only using flies that produced a large number of pulses during the trial (to accurately estimate STD and mean).

To test whether any features of the male sensory environment predict amplitude, we utilized the unbiased generalized linear model (GLM) previously described in chapter 1 (Figure 2.5, [49]), although we use a Gaussian link function as the GLM output (normalized pulse amplitude) is non-binary (see Methods). We divided the tracking data into 9 movement features and compared the performance of models based on each individual feature. Dis was the strongest predictor of pulse amplitude (Figure 3.1e). We repeated this process, combining Dis with each of the remaining movement features and tested two-feature models, and found that mFV was a significant secondary predictor of amplitude (Figure 3.1f). The addition of a third feature provided no further improvement in deviance reduction (data not shown). The inclusion of mFV in an optimal model is perhaps unsurprising given the proposed neural link between the locomotor and song circuits [77]. While we focus primarily on Dis here, we control for any effects of mFV in analyses.

If males are measuring Dis to modulate amplitude, there should be a time delay at which Dis is most predictive. We examined this delay, for both Dis and mFV, by running separate GLMs for at each time point prior to pulse generation. Dis and mFV were most predictive at delays of ∼470ms and ∼100ms respectively (Figure 3.2a). Hereafter, we refer to Dis and mFV at these delays as pre-Dis and pre-mFV. The broad peak of predictive time-points for Dis likely derives the wide auto-correlation, especially when compared with mFV, of this movement feature during natural courtship (Figure 3.2b). For both Dis and

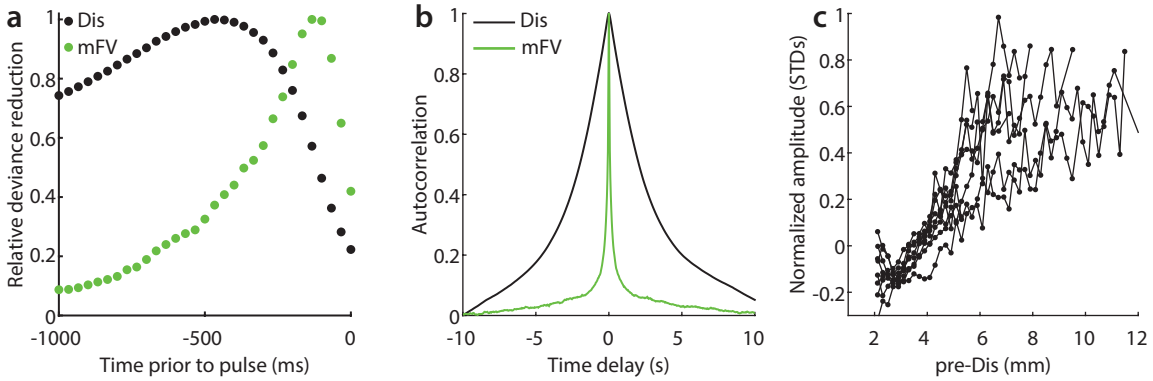

Figure 3.2: Dis predicts pulse amplitude at a delay of 470ms. **a**, The relative deviance reduction for GLMs designed to predict amplitude from Dis (black) or mFV (green) at a specified time delay prior to each pulse. n = 308,071 pulses. 95% confidence intervals are too small to visualize. **b**, The mean autocorrelation for Dis (black) is broader than the autocorrelation for mFV (green). Values are normalized to a correlation with shuffled data and scaled between 0 and 1 for visualization. n = 97 wild type flies courting for > 20mins. **c**, Normalized amplitude increases with pre-Dis (Dis at 470ms prior to pulse, bin width = 0.2mm) for 8 wild type strains, $r^2 \geq 0.82$. Each point is generated from a minimum of 100 pulses. n = 23-38 flies. **a** and **c**, Data came from males singing more than 500 pulses.

mFV, the filter coefficient was positive for every time point (data not shown), indicating that increases in Dis or mFV predict increases in pulse amplitude. In confirmation of this, we found a strong positive correlation between pre-Dis and pulse amplitude for all 8 wild type strains($r^2 \geq 0.82$, Figure 3.2c). Because variations in strain body size can have systematic effects on the distribution of pulse amplitudes (Figure 3.1c-d), small differences between strains at particular values cannot necessarily be attributed to changes in behavior, and for this reason we focus on the overall relationship between amplitude and distance (the r^2 value).

Despite the predictive power of distance, if amplitude was strongly correlated with another pulse parameter, such as IPI, modulation of this acoustic feature could generate a spurious correlation between Dis and amplitude. As expected from the wide autocorrelation of Dis (Figure 3.2b), there is a strong correlation between the amplitude of adjacent pulses (Figure 3.3a-c). However, we found no observable relationship between amplitude and pulse frequency or IPI (Figure 3.3d-i). We conclude that modulation of pulse amplitude cannot be attributed to interactions with other pulse parameters.

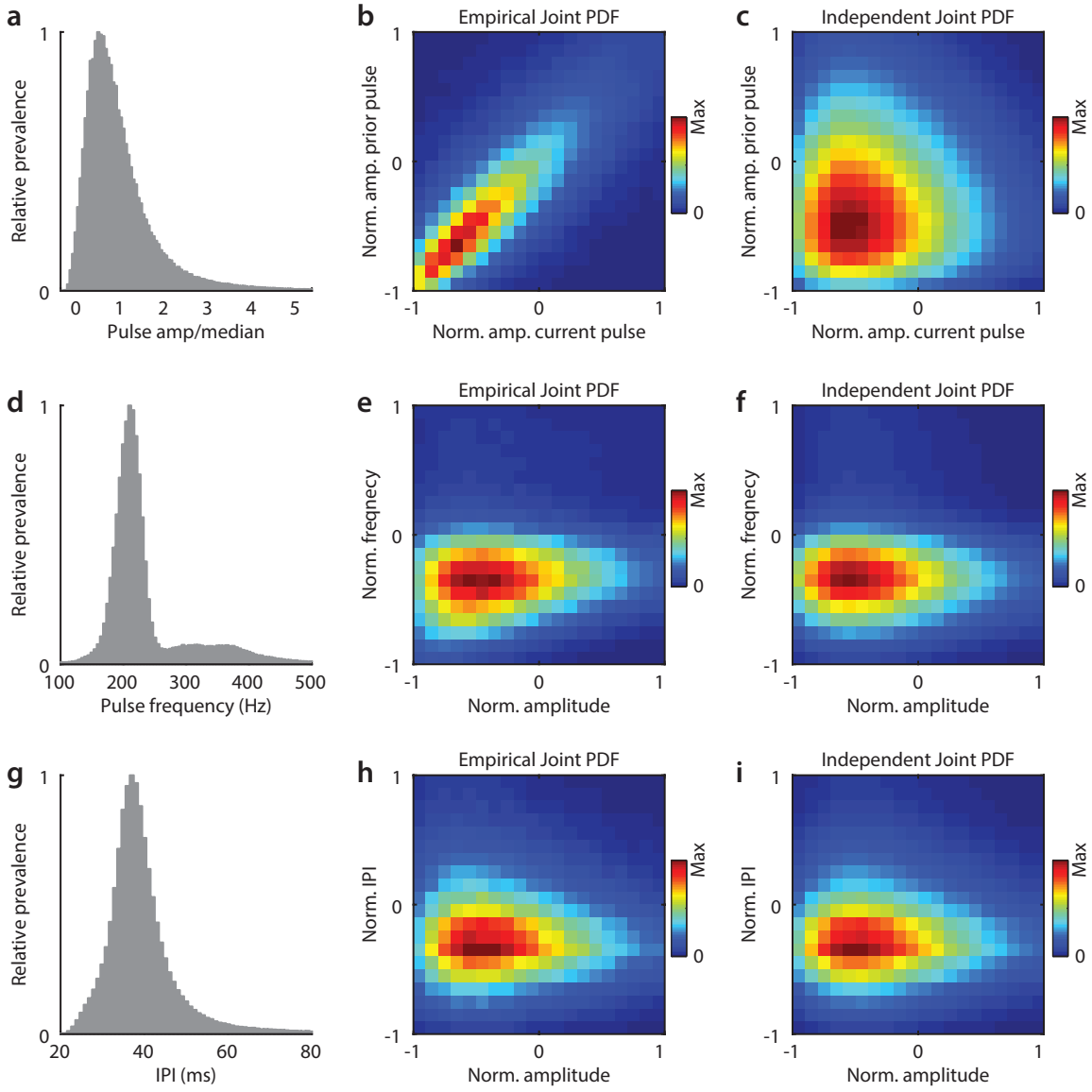

Figure 3.3: Pulse parameters are independent. For all panels, data came from 226 wild type males singing more than 500 pulses. **a**, Relative prevalence of pulse amplitudes as a fraction for the median. n = 466,773 pulses. **b**, The empirical joint probability density function (PDF) of amplitudes for consecutive pairs of pulses (see Methods). n = 312,946 pulses. **c**, As in **b**, but the independent, rather than empirical, joint PDF. The distributions in **b** and **c** are significantly different ($p < 10^{-7}$, two-sample Kolmogorov-Smirnov test). **d**, Relative prevalence of pulse frequencies. n = 466,773 pulses. **e**, The empirical joint PDF of pulse amplitude and frequency. n = 336,973 pulses. **f**, As in **e**, but the independent, rather than empirical, joint PDF. The distributions in **e** and **f** are not significantly different ($p > 0.11$, two-sample Kolmogorov-Smirnov test). **g**, Relative prevalence of pulse IPIs. n = 413,492 pulses. **h**, The empirical joint PDF of pulse frequency and IPI. n = 314,638 pulses. **i**, As in **h**, but the independent, rather than empirical, joint PDF. The distributions in **h** and **i** are not significantly different ($p \sim 1.00$, two-sample Kolmogorov-Smirnov test). For **b-c**, **d-e**, and **h-i**, data were zscored for each fly and values more than 1 STD from the mean were excluded. For **a**, **d**, and **g**, axes are truncated to aid visualization.

3.2.2 Males modulate individual pulses within each train

These data provide direct evidence for a sensorimotor transformation between distance and acoustic amplitude previously unidentified in any invertebrate system. However, the temporal resolution with which males can exercise this modulation is unclear. Males could employ one of two mechanisms (Figure 3.4a): either flies measure Dis prior to the initial pulse and adjust the amplitude of the entire pulse train (M1), or they perform ongoing modulation of individual pulses (M2). While the strong correlation between the amplitude of neighboring pulses appears to support M1 (Figure 3.3b), this could be the result of temporal correlations in the sensory environment. The two mechanisms make divergent predictions about the delay at which Dis would be most predictive for each pulse position within a train (Figure 3.4b). Therefore, to distinguish between these possibilities, we built separate GLMs for each pulse number. With the exception of the first two pulses, the maxima of deviance reduction curves occurred at similar time points for each pulse position within the train, supporting M2 and suggesting that males are capable of modulating amplitude on a pulse-by-pulse basis during song production (Figure 3.4c). As the IPI for *Drosophila melanogaster* is ∼35ms, the rapidity of this sensorimotor transformation is striking. To the best of our knowledge, using visual cues to modulate an ongoing acoustic signal on this timescale is unprecedented in any system and represents a unique opportunity to study the underlying neural mechanisms.

To investigate the reduced GLM performance and atypical curve shape for pulse numbers 1 and 2, we examined the normalized pulse amplitude at each position within a train. Across flies, the initial two pulses were produced at a significantly lower amplitude than the rest (Figure 3.4d). This could result from a mechanical limitation on producing loud pulses at the start of a train or differences in the sensory environment during initial pulses. As initial pulses tend to be produced at larger Dis and mFV (Figure 3.4e), both of which predict larger amplitudes, the low intensity cannot be explained by variations in these variables, suggesting a mechanical limitation is more likely. If this is the case, males should show the same relationship between amplitude and pulse number in the absence of a female.

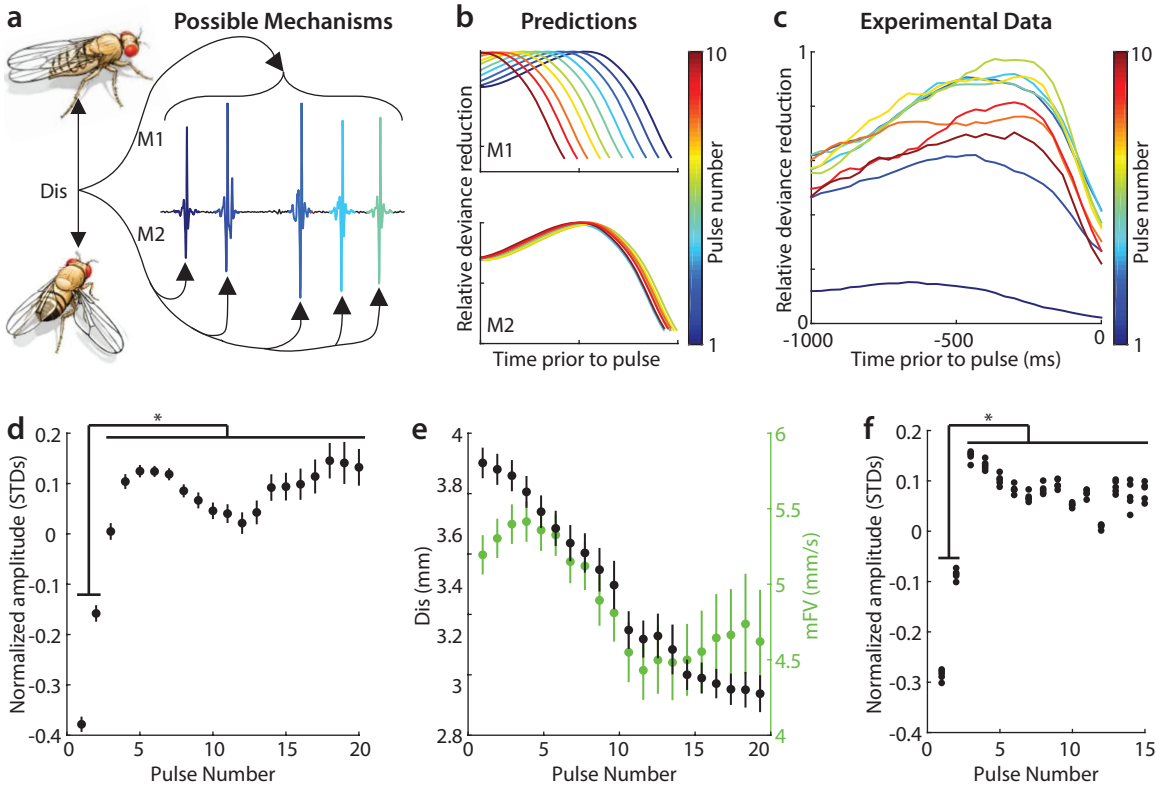

Figure 3.4: Flies modulate individual pulses with distance. **a**, Two possible mechanisms for pulse amplitude modulation. Either flies modulate the amplitude of entire pulse trains based on Dis prior to the initial pulse (top, M1) or each individual pulse is separately modulated (bottom, M2). **b**, Predictions for the two mechanisms in **a** if a separate GLM was built using only pulses at each position within a train. If flies implement M1 (top) the most predictive time-point (as identified by maximal deviance reduction) should shift for each pulse number. Conversely, if flies use M2 (bottom), the maximum for each pulse number should be the same. **c**, GLMs designed to predict amplitude from Dis at specified time delay prior to each pulse, using only pulses at a particular position within pulse trains. Positions beyond 10 were excluded due to data limitations. Results strongly suggest flies modulate each pulse (M2). n = 10,000 - 35,000 pulses for each pulse number. **d**, Normalized pulse amplitude for each pulse number. Error bars indicate SEM. For each point, n = 25-221 flies producing > 50 pulses with that pulse number. $* = p < 10^{-6}$. **e**, As in **d**, but comparing Dis (black) and mFV (green), rather than amplitude, at each pulse number. **f**, As in **d**, but for 5 different heat-activated lines: FRU^{Act}, DSX^{Act}, P1^{Act}, pIP10^{Act}, and dPR1^{Act} (see Methods). Pulse number is truncated at 15 due to data limitations. For each point, n = 2-9 flies. $* = p < 10^{-6}$. **c-e**, data came from 226 wild type males singing > 500 pulses.

Expression of the heat-sensitive cation channel TrpA1 in specific neural subsets is known to activate male song in the absence of female flies [33]. We used this thermogenetic strategy elicit song from isolated males of 5 different genotypes. Two of these involved global activation of neurons expressing the sexually dimorphic genes *fruitless* (FRU^{Act}, ~2000 neurons), or *doublesex* (DSX^{Act}, ~700 neurons), both of which elicit all courtship behaviors [45, 81]. We also activated three sparse neural subsets known to generate song: the putative song command cluster, P1 (15-20 neurons per hemisphere), the descending neuron, pIP10 (1 neuron per hemisphere), and a prothoracic neuron, dPR1 (1 neuron per hemisphere) [33] (Figure 3.12a). When placed at an activating temperature, we refer to these flies as $P1^{Act}$, $pIP10^{Act}$, and $dPR1^{Act}$ respectively. For all 5 genotypes, the initial two pulse of each pulse train were of a significantly lower amplitude than later pulses, corroborating the results from wild type data (Figure 3.4f). We conclude that while sensory cues still weakly predict amplitude at pulse train initiation, mechanical limitations prevent males from properly implementing this sensorimotor transformation. To accurately assess amplitude modulation, we excluded these initial two pulses from further analyses unless otherwise specified; this produced only minor changes in results and didn't alter the maximally predictive delays for Dis or mFV.

3.2.3 A crucial role for vision in amplitude modulation

Which sensory modality could males be using to perform this rapid sensorimotor transformation? Using a panel of genetic and physical manipulations, we eliminated individual male sensory cues and looked for abnormalities in pulse amplitude. Making males deaf (AC) or pheromone insensitive (PI), or using females that were unreceptive (sex-peptide injected, SP [56]) or lacked pheromones (oe^{-}) had little effect. However, blind males (BL) showed an inflated pulse amplitude compared with their wing length (Figure 3.5a). To confirm this resulted from lost visual cues rather than off-target effects of the mutation, we placed WT1 flies with females while alternating between dark and light conditions and found an increase in pulse amplitude during the dark (Figure 3.5b). This suggests that vision is a critical com-

ponent of amplitude modulation. In confirmation, the positive correlation between pre-Dis and amplitude is eliminated in blind flies, but only for pre-Dis > 5mm ($r^2 = 0.00$, Figure 3.5c).

This relationship is unchanged when accounting for any correlation between mFV and Dis (data not shown) and blind flies show a normal relationship between pre-mFV and amplitude (Figure 3.5f). Furthermore, pulse amplitude is much larger at close distances, and the relationship with pre-Dis is abrogated, when a BL male is not facing the female (Ang2 > 90°, $r^2 = 0.12$, Figure 3.5d-e). This suggests that blind males modulate amplitude via a non-visual sensory cue from females at pre-Dis < $5mm$. In an effort to isolate this secondary cue, we made blind males pheromone insensitive (PIBL) or cut their foreleg tarsi to eliminate gustatory and tactile cues from tapping (TCBL). In both cases, no amplitude modulation was observed at pre-Dis > 5mm ($r^2 \leq 0.05$), but neither manipulation prevented amplitude modulation at pre-Dis < 5mm ($r^2 \geq 0.58$, Figure 3.6a). Further, both of these manipulated strains still sing at a significantly lower amplitude when facing the female at close distances (Figure 3.6b-c). Thus, another secondary cue (perhaps received via non-tarsi-mediated tactile sensation or licking [37]) must be by males for amplitude modulation at close distances to the female. Nonetheless, we have shown that vision is exclusively used to modulate pulse amplitude over a large range of Dis (from 5mm to >10mm) and we therefore focus on the visual modulation of pulse amplitude from here on.

3.2.4 Changes in light intensity impact pulse amplitude in isolated males

Our data demonstrated that vision is required for amplitude modulation when flies are separated by more than ∼ 1 body length, but also make predictions about the processing of these visual stimuli. Dis is optimally predictive at a significant delay (∼470ms), yet flies rapidly modulate individual pulses. Thus, we hypothesize that visual information is integrated over hundreds of milliseconds, but new information reaches the song circuit within

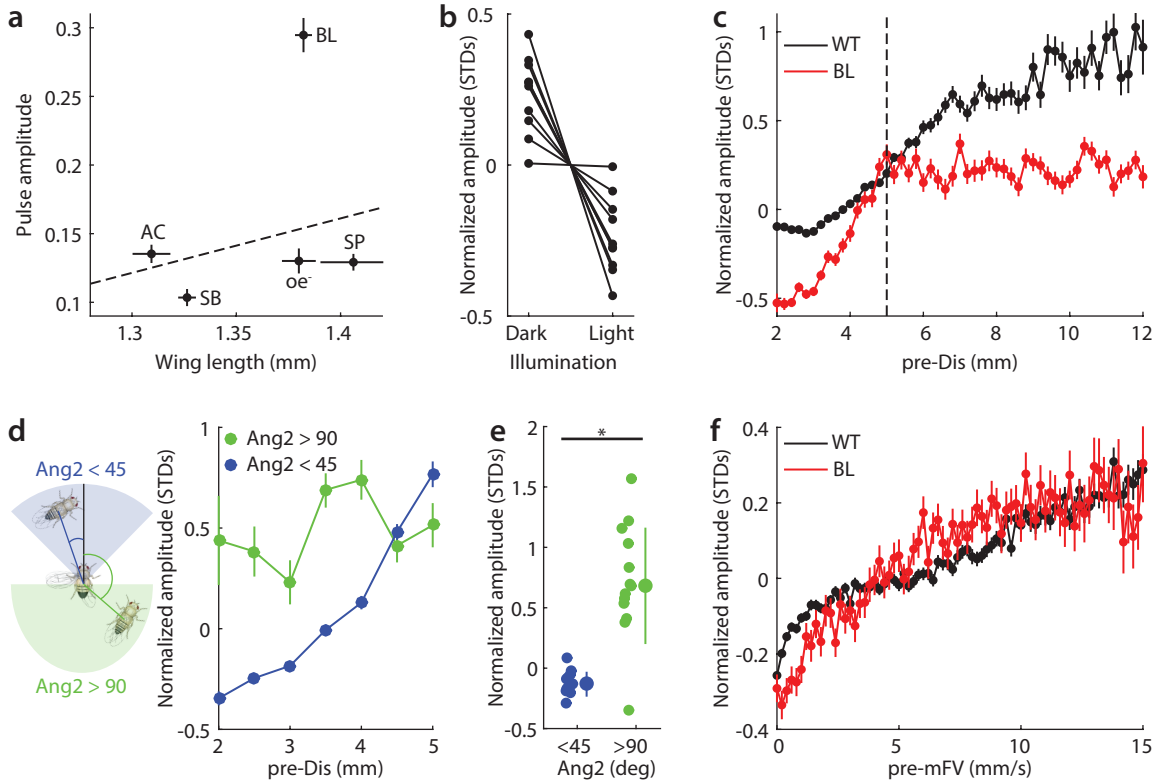

Figure 3.5: Vision is responsible for amplitude modulation at larger distances. **a**, Relationship between mean pulse amplitude (arbitrary units) and wing length for 5 different genetic and physical manipulations of male and female flies. Males were deaf (AC), blind (BL), or pheromone insensitive (PI), and paired with PIBL females. WT1 males were paired with unreceptive females (SP), or females engineered to lack pheromones (oe$^-$). See Table 3.1 for strain details. Linear fit (dashed line) is reproduced from wild type flies. n = 7-30 flies. **b**, Individual WT1 males (paired with PIBL females) produce louder pulses in the dark. * = $p < 10^{-6}$. n = 9 flies singing $\geq$ 200 pulses in each condition. **c**, Normalized amplitude of pulses with increasing pre-Dis (bin-width = 0.2mm) for all WT (black, n = 226 flies) and BL (red, n = 25 flies) males. Dashed line indicates 5mm boundary. For pre-Dis below and above 5mm, $r^2 = 0.87/0.94$ and $r^2 = 0.81/0.00$ for WT/BL flies. Each point is generated from a minimum of 100 pulses. **d**, **Left**, Illustration of regions within the visual field that constitute Ang2 $< 45°$ or Ang2 $> 90°$. **Right**, When considering only pulses produced by BL flies with pre-Dis $<$ 5mm (bin-width = 0.5mm), amplitude is independent of pre-Dis if the male isn't the facing female (Ang2 $> 90°$, green, $r^2 = 0.12$). Conversely, amplitude robustly increases with pre-Dis when he faces the female (Ang2 $< 45°$, blue, $r^2 = 0.94$). Amplitudes were normalized before splitting data, so values are comparable. Each point is generated from a minimum of 25 pulses, n = 25 flies. **e**, When considering distances away from the 5mm boundary (pre-Dis $\leq$ 4mm), BL flies sing at significantly lower amplitudes when facing the female (Ang2 $< 45°$). * = $p < 10^{-5}$, n = 13 flies singing $\geq$ 10 pulses in each conditions. Individual points, mean, and STD is given for each condition. **f**, As in **c**, but for pre-mFV rather than pre-Dis. Unlike with pre-Dis, BL and WT flies show similar amplitude increases with increasing pre-mFV. **c-d**, and **f**, Error bars indicate standard error. **b-f** All males sang more than 500 pulses

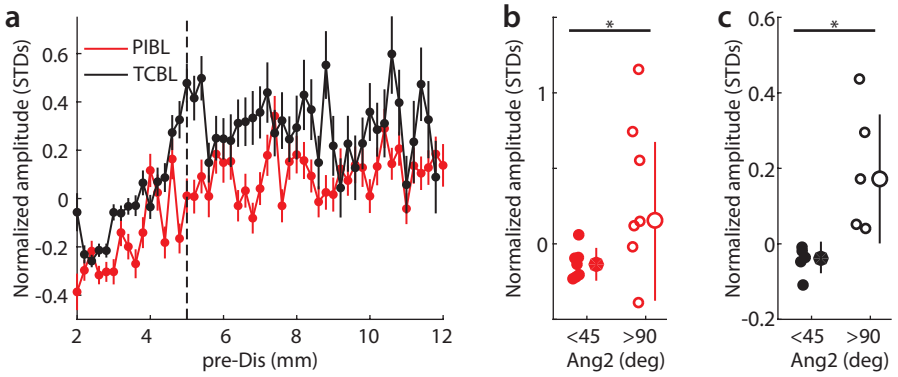

Figure 3.6: Modulation at short distances is independent of foreleg tarsi and pheromones. For all panels, each male sang > 500 pulses. **a**, Normalized amplitude of pulses with increasing pre-Dis (bin-width = 0.2mm) for BL flies that are additionally pheromone insensitive (PIBL, red, n = 7 flies) or missing their foreleg tarsi (TCBL, black, n = 5 flies). For pre-Dis below and above 5mm, $r^2 = 0.58/0.82$ and $r^2 = 0.05/0.01$ for PIBL/TCBL flies. Each point is generated from a minimum of 50 pulses. Error bars indicate standard error. **b**, When considering distances away from the 5mm boundary (pre-Dis $\leq$ 4mm), PIBL flies sing at significantly lower amplitudes when facing the female (Ang2 $< 45°$). * = $p < 0.05$, n = 7 flies singing $\geq$ 10 pulses in each condition. **c**, As in **b**, but for TCBL, rather than PIBL, flies. * = $p < 0.05$, n = 5 flies singing $\geq$ 10 pulses in each conditions. **b-c**, Individual points, mean, and STD is given for each condition.

a single IPI (∼35ms). To test these assertions requires the elimination of confounding female sensory cues and precisely timed perturbations to the visual environment. We recorded song from isolated FRU^{Act} males while cycling the power supply to the chamber light every 15 seconds (see Methods). A sharp change in light intensity should dramatically alter the activity of visual neurons (at least temporarily). Given the critical role for vision in amplitude modulation, we predicted that these changes might have a measurable impact on amplitude. Indeed, this cycling of luminance produced changes in mean pulse amplitude, a change which was absent for headless FRU^{Act} males (Figure 3.7a).

Building on this result, we integrated a voltage controlled light into the chamber, allowing us to modulate ambient light intensity between 0.5lux (moonlit night) and 22000lux (full daylight). Using this system, we provided an uncorrelated sequence of switches between 4 different light levels (650lux, 1800lux, 6500lux, and 20000lux) every 250ms. FRU^{Act} flies showed significant increases in pulse amplitude in response to decreases, but not increases in light intensity (Figure 3.7b). These responses occurred within 30ms of the intensity change,

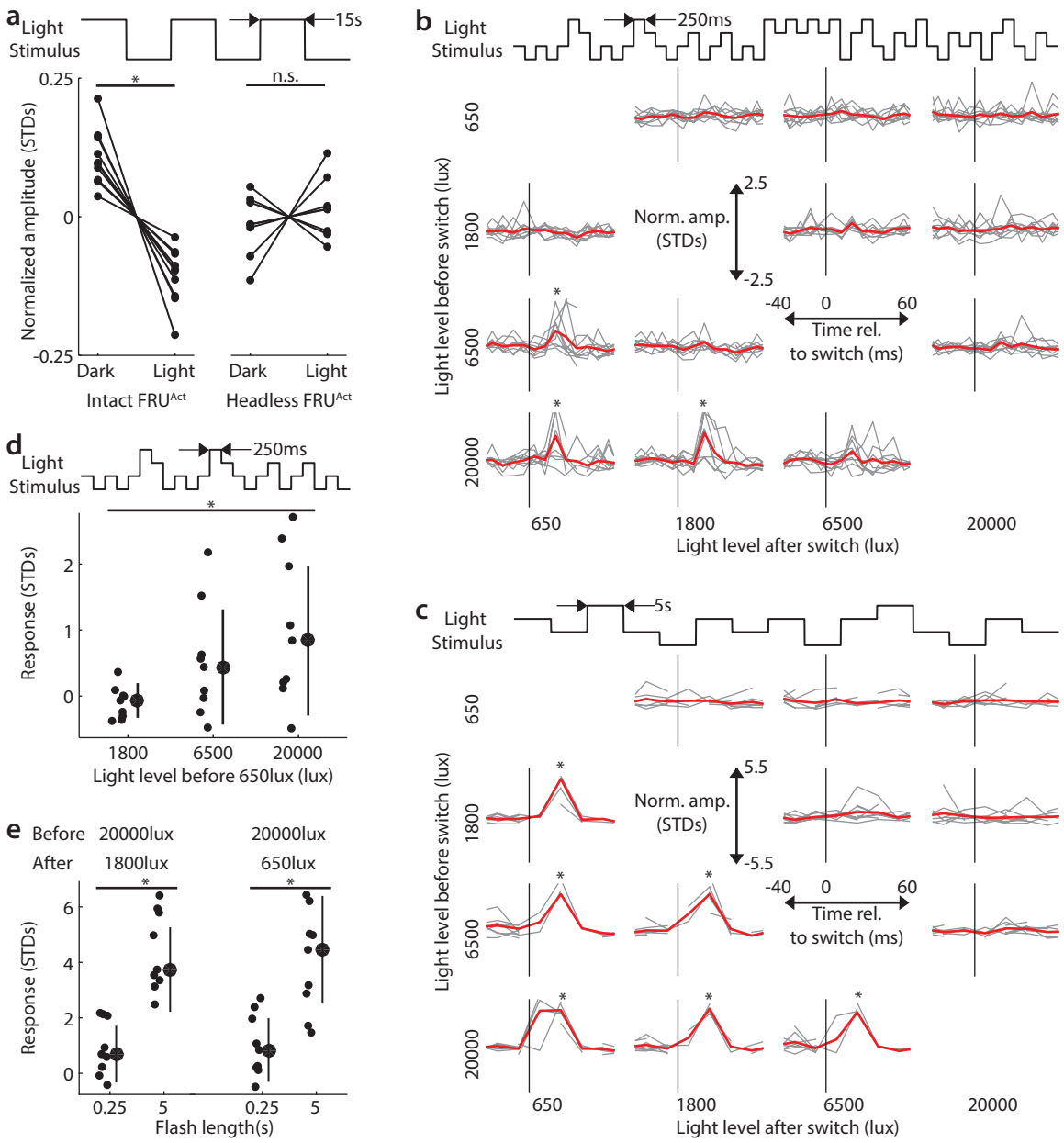

Figure 3.7: Visual information modulates amplitude within 30ms, but is influenced by history. **a**, When the chamber light was cycled on and off every 15s, FRU^{Act} flies sang louder in the dark (left, n = 11, $* = p < 10^{-7}$), but not when heads were removed (right, n = 7, $p > 0.2$). Each fly sang ≥ 200 pulses in each condition. **b**, Normalized amplitude relative to transition time between 4 intensity levels with flash length 250ms (bin-width 10ms, black line = 0ms). Individual flies (grey) and average (red) are shown. $n \leq 9$ FRU^{Act} flies, (varied across time bins). $* = p < 0.01$. **c**, as in **b**, but flash length is 5s rather than 250ms, bin-with is 20ms, and $n \leq 10$ FRU^{Act} flies. Note the change in vertical scale. $* = p < 0.001$. **d**, Response of FRU^{Act} flies (see Methods) for transitions to 650lux increase with the size of transition ($* = p < 0.05$, n = 9 flies). **e**, The response of FRU^{Act} flies for a 20,000lux to 1,800lux transition (left), and a 20,000lux to 650lux transition (right), is larger for a 5s flash (n = 10 flies) than a 250ms flash (n = 9 flies). $* = p < 0.001$. **d-e**, Individual points, mean, and STD is given for each condition.

and response size increased with the magnitude of the intensity difference (Figure 3.7d and Figure 3.8). This conclusively demonstrates that changes in the visual environment can affect pulse amplitude within a single IPI. Since we exclude the initial two pulses of each train, and each IPI is $\sim$ 35ms, the higher amplitudes being generated within 30ms of the transition are from pulse trains which began at least 40ms prior to the intensity change. Thus, these responses must result from modulations within ongoing pulse trains and demonstrate that flies are capable of changing amplitude during ongoing song production. Despite the changing light levels, we were able to effectively track flies (not possible in the "Dark" condition) which improved amplitude normalization and confirmed that changes in amplitude were independent of changes in mFV (Figure 3.8a).

As Dis is most predictive at a delay of 470ms, we hypothesized that historical visual information hundreds of milliseconds prior to the pulse should impact amplitude modulation. To test this, we increased the length of each light level to 5s. If amplitude responses are independent of visual history beyond 250ms, there should be no difference in the response size as a result of this increased flash length. However, in agreement with our prediction, we found a 5s flash period produced much larger responses for all negative light transitions (Figure 3.7c,e), demonstrating a clear effect of visual history on pulse amplitude. We reproduced this result for DSX^{Act} flies, and an independent set of experiments where we replaced the lowest light level (650lux) with "Dark" (0.5lux) (Figure 3.8a-b). Adaptations to the mean intensity and variance in a visual environment have long been known to exist in the *Drosophila* visual system [82], but these adaptations need not have propagated to the song circuit. This highlights the remarkable control males are exercising over their pulse amplitude and the complexities likely to exist in the underlying neural circuit.

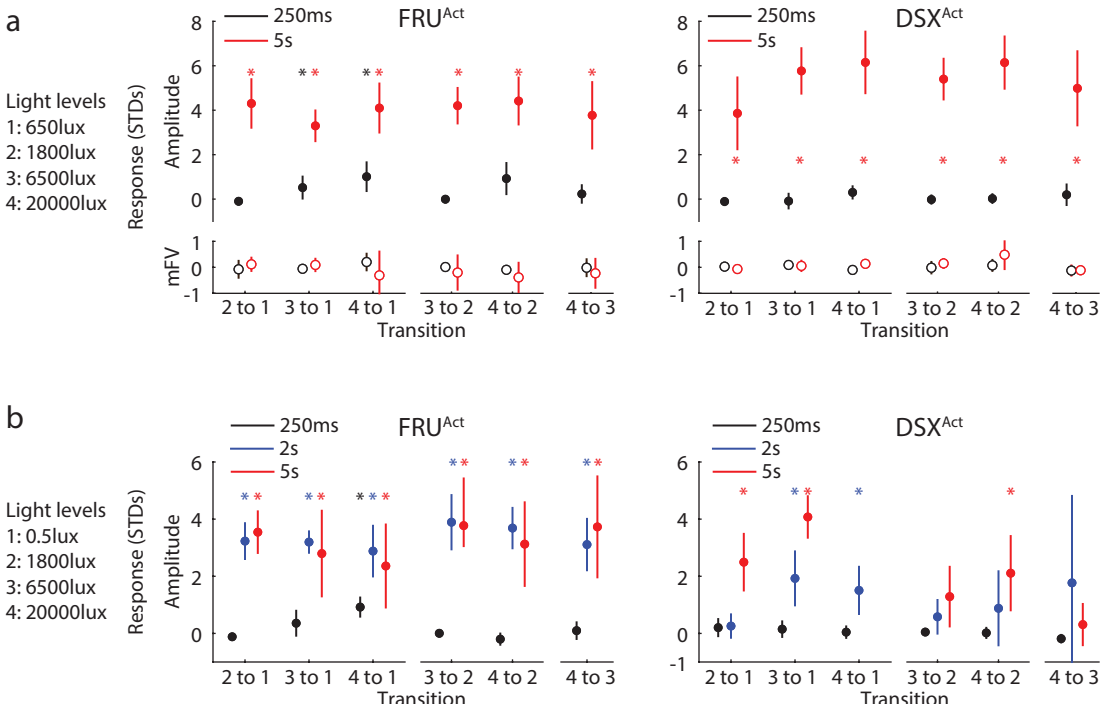

Figure 3.8: FRU^{Act} and DSX^{Act} both show a light flash response independent of velocity. Responses are calculated as described in Methods. **a**, The amplitude (top, closed circles) and velocity (bottom, open circles) responses to light transitions between 4 light levels. Data from FRU^{Act} (left) and DSX^{Act} (right) flies are shown for flash lengths of 250ms (black) and 5s (red). $* = p < 0.05$ and indicates a significant response. The mFV at the time of pulse production showed no significant changes for any light transition. **b**, As in **a**, but with the lowest light level as 0.5lux rather than 650lux. This light level was too low for tracking, so no mFV responses are shown. Additionally, a third flash length of 2s (blue) was recorded. **a-b**, Error bars indicate standard error. Every point represents data from ≥ 5 flies. Only negative light transitions are shown since positive transitions failed to elicit any significant amplitude responses.

3.2.5 Motion-sensitive neurons affect courtship but not amplitude modulation

While the unidirectional nature of the response to intensity changes is intriguing, and perhaps suggests separate roles for the ON and OFF pathways [83], *fruitless* or *doublesex* activation affects too many neurons to make inferences about the underlying circuitry. Fortuitously, recent work in the fly visual system [84] identified the contribution of the 12 classes of lamina neurons to motion vision. As the male must chase the female during courtship, motion vision is likely critical to his success, suggesting that the same visual neurons could be involved in measuring his distance to the female. However, whether these neurons have

any role in courtship is completely untested. We used two separate genetic mechanisms to silence one of three subsets of lamina neurons (L1 and L2, L4, or C2 and C3) in male flies: expressing either Kir2.1 (an inward rectifying potassium channel) or tetanus toxin light chain (TNT, a blocker of synaptic transmission). Prior work has shown that silencing any of these three neural subsets causes severe defects in motion detection [84], but when paired with PIBL, silenced flies showed no gross defect in following ability compared with controls (Figure 3.9a,d). Given this surprising result, we focused our analysis on times at which pulses were produced (i.e. when the male should be actively following the female). Mutant flies (particularly L1L2^{TNT} and C2C3^{Kir}) sang an increased fraction of pulses at Dis $>$ 5mm (Figure 3.9c,e), demonstrating a relatively mild defect (compared with BL flies for example) in the male's ability to maintain a close proximity to the female. This represents the first demonstration of a role for these motion-sensitive neurons in fly courtship. Despite this defect, all three mutant strains showed amplitude modulation extending into the purely visual range (pre-Dis $>$ 5mm) irrespective of the silencing mechanism ($r^2 \geq 0.72$, Figure 3.9c,f).

We performed similar tests on T4 and T5 tangential cells in the lobula plate which have an established role motion detection [85, 86]. Again, we silenced these neurons chronically with Kir (as above) or acutely using flies expressing temperature sensitive shibire (see Methods). While both mutations significantly inhibited the male's ability to pursue the female relative to controls, the were no observable effects on amplitude modulation ($r^2 \geq 0.79$, Figure 3.10). All the visual neurons we silenced are established components of the classical elementary motion detector (EMD) pathway [86]. As amplitude modulation survived all our perturbations of this pathway, we suspect males are measuring distance via an independent neural mechanism. Previous work has established that silencing T4 and T5 cells did not extinguish responses to flickering stimuli (changes in light intensity) in downstream neurons, even if motion responses were completely abolished [85]. Since we have established that changes in light intensity

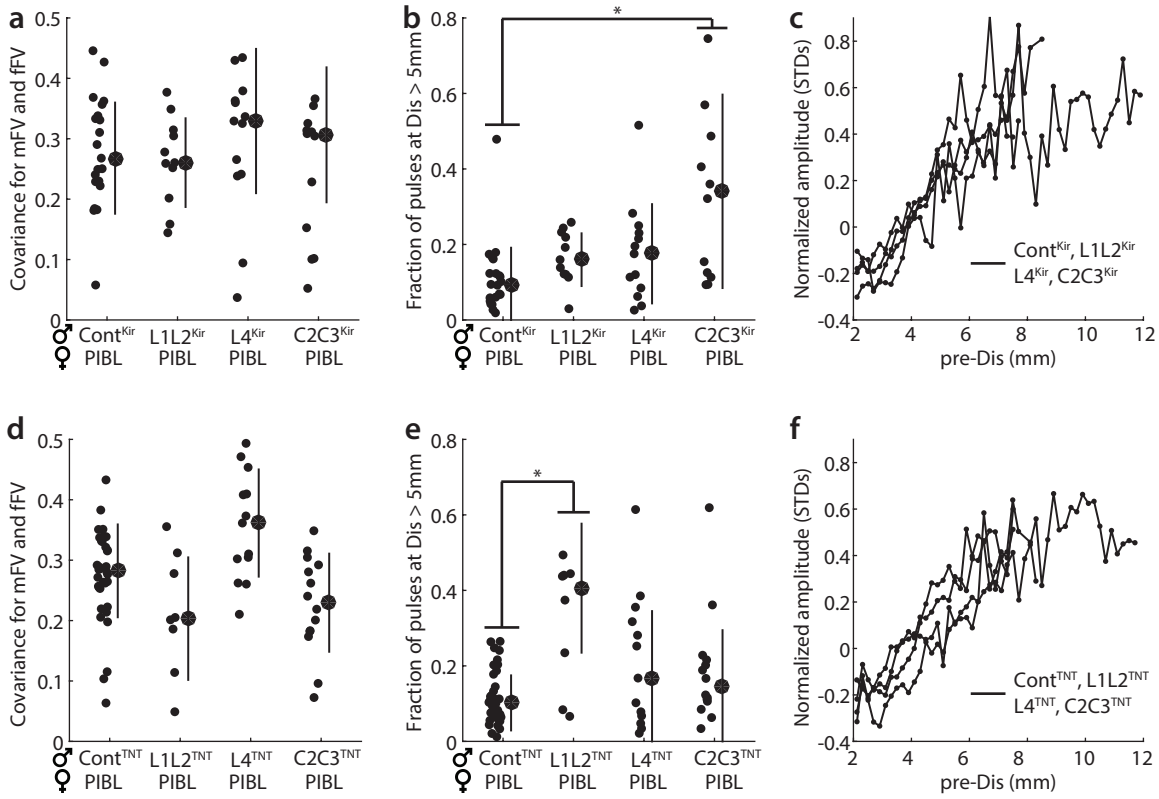

Figure 3.9: Motion-sensitive lamina neurons are not required for amplitude modulation. For all panels, data came from males singing more than 500 pulses. **a**, An estimate of following behavior for males expressing Kir in one of three subsets of lamina neurons (L1 and L2, L4, or C2 and C3). We measured the maximum cross-covariance (normalized by the auto-covariance) between male and female forward velocities, n = 11-21 flies. Perfect following behavior, over the entire trial, would produce a value of 1. No strain deviated significantly from the control. **b**, as in **a**, but comparing the fraction of pulses produced at Dis > 5mm. $* = p < 0.01$. **c**, All strains (from **a**) increase pulse amplitude with pre-Dis (bin width = 0.2mm), extending beyond 5mm, and are indistinguishable from control flies ($r^2 \geq 0.72$). Each point is generated from a minimum of 100 pulses. **d**, As in **a**, but expressing TNT (rather than Kir) in the lamina neurons. No strain deviated significantly from the control. n = 8-34 flies. **e**, As in **b**, but expressing TNT (rather than Kir) in the lamina neurons. $* = p < 0.05$. **f**, As in **c**, but expressing TNT (rather than Kir) in the lamina neurons. ($r^2 \geq 0.81$). **a-b** and **d-e**, Individual points, mean, and STD are given for each strain/genotype.

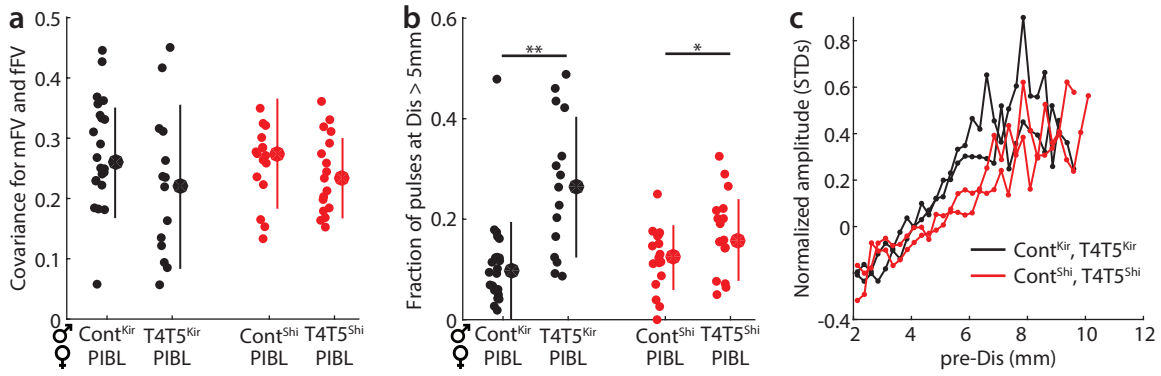

Figure 3.10: T4 and T5 tangential neurons are not required for amplitude modulation. For all panels, data came from males singing more than 250 pulses. T4 and T5 neurons were silenced using the R42F06 GAL4 line [85] and expressing Kir ($T4T5^{Kir}$) or temperature sensitive shibire at permissive ($Cont^{Shi}$) and non-permissive ($T4T5^{Shi}$) temperatures (see Methods). **a**, A comparison of following behavior for silenced T4 and T5 neurons compared with respective controls. We measured the maximum cross-covariance (normalized by the auto-covariance) between male and female forward velocities, n = 15-22 flies. Perfect following behavior, over the entire trial, would produce a value of 1. Neither manipulation deviated significantly from its respective control. **b**, as in **a**, but comparing the fraction of pulses produced at Dis $>$ 5mm. $* = p < 0.05$ and $** = p < 0.001$. **c** All strains (from **a**) increase pulse amplitude with pre-Dis (bin width = 0.2mm), extending beyond 5mm, and are indistinguishable from respective controls ($r^2 \geq 0.79$). Each point is generated from a minimum of 100 pulses. **a-b**, Individual points, mean, and STD are given for each strain/genotype.

generate changes in pulse amplitude (Figure 3.7 and Figure 3.8), this flicker-sensitive pathway may be involved in amplitude modulation.

3.2.6 Amplitude modulation relies on indirect flight muscles

For males to modulate amplitude, visual information must eventually alter muscle activity, but which muscles are used for this behavior? The indirect-flight-muscles (IFMs) are required to increase power during flight [60], presenting the intriguing possibility that they could also be required increase pulse amplitude. Although these muscles are active during courtship song, their role is still unclear. IFM function relies on a myosin light regulatory chain (Dmlc2) unique to this muscle, and mutations of this protein have been used to examine the role of these muscles in flight [87, 88]. A recent study utilized this method to examine the effect of

Dmlc2 mutantations on courtship song, but concluded that the IFM plays a minor role in song production [78].

Here, we use two mutations of the Dmlc2 protein to test for a role of the IFM in amplitude modulation. Phos is an alanine substitution of two myosin light chain kinase phosphorylation sites [89], while Dual is a double mutation, combining Phos with a truncation of the 46 amino acid N-terminal extension [90]. The amplitude of pulses produced by these mutant flies when paired with PIBL females was dramatically reduced compared with their wing length (Figure 3.11a). Furthermore, mutant pulses were of a lower amplitude than those produced by a rescued null strain (Cont^{Dm}, [91]), despite similar mFV at the time of pulse production. Dual flies also demonstrated a significantly lower rate of copulation (Figure 3.11b-c).

Both mutant strains failed to show normal amplitude modulation (Figure 3.11d). Phos flies increased amplitude with pre-Dis, but only at large distances, whereas Dual flies showed abnormal modulation at all distances, tending to decrease pulse amplitude with increasing pre-Dis. The partial behavior displayed by Phos, along with its intermediary rate of copulation, is likely because it is a less extreme Dmlc2 mutation than Dual. These data demonstrate that IFM function is critical for amplitude modulation. Further, since 0% of 18 Dual flies managed to copulate, we hypothesize that this behavior is an important component of courtship success. At short distances, we observed a strong negative correlation between pulse amplitude and pre-Dis for both mutant strains (Figure 3.11d), and we expand upon the possible reasons for this below.

3.2.7 Visual information intersects the song pathway upstream of dPR1

We have examined the visual inputs and muscular outputs of amplitude modulation, but to understand the interface between these two systems, we must examine the point(s) at which visual information intersects with the song circuit. Visual neurons could interface at the early stages of pulse production (song command neurons), late stages (motor-neurons),

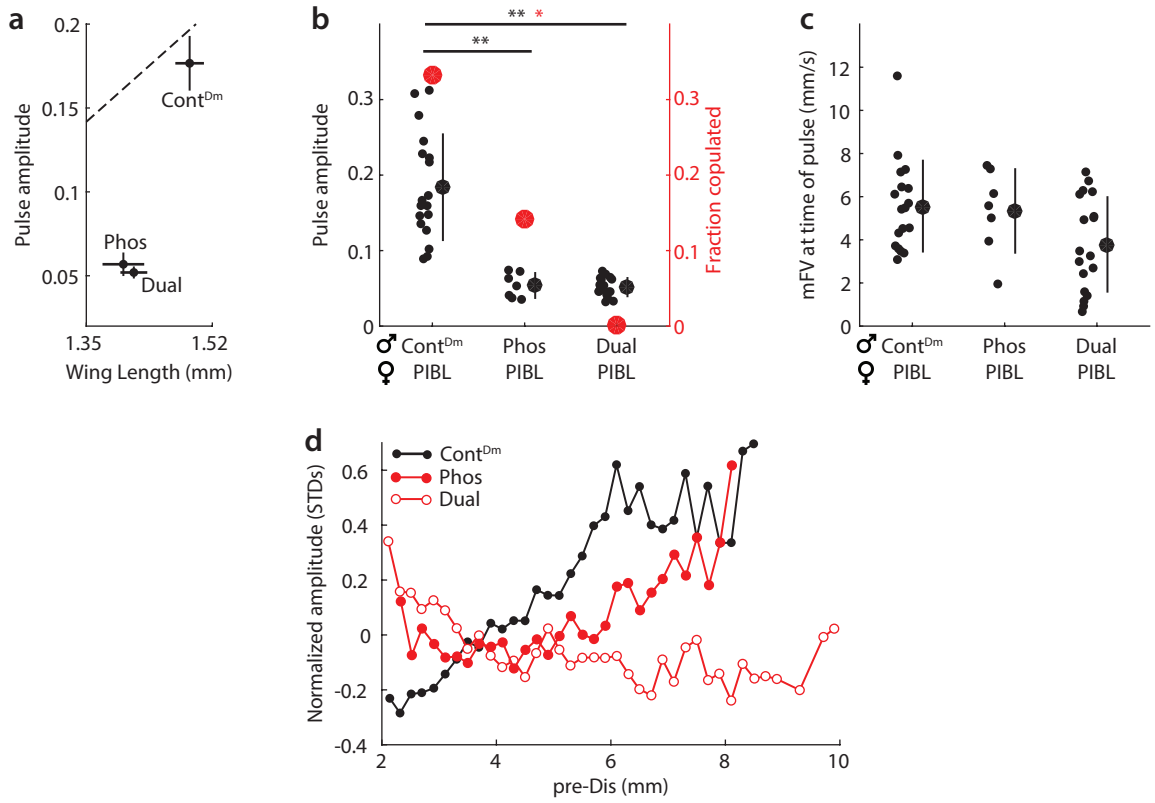

Figure 3.11: Normal IFM function is critical for amplitude modulation. For all panels, n = 18 (Cont^{Dm}), 7 (Phos), or 18 (Dual), and each fly sang > 500 pulses. **a**, The mean pulse amplitude (arbitrary units) for Phos and Dual mutants is smaller than expected given their wing length. Linear fit (dashed line) is reproduced from wild type flies. **b**, Phos and Dual mutants produce pulses with a lower mean amplitude (black, arbitrary units) than Cont^{Dm} flies. Dual flies have a significantly lower rate of successful copulations (red, chi-squared test). $* = p < 0.05$ and $** = p < 10^{-5}$. **c** The mFV during pulse production was similar for all strains ($p > 0.05$) and cannot explain the amplitude difference in **b**. **d**, Relationship between pre-Dis (bin-width 0.2mm) and pulse amplitude. Cont^{Dm} flies display amplitude modulation from 2mm which extends into the purely visual range ($r^2 = 0.79$). Phos flies show some overall modulation ($r^2 = 0.41$) but no modulation below 5mm ($r^2 = 0.00$). Dual flies show abnormal modulation for all distances: pulse amplitude decreases with increasing pre-Dis ($r^2 = 0.61$). Each point is generated from a minimum of 100 pulses. **b-c**, Individual points, mean, and STD are given for each strain/genotype.

or anywhere in between. Unfortunately, little is known of the song pathway, but three putative components have been identified: P1, pIP10, and dPR1 [33] (Figure 3.12a). During song production, neural signals are thought to descend from P1 to pIP10, and then from pIP10 to dPR1, before reaching the song central pattern generator. We thermogenetically activated each neural subset while pairing males with PIBL females, and tested for amplitude modulation. If visual information intersects the song circuit upstream of our activation site, artificial activation should disrupt modulation. In contrast, if visual information intersects downstream, modulation should be unaffected.

pIP10^{Act} flies produced louder pulses than P1^{Act} flies, and moved more quickly than both P1^{Act} and dPR1^{Act} flies, but all three strains produced pulses over a similar Dis range (Figure 3.12b-d). It is possible that these differences could contribute to variations in amplitude modulation (although only for pIP10^{Act}), but it is unlikely as we normalize amplitude for each fly and bin pre-Dis values. Activated flies produce pulses at a large range of distances and angles, some of which will be solely due to artificial activation while others may be elicited in response to the female. Pulses produced when the male faces away from the female (Ang2 $> 90°$) are entirely artificial (as $<0.5\%$ of WT pulses are produced under these conditions), and we would expect little/no amplitude modulation of these pulses. Indeed, P1^{Act} flies showed amplitude modulation up to distances of 15mm, but only for pulses generated when facing the female (Figure 3.12e), demonstrating that these flies display normal amplitude modulation which is dependent on visual information from the female.

pIP10^{Act} flies showed a similar pattern to P1^{Act} (Figure 3.12f), but amplitude modulation in dPR1^{Act} flies was highly abnormal (Figure 3.12g). dPR1^{Act} flies showed a decrease in pulse amplitude with increasing pre-Dis, but only when facing the female. This dramatic change in amplitude modulation for dPR1^{Act} flies indicates that constitutive activation of dPR1 prevents natural modulation of the IFMs and suggests that visual information is integrated into the song pathwat upstream of dPR1, but downstream of P1.

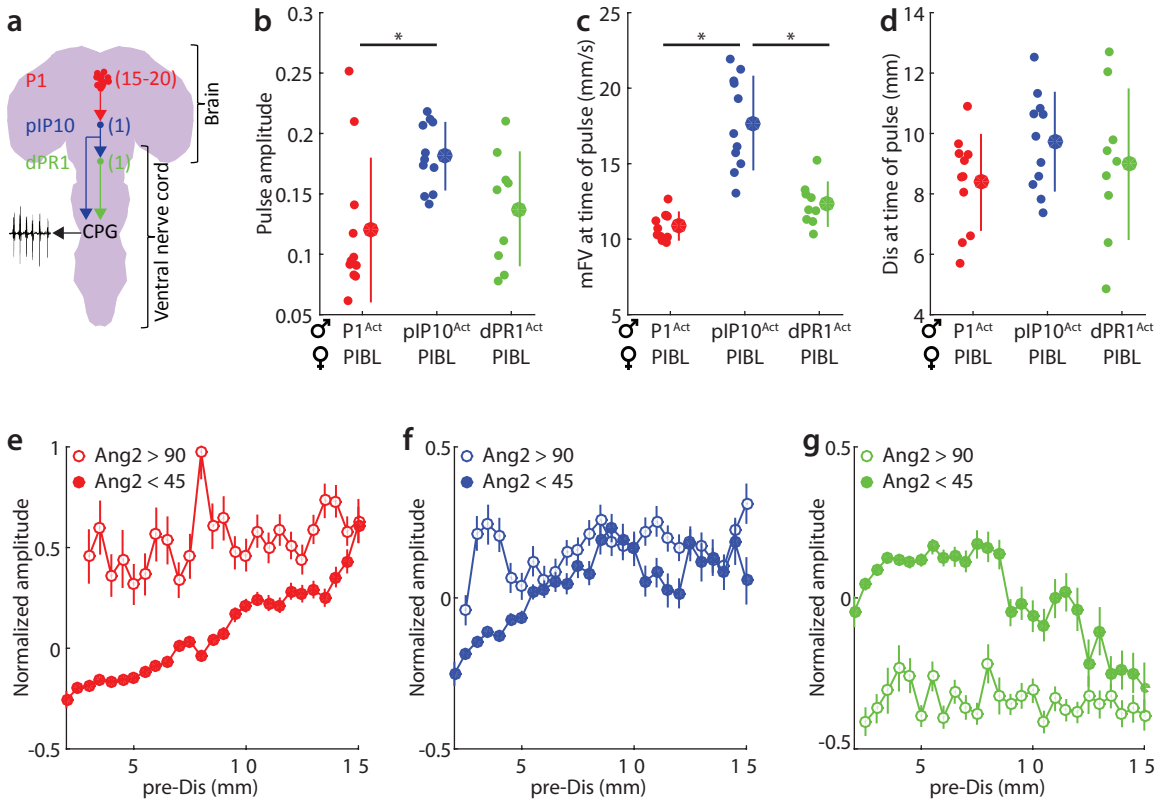

Figure 3.12: Visual information intersects with the song pathway upstream of dPR1. **a**, Diagram of the three identified components of the song circuit, along with the number of neurons in each hemisphere (numbers in brackets) and putative interconnections (arrows) [33]. P1 and pIP10 neurons are located in the brain while dPR1 is in the anterior nerve cord. pIP10 and dPR1 (but not P1) are thought to send projections to the song central pattern generator (as yet unidentified). **b**, The mean pulse amplitude (arbitrary units) for $P1^{Act}$, $pIP10^{Act}$, and $dPR1^{Act}$ males when placed with a PIBL female. $* = p < 0.05$. **c**, As in **b**, but the mean mFV at the time of pulse production, rather than pulse amplitude. $* = p < 0.10^{-4}$. **d**, As in **b**, but the mean Dis at the time of pulse production, rather than pulse amplitude. **e**, Relationship between pre-Dis (bin-width 0.5mm) and pulse amplitude for $P1^{Act}$. Amplitude modulation is observed when the male faces the female (Ang2 $< 45°$, closed circles, $r^2 = 0.94$) but not when facing away (Ang2 $> 90°$, open circles, $r^2 = 0.18$). Each point is generated from a minimum of 100 pulses. Amplitudes were normalized before splitting data, so values are comparable. **f**, As in **e**, but for $pIP10^{Act}$ flies rather than $P1^{Act}$. Amplitude modulation is weak, but present, when facing the female (Ang2 $< 45°$, closed circles, $r^2 = 0.55$) and absent when facing away from the female (Ang2 $> 90°$, open circles, $r^2 = 0.17$). **g**, As in **e**, but for $dPR1^{Act}$ flies rather than $P1^{Act}$. Amplitude modulation is abnormal (negative correlation) when facing the female (Ang2 $< 45°$, closed circles, $r^2 = 0.60$) and absent when facing away from the female (Ang2 $> 90°$, open circles, $r^2 = 0.07$). **b-g**, n = 11 ($P1^{Act}$), 11 ($pIP10^{Act}$), and 9 ($dPR1^{Act}$) and each fly sang > 500 pulses.

The increased amplitude of pulses produced at short distances when dPR1^{Act} flies face the female is akin to the results we observed with Dual and Phos flies at short distances (Figure 3.11d). Thus, when males cannot use distance cues to modulate amplitude, we observe a consistent negative trend in pulse amplitude with increasing pre-Dis. It is known that multiple sensory cues stimulate courtship and impact the activity of the song circuit [77, 92]. An overall increase in activity within the song circuit due to increased courtship drive could be responsible for these spurious changes in amplitude when the (normally dominant) modulation pathway cannot function. However, this mechanism is speculative and is only suggested by our results.

3.2.8 Using an air-supported ball setup to investigate optimal visual stimuli

While our naturalistic behavioral assay was critical in discovering amplitude modulation, it does not allow for experimental manipulations of visual stimuli. To accurately quantify visual walking behaviors in *Drosophila*, prior studies have tethered flies on an air-supported ball while presenting stimuli on a monitor [35, 93]. However, such a setup has never been combined with acoustic recordings, in part because tethered flies rarely produce song in the absence of other sensory cues [92]. We recognized that the amplitude modulation demonstrated by P1^{Act} and pIP10^{Act} flies presented a unique opportunity to overcome this limitation by eliciting pulses artificially.

We tethered P1^{Act} and pIP10^{Act} flies on an air-supported ball while acutely heating the fly head using a laser (Figure 3.13a and Methods). Two microphones were used to record the song from each wing, and synchronized visual stimuli were presented on a monitor at 144Hz. For the visual stimulus, we presented a black square, but modulated the azimuthal angle and horizontal and vertical dimensions in accordance with natural statistics (see Methods). Because our screen is not rounded, the horizontal angular size (hAng) of the stimulus varied with azimuthal position while vAng did not. Initially, we kept the horizontal and vertical di-

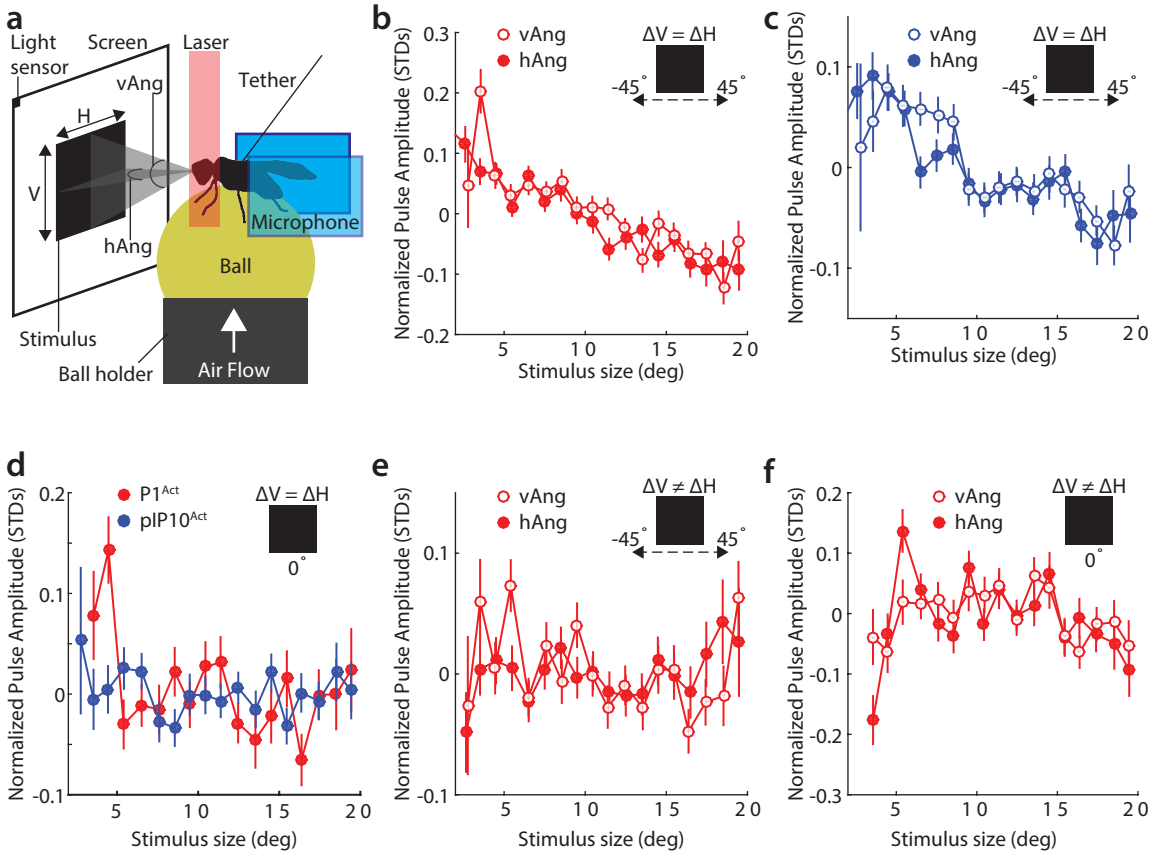

Figure 3.13: Dissecting amplitude modulation using an air-supported ball setup. **a**, Diagram of the air-supported ball setup. Two microphones (blue boxes) are used to record the song produced by each wing while an infrared laser is focused on the head of the fly. Visual stimuli are presented on a monitor at 144Hz and synchronized with acoustic recordings via a light sensor. The horizontal (H) and vertical (V) stimulus dimensions vary according to natural statistics, and the horizontal (hAng) and vertical (vAng) angular size of the stimulus is calculated based on the fly's distance from the screen (100mm). **b**, For $P1^{Act}$ flies (n = 9) viewing a stimulus with equal (but varying) H and V, normalized amplitude decreases with increasing hAng (closed circles, $r^2 = 0.91$) or vAng (open circles, $r^2 = 0.71$). The stimulus center moved between ±45°along the azimuth according to natural statistics. **c**, As in **b**, but for $pIP10^{Act}$ flies. Amplitude decreases with hAng (closed circles, $r^2 = 0.78$) or vAng (open circles, $r^2 = 0.70$). **d**, As in **b**, but the stimulus center remains at 0° in the azimuth (i.e. hAng and vAng are equal at every point in time). Neither $P1^{Act}$ (red, $r^2 = 0.18$, n = 6) or $pIP10^{Act}$ (blue, $r^2 = 0.05$, n = 6) flies show any amplitude modulation. **e**, as in **b**, but the two stimulus dimensions vary independently. $P1^{Act}$ pulse amplitude doesn't correlate with hAng (closed circles, $r^2 = 0.19$) or vAng (open circles, $r^2 = 0.06$). n = 8 flies. **f**, As in **e**, but the stimulus center remains at 0° in the azimuth. $P1^{Act}$ pulse amplitude doesn't correlate with hAng (closed circles, $r^2 = 0.01$) or vAng (open circles, $r^2 = 0.02$). n = 6 flies. **b-f**, Error bars indicate SEM. Each point is generated from ≥ 100 pulses, and each fly sang ≥ 500 pulses. vAng and hAng are calculated at ∼ 470ms before each pulse and binned with bin-width = 1°.

mensions the same at each point in time. When presented with this stimulus, both P1^{Act} and pIP10^{Act} flies increased their pulse amplitude when vAng or hAng decreased (Figure 3.13b-c). This directly confirms our behavioral results, and conclusively demonstrates amplitude modulation in the absence of any non-visual cues.

We repeated this experiment, but without any azimuthal movement in the stimulus. Surprisingly, this completely eliminated amplitude modulation in both P1^{Act} and pIP10^{Act} flies (Figure 3.13d), indicating a critical role of azimuthal movement in the behavior. This suggests that a visual cue alone is insufficient to elicit the behavior if its motion isn't similar to a female. Another possibility is that the receptive field for the neurons controlling this behavior does not cover 0° in the azimuth, although this seems unlikely as this is the region most often occupied by the female during natural behavior [77]. To test this possibility, we presented the same target at different positions in the azimuth, but didn't observe any amplitude modulation (data not shown). This establishes that motion in the azimuth is required for the behavior, and makes its independence from EMD neurons even more surprising.

If male flies are performing amplitude modulation to optimize for the acoustic intensity received by the female, optimal behavior would rely upon distinguishing changes in female distance from changes in female orientation. For example, if the female turns perpendicular to the male, hAng would increase dramatically, despite a negligible difference in inter-fly distance. One mechanism males could employ to avoid responding to orientation changes would be to modulate amplitude only in response to correlated changes in both horizontal and vertical dimensions. To test this, we decoupled the relationship between H and V, and allowed the two parameters to vary independently. Strikingly, when variations in two dimensions were uncorrelated, no amplitude modulation was observed, regardless of the presence of azimuthal motion (Figure 3.13e-f). This result makes an intriguing prediction about the natural behavior: Dis should be a better predictor of pulse amplitude than the angular size of the female projected onto the male's eye (a parameter not previously included

in the model). We ran a GLM to compare these models and found that Dis was indeed a superior predictor of pulse amplitude (data not shown).

3.3 Discussion

Increasing the amplitude of an acoustic communication signal with respect to target distance is a familiar behavior in humans [74], and has been identified in other vertebrates [75], but whether insects were capable of this sensorimotor transformation remained unknown. Here, we demonstrated not only that *Drosophila* modulate song amplitude with distance from the female, but that they modulate each pulse separately with striking rapidity.

Amplitude modulation is entirely dependent on visual cues when fly centers are separated by a space exceeding ~ 1 body length. Using uncorrelated changes in light intensity, we further demonstrate that visual signals reach the musculature within 30ms, and are dependent on the flys visual history over a time period of at least 250ms. Given the relatively slow changes in Dis during natural courtship, it may be advantageous for the male to integrate visual information over several-hundred milliseconds when estimating his distance from the female while still utilizing the most recent information before producing the next pulse.

The appearance of mFV as a secondary predictor pulse amplitude may result from a direct link between the song and motor circuit, as suggested in recent work [77]. However, it has been demonstrated that motion in *Drosophila* can dramatically alter the gain of visual neurons in both walking and flight [35, 36], and spontaneous activity in the visual cortex of rodents is known to increase with running speed [10]. These results hint at an alternative hypothesis: the effect of mFV on amplitude could derive from speed-induced changes in the activity of visual neurons. Since these effects could impact spontaneous activity (and so still exist in the dark), testing this would require neural recordings during visual stimulation while measuring song amplitude (see Future work).

For the first time in any system, we have begun to dissect the sensorimotor-circuit underlying acoustic amplitude modulation. The majority of visual object tracking research in *Drosophila* has centered on identifying components of the classical elementary motion detector (EMD). We demonstrate a previously unidentified role for EMD neurons during courtship, but find that inhibiting EMD neurons had no discernible effect on amplitude modulation. There are behaviors and neural responses that cannot be explained with an EMD model [94, 95, 85], but the neural mechanisms and components of such alternative pathways remain unknown. Amplitude modulation provides a novel opportunity to identify these pathways in the visual system. Futhermore, we demonstrate that amplitude modulation behavior depends on correlated changes in both the vertical and horizontal visual dimensions, and hypothesize that this is to make the behavior robust to changes in female orientation. To our knowledge, this is the first visual behavior identified in *Drosophila* which relies on correlated visual changes across 2 dimensions and suggests a novel neural mechanism may be responsible.

Our results suggest that visual information intersects the song pathway at a stage upstream of dPR1 neurons, but downstream of pIP10 neurons. We also establish a critical role for the IFMs in amplitude modulation which is inline with their part in powering intense flight [60].

Together, our data identify a novel and rapid sensorimotor transformation in *Drosophila* courtship which relies on highly specific and fine-tuned visual stimuli, and illustrate the importance of using naturalistic behaviors to identify and dissect complex neural computations.

3.4 Methods

3.4.1 Fly strains and rearing

For all experiments, we used 3-7 day old virgin flies raised in density-controlled bottles seeded with 8 males and 8 females for 4 days (25°C) or 7 days (18°C). For non-heat-sensitive flies, bottles were kept at 25°C and 60% relative humidity. Heat-sensitive flies were maintained at 18°C or 20°C. Virgined flies were then housed individually and kept in behavioral incubators (TriKinetics) under 12hr/12hr light/dark cycling. When recording with a female, males were painted with a small spot of opaque ultraviolet-cured glue (Norland Optical and Electronic Adhesives) on the dorsal mesothorax to facilitate identification during tracking. All wild-type strains, except for the laboratory colony Canton-S (WT2), were supplied by the Andolfatto group at Princeton University. These strains descended from single females caught in geographically diverse locations (Table 3.1). For several experiments, we used genetically modified flies; their genotypes were:

PIBL (pheromone-insensitive and blind): *w+/w+; GMR-hid/+; orco-/ orco-*

oe- (oenocyte-less and PIBL): *GMR-hid/+; PromE800-Gal4, Tub-Gal80ts/UAS-hid,UAS-stringerll; orco-/orco-*

PI (pheromone-insensitive): *w+/w+; ; orco-/ orco-*

BL (blind): *w+/w+; GMR-hid/GMR-hid*

Cont^{Kir} (UAS-Kir2.1 with half of split-GAL4) : *R53G02AD attP40/UAS-Kir2.1* and *+/UAS-Kir2.1 ; R19C10DBD attP2/+*

Cont^{TNT} (UAS-TNT with half of split-GAL4) : *R53G02AD attP40/UAS-TNT* and *+/UAS-TNT ; R19C10DBD attP2/+*

L1L2^{Kir} (Kir2.1 in L1 and L2 lamina neurons) : *R75H09AD attP40/UAS-Kir2.1; R29G11DBD attP2*

L1L2^{TNT} (TNT in L1 and L2 lamina neurons) : *R75H09AD attP40/UAS-TNT; R29G11DBD attP2*

C2C3^{Kir} (Kir2.1 in C2 and C3 lamina neurons) : *R20C11AD attP40/UAS-Kir2.1; R48D11DBD attP2*

C2C3^{TNT} (TNT in C2 and C3 lamina neurons) : *R20C11AD attP40/UAS-TNT; R48D11DBD attP2*

L4^{Kir} (Kir2.1 in L4 lamina neurons) : *R31C06AD su(Hw)attP2/UAS-Kir2.1; R34G07DBD attP2*

L4^{TNT} (TNT in L4 lamina neurons) : *R31C06AD su(Hw)attP2/UAS-TNT; R34G07DBD attP2*

T4T5^{Kir} (Kir2.1 in T4 and T5 lobula plate neurons) : *R42F06/UAS-Kir2.1*

T4T5^{Shi} and Cont^{Shi} (Temperature-sensitive shibire expressed in T4 and T5 lobula plate neurons) : *R42F06/UAS-shi^{ts}; +/UAS-shi^{ts}*

Cont^{Dm} (Full length Dmlc2 gene expressed in a null Mlc2E38 background): *w; P[mlc2^{+},w+]/P[mlc2^{+},w+] ; mlc2$^{E38.13}$/mlc2^{E38e}*

Phos (Transgenic line expressing Dmlc2 with phosphorylation sites serines 66 and 67 replaced by alanines) : *w ; P[mlc2^{S66A,S67A},w+]/P[mlc2^{S66A,S67A},w+] ; mlc2$^{E38.13}$/mlc2^{E38e}*

Dual (Transgeneic line expressing Dmlc2 with Phos mutations and lacking amino acids 2-46) : *w ; P[mlc2$^{\Delta 2-46;S66A,S67A}$,w+]/P[mlc2$^{\Delta 2-46;S66A,S67A}$,w+] ; mlc2$^{E38.13}$/mlc2^{E38e}*

FRU^{Act} (TrpA1 expressed in all *fruitless*-positive neurons): *UAS-TrpA1/+; fruP1-GAL4/+*

DSX^{Act} (TrpA1 expressed in all *doublesex*-positive neurons): *UAS-TrpA1/+; dsx-GAL4/+*

P1^{Act} (TrpA1 expressed in the P1 neural cluster): *UAS-frtstopfrt-TrpA1/+; fru P1-FLP/NP2631*

pIP10^{Act} (TrpA1 expressed in pIP10 neurons): *UAS-frtstopfrt-TrpA1/+; fru P1-FLP/VT40556*

dPR1^{Act} (TrpA1 expressed in dPR1 neurons): *UAS-frtstopfrt-TrpA1/+; fru P1-FLP/VT41688*

We acquired *GMR-hid* and *UAS-shi^{ts}* flies from the Bloomington Stock Center, *orco-* flies from Leslie Vosshall, *fru P1-GAL4*, *fru P1-FLP*, *VT41688*, and *VT40556* flies from Barry Dickson, NP2631 flies from the Kyoto stock center, and *DSX-GAL4* flies from Stephen Goodwin. Michael Reiser provided all split-GAL4 lines for labeling lamina neurons [84], and Cont^{Dm} [91], Phos [89], and Dual [90], lines were provided by Jim O. Vigoreaux.

For arista- and tarsi- cutting paradigms (AC and TCBL), to render flies deaf (AC) or remove gustatory cues (TCBL), WT1 (for AC) or BL (for TCBL) flies were anesthetized with CO^2, and aristae or tarsi were removed with fine scissors >20 hours prior to recording. To generate SP flies, *Drosophila melanogaster* sex peptide [56] was injected into PIBL virgin females 12-24 hours prior to recording. These flies were anesthetized on ice during injections. For recordings from headless FRU^{Act} flies, heads were removed during cold anesthesia < 5 minutes before recording.

3.4.2 Behavioral chamber

The recording chamber used for all untethered experiments was as described in [77] with minor alterations. We used a sectional LED ring light (edmund optics) for experiments with constant or light/dark illumination, and a 3" white LED ring light (edmund optics) when switching between 4 light intensity levels. Finally, we used an external triggering system to record video at 60Hz.

3.4.3 Air-supported ball

Designs for the ball holder were supplied by Vivek Jayaraman, and 6mm diameter HDPE balls (Craig Technologies) were roughened slightly with sand-paper before use. Flies were tethered to a 0.005" tungsten rod (A-M Systems) using a small spot of ultraviolet-cured glue (Norland Optical and Electronic Adhesives) on the anterior mesothorax under cold anesthesia. All flies were tethered < 30 minutes prior to recording.

Song signals were recorded with 2 NR23158 microphones placed either side of the fly (Knowles Electronics). Both microphones were connected to a custom-built amplifier [70]. Stimuli were presented on an XL2411T monitor (BenQ) at 144Hz using Psychtoolbox-3, and synchronized with microphone recordings via a light sensor (GA1A12S202, Adafruit). A 808nm laser (Dragon Lasers), passing through a 780nm collimation fiber (Thor labs) and focused on the fly head, was used to heat flies. For each recording, laser power was increased until flies began singing, and then held constant throughout the recording. All recordings lasted 15 minutes.

3.4.4 Courtship assay

When recording male/female pairs, the chamber was prepared as previously describe [77]. Flies were loaded individually into the chamber using a custom-built aspirator. To optimize for peak fly activity, we began recordings within 150 minutes of the behavioral incubator lights switching on. Recordings were terminated when copulation occurred or after 30 minutes (classified as no copulation). Recordings with no song in the first 5 minutes were terminated early and disregarded.

3.4.5 Wing Measurement

Wings were measured after behavioral experiments with wing length defined as previously described [79]: the distance from the intersection of the anterior cross vein and longitudinal vein 3 (L3) to the intersection of L3 with the distal wing margin. All wing lengths were measured at 5x magnification using a reticule inserted into a microscope eyepiece.

3.4.6 Thermogenetic activation in the behavioral chamber

For thermogenetic activation of FRU, DSX, P1, pIP10, and dPR1 neurons in males, the chamber was heated with a coil (HSTAT, BriskHeat) to 26°C (for FRU activation), 27°C

(for DSX activation), or 32-34°C (for P1, pIP10, and dPR1 activation). For experiments in which a heat activated fly was placed with a female (see Figure 3.12), activated song was confirmed prior to female introduction, and after female removal at the end of the 30 minute trial. If either of these criteria were not met, the trial was discarded. When heat-activated flies were recorded in the absense of a female (see Figure 3.4f), recordings were not timed to peaks in circadian activity.

3.4.7 Dark/Light transition assay

For acute transitions between dark/light conditions (see Figure 3.5b and Figure 3.7a), the chamber was covered completely with BK5 Blackout Fabric (Thor Labs), and flies were loaded in darkness. A custom built voltage switch was used in combination with a Master 8 (A.M.P.I.) pulse generator to cycle power to the sectional LED ring light (Edmund Optics) with a period of 30s (15s on/off). On/off periods were detected post-experiment using the light-intensity during each camera frame. As flies were activated in isolation, recordings were not timed to peaks in circadian activity.

3.4.8 Multi-level light intensity assay

The intensity of a 3" white LED ring light (edmund optics) was adjusted using an analog voltage signal generated from the same data acquisition terminal (National Instruments) used to acquire amplifier signals from the microphones and trigger the camera. This ensured synchrony between all components. Lux levels were calibrated by placing a light sensor (GA1A12S202, Adafruit) in the behavioral chamber and recording the output over the entire range of light intensities. For each recording, the sequence of light intensities presented was randomly generated using a truncated 4-level maximum length sequence; this eliminated any confounds of periodicity while ensuring an even distribution of transitions [96].

In experiments where 0.5lux was one of the light intensities used, the chamber was covered completely with BK5 Blackout Fabric (Thor Labs) to avoid light contamination from the

computer monitor. If 650lux was the lowest light intensity, the shutter time of the camera was continually adjusted throughout the experiment to prevent image saturation at higher light intensities and allow for fly tracking. As flies were activated in isolation, recordings were not timed to peaks in circadian activity.

3.4.9 Inactivation of motion-sensitive neurons

Chronic silencing of motion-sensitive lamina neurons with TNT and Kir2.1 (see Figure 3.9), and chronic silencing of T4 and T5 lobula plate neurons with Kir2.1, (see Figure 3.10), were achieved using the genetic crosses described above.

We performed acute inactivation of T4 and T5 cells using temperature sensitive shibire. Control flies ($Cont^{shi}$) were paired with PIBL females at a permissive temperature (∼22°C). Experimental flies were placed at a non-permissive temperature (∼27°C) ∼30mins prior to being paired with a PIBL female, and the entire courtship bout was recorded at the non-permissive temperature.

3.4.10 Data processing and analysis

All data processing and analysis was conducted in MATLAB (MathWorks, Inc.).

Significance Testing

Unless otherwise specified in the text, significance tests were as follows: To determine significant differences between means, we used one-way ANOVA or KruskalWallis analyses, depending on whether the distributions in question were non-normal (as identified by the Jarque-Bera test for normality). For confidence intervals in Figure 3.1e-f, non-overlap was used as a conservative estimate of significant differences. For normally distributed data, variance was estimated to be similar between groups, as required for applying ANOVA. Given variability in behavior, we sampled a large number of flies for each wild type strain (~ 40) before performing any statistical tests. After observing the effect size in wild type data, we

then collected between 5 and 40 flies (depending on the analysis) for other genotypes and manipulations. Blinding was not necessary for these experiments because all data analyses were automated. As all statistical tests were performed between different fly strains, or between flies of the same strain with an internal control, randomization of animal groups was not necessary.

Normalizing pulse amplitude in the behavioral chamber

We defined the raw amplitude of each pulse as its maximum noise-subtracted amplitude averaged across the three microphones with the largest signal. We took a total of 600,000 pulse amplitudes produced by our 8 wild type strains when courting PIBL, SP, or AC females. To avoid normalizing for differences in Dis throughout the chamber, we ordered these pulses by the Dis at which they were produced and split them into groups of 20,000 (all results in this paper are effectively unchanged without this step). For each group of 20,000 pulses, we divided the pulse amplitude produced at each point within the chamber (bin-width 0.5mm) by the mean amplitude produced by that particular fly (within that distance-based group of 20,000 pulses). All pulses produced >11mm from the center of the chamber were excluded due to data limitations (∼10% of pulses), and flies which did not produce >20 pulses within the group of 20,000 were not included.

We then recombined the 600,000 pulses and calculated the fractional deviation from the mean (across all locations) at each position in the chamber with 2-dimensional kernel density estimation (see Figure 3.1b). Using this map of fractional deviation, all pulse amplitudes were scaled depending on the position of the male at the time of pulse production. These values were then used to compare the song amplitudes produced by different strains and genetic manipulations (see Figure 3.1c-d, Figure 3.5a, Figure 3.11a-b, and Figure 3.12b.

For analyses involving "Normalized amplitude" (throughout the paper), pulse amplitudes were further normalized before combining individual flies. Flies were required to sing a minimum number of pulses (specified in each figure legend) and the amplitudes were then

z-scored (mean subtracted and then divided by the STD). Thus, values of "Normalized amplitude" represent the number of standard deviations from the mean amplitude and can take postitive and negative values.

Normalizing pulse amplitude for tethered flies

To control for small differences in the size and position of each fly, and differences in the sensitivity of the two microphones, we separately normalized the amplitude of pulses produced by each wing. Pulses which were recorded with approximately equal amplitude on each microphone (within 25%) were excluded as these could not be attributed to a particular wing. The remaining pulses were then grouped by wing and z-scored separately before being combined for analysis. Thus, the tethered version of "Normalized amplitude" is also measured in standard deviations from the mean amplitude.

Fly tracking and song segmentation

Both tracking and segmentation were as previously described [77].

Quantification of movement parameters

Males can approach the female from either side during courtship. As a result, distinctions between left/right lateral movement and anticlockwise/clockwise rotations or angles are not meaningful for the analyses we performed. For this reason, only forward velocities were allowed to take negative vales and we use absolute values for lateral movements and rotations.

GLM implementation

For this work, we used GLMs only for model selection, and so used 100% of the data for model fitting (see Figure 3.1e-f, Figure 3.2a). We fit all models using the method described in [49], which uses a sparseness prior to penalize redundant features. Movement features were z-scored for each fly before running the model to account for any trivial differences in

behavior. Given the non-binary nature of our model output (normalized pulse amplitudes) we used a Gaussian link function. To calculate the deviance reduction for each fit, data were randomly split into 4 equal subgroups for cross-validation, and this process was repeated 1000 times to estimate 95% confidence intervals.

Model selection

When determining which movement features were most predictive of normalized pulse amplitude (see Figure 3.1e-f), we considered a stimulus history of 1s prior to pulse production for all features. We first selected the single feature which produced the largest deviance reduction (Dis), and then re-ran models with paired inputs (e.g. Dis and mFV), to determine if adding a second feature improved model performance. Subsequent features were added until the relative improvement from an additional feature was not significantly different from zero, but adding a third feature beyond Dis and mFV produced no significant improvement in deviance reduction.

Natural autocorrelation in movement features

We extracted movement features from all wild type flies courting PIBL females whose trials lasted longer than 20 minutes (to obtain sufficient data for the autocorrelation). For each delay, the autocorrelation was normalized by a correlation with shuffled data. The mean correlation across flies was scaled to have a minimum of zero and maximum of 1 for ease of visualization (see Figure 3.2b).

Amplitude modulation curves

When testing for amplitude modulation (for example, see Figure 3.2c) we binned the normalized pulse amplitudes produced by all flies of a particular strain/manipulation according to the pre-Dis (or Dis) for each pulse. We used a bin-width of 0.2mm unless data-limited (for example, when analyzing pulses produced when facing away from the female, Figure

3.5d). After combining flies, bins with <100 pulses were excluded (unless otherwise specified in figure legends), before r^2 values were calculated. SEM values are included only for illustrative purposes as subsequent pulses cannot be considered independent samples.

All pulses produced at Dis<1.99mm were excluded as tracking errors because fly centers are very unlikely be this close given their body length (∼0.5% of pulses). For non-heat-activated flies, pulses produced at Dis>12.01mm were also excluded as segmentation errors since flies rarely naturally sing beyond that distance (∼0.8% of pulses).

When testing for amplitude modulation in tethered flies, we used the same methodology, but binned hAng or vAng, rather than pre-Dis, with a bin-width of 1°.

Testing for correlations between pulse parameters

For Figure 3.3b, e, and h, empirical joint probability density functions (PDFs) were calculated by binning data in 2 dimensions. For Figure 3.3c, f, and i, independent PDFs were calculated as the outer product of the empirical marginal PDFs. In all cases, PDFs were calculated using only values within 1 STD of the mean, with bin-width 0.1 STDs, because the sparsity of values prevented accurate empirical PDF estimation beyond this range. Since two pulses are required to calculate an IPI, the initial pulses of each train were not included when testing for a correlation between IPI and amplitude.

Responses to multi-level changes in light intensity

For Figure 3.7b-c, peaks were defined as significant if the mean normalized amplitude produced by flies at the peak was significantly different from the mean normalized amplitude produced during the 10 time-points preceding the intensity transition. This analysis was aimed at identifying the speed of intensity responses and necessitated narrow bins within the time domain. For later analyses (see Figure 3.7d-e and Figure 3.8) a "response" is calculated from the difference in normalized amplitude between pulses produced up to 45ms

before the switch, and between 15ms and 60ms after the switch. Thus, a positive response indicates that males produced louder pulses after the light intensity transition.

Visual stimuli presented to tethered flies

Visual stimuli were generated using tracking statistics from P1^{Act} males paired with PIBL females. We concatenated the data from 11 flies and eliminated all sections where the female moved more than 45° from the males line of sight (i.e. Ang2 >45°, see Figure 3.5d). This produced >115 minutes of natural variations in Ang2 from which we randomly selected a 15 minute segment for each trial. To replicated naturalistic variations in the size of the stimulus, we extracted 15 minutes of Dis values from the same sample of time-points. The random selection of Ang2 and Dis sections were independent, so the azimuthal location of the stimulus was uncorrelated with its size. Relative changes in Dis were used to control the dimensions of the stimulus. For example, if Dis doubled, the vertical and horizontal dimensions of the stimulus halved. This naturalistic stimulus was used for Figure 3.13b-c.

For experiments where the stimulus was stationary in the azimuth, variations in size were still produced in the same way (Figure 3.13d). To independently vary the stimulus size along horizontal and vertical dimensions, we randomly selected two different 15 minute segments of Dis (Figure 3.13e-f).

Chapter 4

Future directions and Conclusions

4.1 Future work

There are two major future directions leading directly from this work which I will discuss here. Both have already been initiated in collaboration with other members of the Murthy lab, and promise to push our understanding of the natural dynamics of this behavior, and its neural circuitry, to new levels.

4.1.1 Fly triplets with automated song segmentation

In nature, *Drosophila* courtship is not limited to interactions between a lone pair of flies, and when multiple males are placed with a single female, they will compete to copulate with her [97, 98]. Similarly, if a male is placed with multiple females, he will not limit his courtship to a single fly, and will attempt to copulate with all females until one accepts him. Prior studies have demonstrated that a male with undamaged wings will out-compete a male with his wings removed or partially damaged [80]. It has also been shown that when presented with two females, one of which has limited or non-functional hearing, a male is more likely to copulate with the normal female [97]. Furthermore, courtship song doesnt exclusively effect female behavior. When males hear song, they show dramatically increased activity levels,

and when placed with other males, will follow each other and sing, forming courtship chains [99].

These studies indicate that courtship song plays an important role in mate selection, and suggests that the song of one male could have a dramatic effect on competing males. However, this has never been studied in detail because no behavioral assay has been capable of automatically segmenting songs produced by separate males in the same chamber. Our microphone array presents an opportunity to solve this problem by utilizing the pattern of signals across the microphones to localize each bout of song to a specific male.

Using our data set of single males, we have already performed this localization in our nine-microphone chamber, and our estimates of male location have a median error of $\sim$2mm for song pulses. To maximize the accuracy of this system, we have redesigned the chamber to include 16 microphones without expanding the diameter. This increases the number of microphones detecting each pulse—a critical determinant of localization accuracy. This new system will allow us to place two males with a single female and automatically pair each pulse with the male that produced it (using the information from our tracking software). A preliminary data set of triplets (two males competing for a single female) has already been recorded in this chamber and we observe highly dynamic interactions between the three flies.

We expect these experiments to advance the field in three distinct ways. Firstly, our tracking data will provide new insights into the movements produced by males when competing for a single female. We can apply computational modeling to dissect how the movements of a secondary male impact the male-female interactions we've already observed in single pairs and use genetic manipulations to assess the sensory modalities responsible for these effects. Secondly, we will have a unique opportunity to determine how songs produced by one male impact the singing decisions of a second male, and whether such inter-male effects are dependent on their location relative to female. Third, since we are presenting the female with a choice between different flies, we can use her mating decision as an indicator of song

preference. Since we are also able to separate the songs of the two males, we can determine which features of winning songs are most predictive of male success.

This extension of our current system will develop our understanding of natural courtship behavior and the underlying computations which must be performed when males are in the presence of multiple competitors or targets.

4.1.2 Calcium imaging and electrophysiology during song production

While genetic manipulations, quantitative behavior, and modeling have given us important insights into the neural mechanisms underlying song patterning, these techniques do not allow the observation of neural activity during behavior. Developing such a technique is vital to fully understand the ongoing dynamics of the neural network responsible for song production in response to sensory cues. Techniques exist to image calcium transients in the fly brain while keeping the wings unobstructed as flies walk on an air-supported ball [35]. However, males rarely sing under such conditions, even when presented with a female abdomen to provide olfactory and gustatory stimulation [92]. When these stimuli succeed in eliciting song, the sensory stimulus is difficult to quantify as it relies on the males decision to tap or taste the female abdomen, a behavior which will differ during every presentation. In amplitude modulation, we have identified of a sensory-driven modulation of ongoing song production, and this presents an opportunity to overcome these obstacles.

We have already demonstrated that song elicited from P1^{Act} and pIP10^{Act} flies can be modulated by artificial visual stimuli while males walk on an air-supported ball. These stimuli are highly quantifiable, repeatable, and easily manipulated to probe neural network function during stimulus presentation. We have recently developed a genetic strategy within the Murthy lab to activate song command neurons while recording neural activity in downstream regions. In brief, P1^{Act} flies, which express TrpA1 via the GAL-UAS binary expression system [33], are further genetically modified to express GCaMP6f (a genetically

encoded calcium indicator with fast kinetics [34]) pan-neuronally using a second binary expression system (LexA-LexAop). This allows us to activate the song circuit by raising the temperature of the brain (to depolarize P1 neurons) while imaging activity levels in separate neural populations via changes in calcium florescence—a technique which has already been successfully employed in the lab. This genetic system can easily be modified to activate P1 optogenetically for increased temporal resolution [31]. With this system we can functionally isolate the areas that respond to P1 activation and are modulated by visual stimuli. Further, we can record ball motion using a filter lens to select for a wavelength outside of those used for imagine or optogenetic activation which, when combined with microphone recordings, will give an accurate readout of fly motion and pulse amplitude at every point in time.

While this strategy will provide insights into the interaction between visual stimuli and song neurons in the brain, many neurons in the song circuit, including the central pattern generator and motorneurons, are in the ventral nerve cord. We have developed a strategy for recording from these neurons in the fly, but the dissection is not compatible with song recording, or tethered walking, as the legs are removed and wing motion is blocked. However, the nerve comprising most of the motor neurons involved in song production (ADM nerve [60]) remains accessible. Neural spikes can be recorded from this nerve using a suction electrode and sorted with an unsupervised algorithm [100]. Thus, it may be possible to infer pulse amplitude from ADM nerve activity. The same genetic strategy (heating $P1^{Act}$ flies which also express GCaMP6f in all neruons) could then be using to image neural activity in the ventral nerve cord in response to P1 activation combined with visual stimulation.

4.2 Conclusions

Through quantitative analysis of a rich, natural behavior in *Drosophila*, combined with genetic manipulations and computational modeling, we have made strides toward understanding the behavioral and neural complexities inherent to courtship song production. Variability

in acoustic signal production was commonly assumed to stem from noise in underlying neural circuits [43]. In direct contrast, we have demonstrated that flies use sensory signals not only to pattern the structure of their song over hundreds of milliseconds (Chapter 2), but that even variations in song amplitude result from the strategic exploitation of sensory cues with extraordinary rapidity (Chapter 3).

Thus, rather than a fixed action pattern, *Drosophila* song production is a sequence of rapid decisions designed to increase the chance of copulation. Our data suggest that male flies integrate sensory information on ethologically relevant timescales, and require naturalistic stimulus in order to engage this decision-making circuitry. This reinforces the importance of studying natural behavior to fully understand how sensory stimuli influence behavior.

However, even at the behavioral level, many questions still remain. We have demonstrated a role for sensory cues in song production, but similar cues must influence the male's decision to perform other behaviors, such as licking and attempted copulation. From our data, it seems unlikely that these behavioral transitions are the result of neural noise in underlying circuits, and like song, the the classification of these behaviors may also be too simplistic.

More generally, we hypothesize that variability in "stereotyped" insect behaviors may indicate undiscovered complexity in neural circuits which would be revealed through accurate quantification of natural behavior.

Bibliography

[1] Matteo Carandini and Anne K Churchland. Probing perceptual decisions in rodents. *Nature neuroscience*, 16(7):824–831, 2013.

[2] O'Connor, Daniel H, Nathan G Clack, Daniel Huber, Takaki Komiyama, Eugene W Myers, and Karel Svoboda. Vibrissa-based object localization in head-fixed mice. *The Journal of neuroscience : the official journal of the Society for Neuroscience*, 30(5):1947–1967, 2010.

[3] Mark H Histed, Lauren A Carvalho, and John H Maunsell. Psychophysical measurement of contrast sensitivity in the behaving mouse. *Journal of neurophysiology*, 107(3):758–765, 2012.

[4] Kenneth H Britten, Michael N Shadlen, William T Newsome, and J Anthony Movshon. Responses of neurons in macaque MT to stochastic motion signals. *Visual Neuroscience*, 10(6):1157–1169, 1993.

[5] Joshua I. Gold and Michael N. Shadlen. Representation of a perceptual decision in developing oculomotor commands. *Nature*, 404(6776):390–394, 2000.

[6] Joshua I Sanders and Adam Kepecs. Choice ball: a response interface for two-choice psychometric discrimination in head-fixed mice. *Journal of neurophysiology*, 108(12):3416–3423, 2012.

[7] Bingni W. Brunton, Matthew M. Botvinick, and Carlos D. Brody. Rats and humans can optimally accumulate evidence for Decision-Making. *Science*, 340(6128):95–98, 2013.

[8] Shankar Sachidhanandam, Varun Sreenivasan, Alexandros Kyriakatos, Yves Kremer, and Carl C H Petersen. Membrane potential correlates of sensory perception in mouse barrel cortex. *Nature Neuroscience*, 16(11):1671–1677, 2013.

[9] Christopher D. Harvey, Philip Coen, and David W. Tank. Choice-specific sequences in parietal cortex during a virtual-navigation decision task. *Nature*, 484(7392):62–68, 2012.

[10] Aman B Saleem, Asl Ayaz, Kathryn J Jeffery, Kenneth D Harris, and Matteo Carandini. Integration of visual motion and locomotion in mouse visual cortex. *Nature Neuroscience*, 16(12):1864–1869, 2013.

[11] Gidon Felsen and Yang Dan. A natural approach to studying vision. *Nature neuroscience*, 8(12):1643–1646, 2005.

[12] Alex Gomez-Marin, Joseph J Paton, Adam R Kampff, Rui M Costa, and Zachary F Mainen. Big behavioral data: psychology, ethology and the foundations of neuroscience. *Nature Neuroscience*, 17(11):1455–1462, 2014.

[13] David J Anderson and Pietro Perona. Toward a science of computational ethology. *Neuron*, 84(1), 2014.

[14] Yi Deng, Philip Coen, Mingzhai Sun, and Joshua W Shaevitz. Efficient multiple object tracking using mutually repulsive active membranes. *PloS one*, 8(6), 2013.

[15] Fabrice de Chaumont, Renata Dos-Santos Coura, Pierre Serreau, Arnaud Cressant, Jonathan Chabout, Sylvie Granon, and Jean-Christophe Olivo-Marin. Computerized video analysis of social interactions in mice. *Nature Methods*, 9(4):410–417, 2012.

[16] Gordon J. Berman, Daniel M. Choi, William Bialek, and Joshua W. Shaevitz. Mapping the stereotyped behaviour of freely moving fruit flies. *Journal of The Royal Society Interface*, 11(99), 2014.

[17] Joshua T Vogelstein, Youngser Park, Tomoko Ohyama, Rex A Kerr, James W Truman, Carey E Priebe, and Marta Zlatic. Discovery of brainwide neural-behavioral maps via multiscale unsupervised structure learning. *Science*, 344(6182):386–392, 2014.

[18] Eviatar Yemini, Tadas Jucikas, Laura J Grundy, André E X Brown, and William R Schafer. A database of caenorhabditis elegans behavioral phenotypes. *Nature Methods*, 10(9):877–879, 2013.

[19] Adam J Calhoun, Sreekanth H Chalasani, and Tatyana O Sharpee. Maximally informative foraging by caenorhabditis elegans. *eLife*, 3, 2014.

[20] C C Ioannou, V Guttal, and I D Couzin. Predatory fish select for coordinated collective motion in virtual prey. *Science*, 337(6099):1212–1215, 2012.

[21] M Mller and R Wehner. The hidden spiral: systematic search and path integration in desert ants, cataglyphis fortis. *Journal of Comparative Physiology A*, 175(5):525–530, 1994.

[22] Rdiger Wehner and Bruno Lanfranconi. What do the ants know about the rotation of the sky? *Nature*, 293(5835):731–733, 1981.

[23] Matthias Wittlinger, Rdiger Wehner, and Harald Wolf. The ant odometer: stepping on stilts and stumps. *Science*, 312(5782):1965–1967, 2006.

[24] M Wittlinger, R Wehner, and H Wolf. The desert ant odometer: a stride integrator that accounts for stride length and walking speed. *Journal of Experimental Biology*, 210(2):198–207, 2007.

[25] M Wittlinger, H Wolf, and R Wehner. Hair plate mechanoreceptors associated with body segments are not necessary for three-dimensional path integration in desert ants, cataglyphis fortis. *Journal of Experimental Biology*, 210(3):375–382, 2007.

[26] Sabine Wintergerst and Bernhard Ronacher. Discrimination of inclined path segments by the desert ant cataglyphis fortis. *Journal of Comparative Physiology A*, 198(5):363–373, 2012.

[27] David W. Franklin and Daniel M. Wolpert. Computational mechanisms of sensorimotor control. *Neuron*, 72(3):425–442, 2011.

[28] Myrka Zago, Gianfranco Bosco, Vincenzo Maffei, Marco Iosa, Yuri P Ivanenko, and Francesco Lacquaniti. Internal models of target motion: expected dynamics overrides measured kinematics in timing manual interceptions. *Journal of neurophysiology*, 91(4):1620–1634, 2004.

[29] T. S. Collett and M. F. Land. How hoverflies compute interception courses. *Journal of comparative physiology*, 125(3):191–204, 1978.

[30] Matteo Mischiati, Huai-Ti Lin, Paul Herold, Elliot Imler, Robert Olberg, and Anthony Leonardo. Internal models direct dragonfly interception steering. *Nature*, 517(7534):333–338, 2015.

[31] Hidehiko K Inagaki, Yonil Jung, Eric D Hoopfer, Allan M Wong, Neeli Mishra, John Y Lin, Roger Y Tsien, and David J Anderson. Optogenetic control of drosophila using a red-shifted channelrhodopsin reveals experience-dependent influences on courtship. *Nature Methods*, 11(3):325–331, 2014.

[32] Daniel E Bath, John R Stowers, Dorothea Hrmann, Andreas Poehlmann, Barry J Dickson, and Andrew D Straw. FlyMAD: rapid thermogenetic control of neuronal activity in freely walking drosophila. *Nature Methods*, 11(7):756–762, 2014.

[33] Anne C von Philipsborn, Tianxiao Liu, Jai Y Yu, Christopher Masser, Salil S Bidaye, and Barry J Dickson. Neuronal control of drosophila courtship song. *Neuron*, 69(3):509–522, 2011.

[34] Tsai-Wen Chen, Trevor J. Wardill, Yi Sun, Stefan R. Pulver, Sabine L. Renninger, Amy Baohan, Eric R. Schreiter, Rex A. Kerr, Michael B. Orger, Vivek Jayaraman, Loren L. Looger, Karel Svoboda, and Douglas S. Kim. Ultrasensitive fluorescent proteins for imaging neuronal activity. *Nature*, 499(7458):295–300, 2013.

[35] Eugenia M Chiappe, Johannes D Seelig, Michael B Reiser, and Vivek Jayaraman. Walking modulates speed sensitivity in drosophila motion vision. *Current Biology*, 20(16):1470–1475, 2010.

[36] Gaby Maimon, Andrew D Straw, and Michael H Dickinson. Active flight increases the gain of visual motion processing in drosophila. *Nature Neuroscience*, 13(3):393–399, 2010.

[37] MB Sokolowski. Drosophila: genetics meets behaviour. *Nature Reviews Genetics*, 2(11):879–890, 2001.

[38] Florian von Schilcher. The role of auditory stimuli in the courtship of drosophila melanogaster. *Animal Behaviour*, 24(1):18–26, 1976.

[39] H C Bennet-Clark and A W Ewing. Pulse interval as a critical parameter in the courtship song of drosophila melanogaster. *Animal Behaviour*, 17(4):755–759, 1969.

[40] null and null. BIRDSONG AND HUMAN SPEECH: common themes and mechanisms. *Annual Review of Neuroscience*, 22(1), 1999.

[41] D Bentley and RR Hoy. The neurobiology of cricket song. *Scientific American*, 231(2):34–50, 1974.

[42] Jon T Sakata and Michael S Brainard. Online contributions of auditory feedback to neural activity in avian song control circuitry. *Journal of neuroscience*, 28(44):11378–11390, 2008.

[43] Dezhe Z Jin and Alexay A Kozhevnikov. A compact statistical model of the song syntax in bengalese finch. *PLoS computational biology*, 7(3), 2011.

[44] JC Hall. The mating of a fly. *Science*, 264(5166):1702–1714, 1994.

[45] Ebru Demir and Barry J Dickson. fruitless splicing specifies male courtship behavior in drosophila. *Cell*, 121(5):785–794, 2005.

[46] Anna B Ziegler, Berthelot-Grosjean, Martine, and Yael Grosjean. The smell of love in drosophila. *Frontiers in physiology*, 4, 2013.

[47] BS Baker, BJ Taylor, and JC Hall. Are complex behaviors specified by dedicated regulatory genes? reasoning from drosophila. *Cell*, 105(1):13–24, 2001.

[48] Pingkalai R Senthilan, David Piepenbrock, Guvanch Ovezmyradov, Bjrn Nadrowski, Susanne Bechstedt, Stephanie Pauls, Margret Winkler, Wiebke Mbius, Jonathon Howard, and Martin C Gpfert. Drosophila auditory organ genes and genetic hearing defects. *Cell*, 150(5):1042–1054, 2012.

[49] Patrick J. Mineault, Simon Barthelmé, and Christopher C. Pack. Improved classification images with sparse priors in a smooth basis. *Journal of Vision*, 9(10):1–24, 2009.

[50] Ana Calabrese, Joseph W. Schumacher, David M. Schneider, Liam Paninski, and Sarah M. N. Woolley. A generalized linear model for estimating spectrotemporal receptive fields from responses to natural sounds. *PLoS ONE*, 6(1), 2011.

[51] Jonathan W Pillow, Jonathon Shlens, Liam Paninski, Alexander Sher, Alan M Litke, EJ Chichilnisky, and Eero P Simoncelli. Spatio-temporal correlations and visual signalling in a complete neuronal population. *Nature*, 454(7207):995–999, 2008.

[52] Tatyana Sharpee, Nicole C Rust, and William Bialek. Analyzing neural responses to natural signals: maximally informative dimensions. *Neural computation*, 16(2):223–250, 2004.

[53] Alexander R. Trott, Nathan C. Donelson, Leslie C. Griffith, and Aki Ejima. Song choice is modulated by female movement in drosophila males. *PLoS ONE*, 7(9), 2012.

[54] Chun Siong Soon, Marcel Brass, Hans-Jochen Heinze, and John-Dylan Haynes. Unconscious determinants of free decisions in the human brain. *Nature Neuroscience*, 11(5):543–545, 2008.

[55] Emmanuel Perisse, Yan Yin, Andrew C Lin, Suewei Lin, Wolf Huetteroth, and Scott Waddell. Different kenyon cell populations drive learned approach and avoidance in drosophila. *Neuron*, 79(5):945–956, 2013.

[56] Nilay Yapici, Young-Joon J Kim, Carlos Ribeiro, and Barry J Dickson. A receptor that mediates the post-mating switch in drosophila reproductive behaviour. *Nature*, 451(7174):33–37, 2008.

[57] D. J. McFarland. Decision making in animals. *Nature*, 269(5623):15–21, 1977.

[58] Jon T Sakata and Michael S Brainard. Real-time contributions of auditory feedback to avian vocal motor control. *Journal of neuroscience*, 26(38):9619–9628, 2006.

[59] Eric S Fortune, Carlos Rodríguez, David Li, Gregory F Ball, and Melissa J Coleman. Neural mechanisms for the coordination of duet singing in wrens. *Science*, 334(6056):666–670, 2011.

[60] Arthur W. Ewing. The neuromuscular basis of courtship song inDrosophila: the role of the direct and axillary wing muscles. *Journal of comparative physiology*, 130(1):87–93, 1978.

[61] Troy R Shirangi, David L Stern, and James W Truman. Motor control of drosophila courtship song. *Cell reports*, 5(3):678–686, 2013.

[62] Dmitriy Aronov, Lena Veit, Jesse H Goldberg, and Michale S Fee. Two distinct modes of forebrain circuit dynamics underlie temporal patterning in the vocalizations of young songbirds. *Journal of neuroscience*, 31(45):16353–16368, 2011.

[63] Barry J Dickson. Wired for sex: the neurobiology of drosophila mating decisions. *Science*, 322(5903):904–909, 2008.

[64] Bence P lveczky, Aaron S Andalman, and Michale S Fee. Vocal experimentation in the juvenile songbird requires a basal ganglia circuit. *PLoS Biology*, 3(5), 2005.

[65] N Tinbergen. *The study of instinct.* Clarendon Press/Oxford University Press, 1951.

[66] Andrea Censi, Andrew D Straw, Rosalyn W Sayaman, Richard M Murray, and Michael H Dickinson. Discriminating external and internal causes for heading changes in freely flying drosophila. *PLoS computational biology*, 9(2), 2013.

[67] Chaoming Song, Zehui Qu, Nicholas Blumm, and Albert-László L Barabási. Limits of predictability in human mobility. *Science*, 327(5968):1018–1021, 2010.

[68] Peter Verleyen, Jurgen Huybrechts, Geert Baggerman, Alfons Van Lommel, Arnold De Loof, and Liliane Schoofs. SIFamide is a highly conserved neuropeptide: a comparative study in different insect species. *Biochemical and biophysical research communications*, 320(2):334–341, 2004.

[69] Jasper C Simon and Michael H Dickinson. A new chamber for studying the behavior of drosophila. *PloS one*, 5(1), 2010.

[70] Benjamin J Arthur, Sunayama-Morita, Tomoko, Philip Coen, Mala Murthy, and David L Stern. Multi-channel acoustic recording and automated analysis of drosophila courtship songs. *BMC biology*, 11(1), 2013.

[71] Kirsten M Parris. More bang for your buck: the effect of caller position, habitat and chorus noise on the efficiency of calling in the spring peeper. *Ecological Modelling*, 156(2-3):213–224, 2002.

[72] Nicolas Mathevon, Thierry Aubin, and Torben Dabelsteen. Song degradation during propagation: Importance of song post for the wren troglodytes troglodytes. *Ethology*, 102(3):397–412, 1996.

[73] Henrik Brumm and Dietmar Todt. Facing the rival: directional singing behaviour in nightingales. *Behaviour*, 140(1):43–54, 2003.

[74] DD Michael, GM Siegel, and HL Pick. Effects of distance on vocal intensity. *Journal of speech and hearing research*, 38(5):1176–1183, 1995.

[75] Henrik Brumm and Peter JB Slater. Animals can vary signal amplitude with receiver distance: evidence from zebra finch song. *Animal Behaviour*, 72(3):699–705, 2006.

[76] Richard D Alexander. Aggressiveness, territoriality, and sexual behavior in field crickets (Orthoptera: gryllidae). *Behaviour*, 17(2-3):130–223, 1961.

[77] Philip Coen, Jan Clemens, Andrew J. Weinstein, Diego A. Pacheco, Yi Deng, and Mala Murthy. Dynamic sensory cues shape song structure in drosophila. *Nature*, 507(7491):233–237, 2014.

[78] Samya Chakravorty, Hien Vu, Veronica Foelber, and Jim O Vigoreaux. Mutations of the drosophila myosin regulatory light chain affect courtship song and reduce reproductive success. *PLoS ONE*, 9(2), 2014.

[79] Linda Partridge, Ary Hoffmann, and J S Jones. Male size and mating success in drosophila melanogaster and d. pseudoobscura under field conditions. *Animal Behaviour*, 35(2):468–476, 1987.

[80] Arthur W. Ewing. The influence of wing area on the courtship behaviour of drosophila melanogaster. *Animal Behaviour*, 12(2):316–320, 1964.

[81] Yufeng Pan, Carmen C. Robinett, and Bruce S. Baker. Turning males on: Activation of male courtship behavior in drosophila melanogaster. *PLoS ONE*, 3(3), 2011.

[82] Mikko Juusola and Roger C. Hardie. Light adaptation in drosophila photoreceptors i. response dynamics and signaling efficiency at 25°C. *The Journal of General Physiology*, 117(1):3–25, 2001.

[83] James A Strother, Aljoscha Nern, and Michael B Reiser. Direct observation of ON and OFF pathways in the drosophila visual system. *Current Biology*, 24(9):976–983, 2014.

[84] John C Tuthill, Aljoscha Nern, Stephen L Holtz, Gerald M Rubin, and Michael B Reiser. Contributions of the 12 neuron classes in the fly lamina to motion vision. *Neuron*, 79(1):128–140, 2013.

[85] Bettina Schnell, Shamprasad Varija Raghu, Aljoscha Nern, and Alexander Borst. Columnar cells necessary for motion responses of wide-field visual interneurons in drosophila. *Journal of Comparative Physiology A*, 198(5):389–395, 2012.

[86] Rudy Behnia, Damon A. Clark, Adam G. Carter, Thomas R. Clandinin, and Claude Desplan. Processing properties of ON and OFF pathways for drosophila motion detection. *Nature*, 512(7515):427–430, 2014.

[87] JR Moore, MH Dickinson, JO Vigoreaux, and DW Maughan. The effect of removing the n-terminal extension of the drosophila myosin regulatory light chain upon flight ability and the contractile dynamics of indirect flight muscle. *Biophysical journal*, 78(3):1431–1440, 2000.

[88] Mark S Miller, Gerrie P Farman, Joan M Braddock, Soto-Adames, Felipe N, Thomas C Irving, Jim O Vigoreaux, and David W Maughan. Regulatory light chain phosphorylation and n-terminal extension increase cross-bridge binding and power output in drosophila at in vivo myofilament lattice spacing. *Biophysical journal*, 100(7):1737–1746, 2011.

[89] R Tohtong, H Yamashita, M Graham, J Haeberle, A Simcox, and D Maughan. Impairment of muscle function caused by mutations of phosphorylation sites in myosin regulatory light chain. *Nature*, 374(6523):650–653, 1995.

[90] Gerrie P Farman, Mark S Miller, Mary C Reedy, Felipe N Soto-Adames, Jim O Vigoreaux, David W Maughan, and Thomas C Irving. Phosphorylation and the n-terminal extension of the regulatory light chain help orient and align the myosin heads in drosophila flight muscle. *Journal of Structural Biology*, 168(2):240–249, 2009.

[91] J Warmke, M Yamakawa, J Molloy, S Falkenthal, and D Maughan. Myosin light chain-2 mutation affects flight, wing beat frequency, and indirect flight muscle contraction kinetics in drosophila. *The Journal of Cell Biology*, 119(6):1523–1539, 1992.

[92] Soh Kohatsu, Masayuki Koganezawa, and Daisuke Yamamoto. Female contact activates Male-Specific interneurons that trigger stereotypic courtship behavior in drosophila. *Neuron*, 69(3):498–508, 2011.

[93] Armin Bahl, Georg Ammer, Tabea Schilling, and Alexander Borst. Object tracking in motion-blind flies. *Nature Neuroscience*, 16(6):730–738, 2013.

[94] Yu-Jen Lee and Karin Nordstrm. Higher-order motion sensitivity in fly visual circuits. *Proceedings of the National Academy of Sciences*, 109(22):8758–8763, 2012.

[95] Roel de Haan, Yu-Jen J Lee, and Karin Nordstrm. Novel flicker-sensitive visual circuit neurons inhibited by stationary patterns. *Journal of neuroscience*, 33(21):8980–8989, 2013.

[96] Giedrius T Buraas and Geoffrey M Boynton. Efficient design of Event-Related fMRI experiments using M-Sequences. *NeuroImage*, 16(3):801–813, 2002.

[97] Barrie Burnet, Kevin Connolly, and Leslie Dennis. The function and processing of auditory information in the courtship behaviour of drosophila melanogaster. *Animal Behaviour*, 19(2):409–415, 1971.

[98] Pau Carazo, Cedric K. W. Tan, Felicity Allen, Stuart Wigby, and Tommaso Pizzari. Within-group male relatedness reduces harm to females in drosophila. *Nature*, 505(7485):672–675, 2014.

[99] Jeonghyeon Yoon, Eriko Matsuo, Daichi Yamada, Hiroshi Mizuno, Takako Morimoto, Hiroyoshi Miyakawa, Setsuo Kinoshita, Hiroshi Ishimoto, and Azusa Kamikouchi. Selectivity and plasticity in a Sound-Evoked Male-Male interaction in drosophila. *PLoS ONE*, 8(9), 2013.

[100] RQ Quiroga, Z Nadasdy, and Ben-Shaul, Y. Unsupervised spike detection and sorting with wavelets and superparamagnetic clustering. *Neural computation*, 16(8):1661–1687, 2004.